CELL FREE PRODUCTION OF ISOBUTANOL

Matthew Wong

Submitted in Partial Fulfillment of the Requirements

for the degree of

DOCTOR OF PHILOSOPHY

Approved by:

Dr. Georges Belfort, Chair
Dr. Mattheos Koffas
Dr. Marlene Belfort
Dr. Jonathan Dordick
Dr. Catherine Royer

Department of Chemical and Biological Engineering

Rensselaer Polytechnic Institute
Troy, New York

[August 2022]
Submitted July 2022

TABLE OF CONTENTS

LIST OF TABLES v
LIST OF FIGURES vi
ACKNOWLEDGEMENTS ix
ABSTRACT xi
BACKGROUND 1
1.1 Biofuel Production 1
1.2 Metabolic Engineering for Butanol Production 2
1.3 In Vitro vs In Vivo 2
1.4 Cell-free Butanol Production 4
1.4.1 Ketoisovalerate Decarboxylase 6
1.4.2 Alcohol Dehydrogenase 7
1.4.3 Formate Dehydrogenase 8
1.5 Objectives and Goals 9
CLONING AND MUTAGENESIS OF ENZYMES 11
2.1 Introduction 11
2.1.1 Mutagenesis of Enzymes 11
2.1.2 Fusion Proteins 12
2.1.2.1 Maltose Bind Protein 13
2.1.2.2 HIS Tag 13
2.2 Materials and Methods 13
2.2.1 Materials 13
2.2.2 Plasmid Construction 13
2.2.3 Expression and Purification 15
2.2.4 Activity Assays 16
2.2.5 Kinetic Assays 17
2.2.6 Fusion Protein Development 17
2.2.7 Heat Stability Screening Conditions 17
2.2.8 pH Stability Screening Conditions 18
2.2.9 Isobutanol Stability Screening Conditions 18
2.3 Results and Discussion 19
2.3.1 Purification 19
2.3.2 Kinetic Assays of Wild Types 21

2.3.3 Activity Assays 22
2.3.4 Isobutanol Stability Enzyme Screening 24
2.3.5 Temperature Stability Enzyme Screening 26
2.3.6 pH Stability Enzyme Screening 28
2.4 Conclusions 30
IN VIVO TO *IN VITRO* PRODUCTION OF ISOBUTANOL 31
3.1 Introduction 31
3.1.1 Keto Acid Production 31
3.1.2 CRISPR 32
3.2 Materials and Methods 32
3.2.1 Culture Conditions 32
3.2.2 Fed-batch Conditions 33
3.2.3 KIV Minimum Inhibitory Concentration 33
3.2.4 In Vivo to In Vitro Reaction 33
3.2.5 Overexpression of the KIV Pathway 34
3.2.6 Analytical Methods 34
3.3 Results 34
3.3.1 Minimum Inhibitory Concentration 34
3.3.2 Bioreactor Run 35
3.3.3 In Vivo to In Vitro Reaction 36
3.3.4 Copy Number 37
3.4 Conclusions 38
IRREVERSIBLE IMMOBILIZATION 39
4.1 Introduction 39
4.1.1 NHS Ester 40
4.1.2 Epoxy Resin 41
4.1.3 Immobilized Reaction 42
4.2 Materials and Methods 43
4.2.1 Materials 43
4.2.2 Enzyme Immobilization- EDC NHS 43
4.2.3 Enzyme Immobilization- Epoxy Methacrylate 43
4.2.4 Enzyme Activity Assay 44
4.2.5 Immobilized Reaction Conditions 44
4.3 Results and Discussion 44

4.3.1 EDC-NHS vs Epoxy 44
4.3.2 Immobilized Enzyme Activity 45
4.3.3 Immobilized In Vitro Reaction 48
4.4 Conclusions 50
COHESIN AND DOCKERIN SCAFFOLD 51
5.1 Introduction 51
5.1.1 Affinity Binding 51
5.1.2 Cohesin and Dockerin 52
5.2 Materials and Methods 53
5.2.1 Materials 53
5.2.2 Fusion Enzyme Assembly 54
5.2.3 Expression 54
5.2.4 Purification 56
5.2.5 Activity Assays 56
5.2.6 Binding Experiments 57
5.2.7 Complete Immobilization 57
5.2.8 Immobilized Reaction 57
5.3 Results 58
5.3.1 Expression of Dockerin Fusions 58
5.3.2 Fusion Activity 61
5.3.3 Binding to Cohesin Scaffold 62
5.3.4 Doc V FDH_{WT} Redesign 64
5.3.5 Immobilized Reaction 67
5.4 Conclusions 70
SUMMARY AND FUTURE WORK 71
6.1 Summary 71
6.2 Future Plans 72
6.2.1 Optimization of In Vivo to In Vitro System 72
6.2.2 Optimization of the Scaffold System 72
6.2.3 Engineering the Pathway 73
6.2.4 Separation of Biofuel 75
REFERENCES 76

LIST OF TABLES

Table 1: Primers for mutagenesis. All primers purchased from Integrated DNA Technologies (Coralville, Iowa). 29C8 mutation is in addition to RE1 mutations. 15

Table 2: Primers for Gibson Assembly. All primers purchased from Integrated DNA Technologies (Coralville, Iowa). Melting temperature calculated using overlap sequence inside brackets. 18

Table 3: Michaelis-Menten kinetic parameters. Calculated at 25 °C. 22

Table 4: Immobilized enzyme reaction scheme. The three enzymes used here were MBP-$KIVD_{LLM4}$, FDH_{WT} and ADH_{29C8}: Reaction conditions 24 h, shaking, 35ºC, pH 7.4, 1 mL total volume, 1 μmol of NADH, excess formate. 48

Table 5: Isobutanol production *in vivo* and *in vitro*. (*) Reaction was partially immobilized: ADH_{WT} and MBP-$KIVD_{WT}$ immobilized, FDH_{WT} free in solution 50

Table 6: Primers for assembly of fusions. Primers purchased from Integrated DNA Technologies (Coralville, Iowa). 55

Table 7: Primers for Doc V linker FDH design. Primers purchased from Integrated DNA Technologies (Coralville, Iowa). 56

LIST OF FIGURES

Figure 1: Two step enzymatic production of isobutanol with cofactor recycling using Keto-acid decarboxylase (KIVD), alcohol dehydrogenase (ADH), and formate dehydrogenase (FDH). 5

Figure 2: Structure of KIVD (PDB ID: 2VBF) from L. lactis. C-terminus highlighted in orange, N-terminus highlighted in blue, lysines highlighted in red, and mutations of $KIVD_{LLM4}$ highlighted in purple. Figure adapted from [45]. 7

Figure 3: Structure of ADH (PDB ID: 4EEZ) from L. lactis. C-terminus highlighted in orange, N-terminus highlighted in blue, lysines highlighted in red, and mutations of ADH_{29C8} highlighted in purple. Figure adapted from [49]. 8

Figure 4: Structure of FDH (PDB ID: 2J6I) from C. boidinii. C-terminus highlighted in orange, N-terminus highlighted in blue, lysines highlighted in red, and mutations of FDH_{WT} highlighted in purple. Figure adapted from [53]. 9

Figure 5: SDS-PAGE gel of wild type enzymes. I: induced, W#: wash number, E#: elution number, and C: buffer exchanged. Purified bands highlighted with red box. KIVD is 63 kDa, ADH is 37 kDa, and FDH is 41 kDa. 20

Figure 6: SDS-PAGE gel of mutant enzymes. (A) is the first set of mutants; (B) is the second set of mutants. I: induced, W#: wash number, E: elution, and C: buffer exchanged. Purified bands highlighted with red box. KIVD is 63 kDa, ADH is 37 kDa, and FDH is 41 kDa. 20

Figure 7: Enzyme activity assays. (A) $KIVD_{WT}$ (●), $KIVD_{LLM3}$ (▲), and $KIVD_{LLM4}$ (■), normalized by initial ketoisovaleric acid concentration (4.4 mg/mL); (B) ADH_{WT} (●), ADH_{RE1} (▲), and ADH_{29C8} (■), normalized by initial NADH concentration (0.034 mg/mL); and (C) FDH_{WT} (●), FDH_{K47E} (▲), and FDH_{K328V} (■), normalized by final wild type NADH concentration (0.13 mg/mL). 23

Figure 8: MBP KIVD activity assay. KIVD WT (red) and MBP-KIVD WT (blue) activity assay, normalized by initial ketoisovaleric acid concentration (4.4 mg/mL). 24

Figure 9: Enzyme isobutanol stability. (A) $KIVD_{WT}$, $KIVD_{LLM4}$, MBP-$KIVD_{WT}$, and MBP-$KIVD_{LLM4}$. (B) ADH_{WT} and ADH_{29C8} (empty). (C) FDH_{WT} and FDH_{K328V}. The 20% concentration is phase separated into two phases with isobutanol concentrations of 10% and 87% (v/v). 26

Figure 10: Enzyme temperature stability. The resulting activity was normalized by the room temperature result. (A) $KIVD_{WT}$, $KIVD_{LLM4}$, MBP-$KIVD_{WT}$, and MBP-$KIVD_{LLM4}$. (B) ADH_{WT} and ADH_{29C8}. (C) FDH_{WT} and FDH_{K328V}. 28

Figure 11: Enzyme pH stability. (A) $KIVD_{WT}$, $KIVD_{LLM4}$, MBP-$KIVD_{WT}$, and MBP-$KIVD_{LLM4}$. Normalized by pH 6.5. (B) ADH_{WT} and ADH_{29C8}. Normalized by pH 7.4. (C) FDH_{WT} and FDH_{K328V}. Normalized by pH 7.4. 29

Figure 12: Delta OD600 vs concentration of KIV. Each concentration was done in triplicate. A linear interpolation based on the data is found in the graph. 35

Figure 13: KIV and acetate production pattern in glucose fed batch reactor at different growth stages of MG03. OD600 (-), KIV (g/L) , and Acetate (g/L) share the left axis, while Glucose Consumed (g) utilizes the right axis. 36

Figure 14: Copy number effect on KIV production. (A) OD of cultures grown at 37oC with and without the inducible KIV pathway plasmid. (B) KIV concentration for cultures grown at 37^{o}C with and without the inducible KIV pathway plasmid. 37

Figure 15: EDC-NHS enzyme immobilization. 41

Figure 16: Epoxy enzyme immobilization. 42

Figure 17: Wild type enzyme epoxy immobilized activity (■) vs EDC-NHS immobilized activity (▲). Absorbance over time was normalized by initial absorbance (1.82). 45

Figure 18: Wild type KIVD immobilized activity (■) vs free in solution (●). Normalized by initial absorbance (0.312). 46

Figure 19: Wild type enzyme immobilized activity (■) vs free in solution (●). (A) MBP-KIVD normalized by initial absorbance (0.742), (B) ADH normalized by initial absorbance (1.82), and (C) FDH normalized by final free in solution absorbance (3.43). 47

Figure 20: Cell-free production of isobutanol on a scaffold-CBM: cellulose binding module; G, T, V denote cohesin from *A. fulgidus, C. thermocellum,* and *C. clariflavum* respectively; enzymes are shown in monomer form for ease of visualization. 53

Figure 21: SDS-PAGE gel of N-terminal dockerin fusion enzymes. F: flowthrough, W#: wash number, E: elution. Purified band highlighted with red box. Theoretical location of purified bands highlighted with green box. MBP $KIVD_{LLM4}$ Doc G is 115 kDa, ADH_{29C8} Doc T is 45 kDa, and FDH_{WT} Doc V is 50 kDa. 59

Figure 22: SDS-PAGE gel of dockerin N-terminal ADH Doc T. L: Lysate, LD: diluted lysate, F: flowthrough, W#: wash number, E: elution. Expressed band highlighted with red box. ADH Doc T is 45 kDa. 59

Figure 23: SDS-PAGE gel of dockerin N-terminal ADH Doc T in different cell lines. L: lysate, C: clarified lysate, F: flowthrough, W: wash, E: elution. Expressed band highlighted with red box. ADH Doc T is 45 kDa. 60

Figure 24: ADH Doc T activity assay. Absorbance normalized by initial NADH absorbance. 61

Figure 25: Enzyme activity assays. (A) Comparison of fused and non-fused MBP $KIVD_{LLM4}$ variants. Position of Doc G in label denoted position in fusion. Absorbance normalized by initial ketoisovaleric acid absorbance; (B) comparison of fused and non-fused ADH_{29C8} variants. Absorbance normalized by initial NADH absorbance; and (C) comparison of fused and non-fused FDH_{WT}. 62

Figure 26: SDS-PAGE gel of enzyme binding. (A) MBP KIVD Doc G serial dilution and binding, A: 0.43 mg/mL, B: 0.25 mg/mL, C: 0.12 mg/mL, D: 0.06 mg/mL, and E: 0.03 mg/mL; (B) ADH_{29C8} Doc T serial dilution and binding, A: 0.18 mg/mL, B: 0.1 mg/mL, C: 0.05 mg/mL, D: 0.03 mg/mL, and E: 0.01 mg/mL; and (C) Doc V FDH_{WT} serial dilution and binding, A: 0.03 mg/mL, B: 0.07 mg/mL, C: 0.1 mg/mL, D: 0.14 mg/mL, and E: 0.17 mg/mL. Before denotes enzyme solution before contact with

cellulose bound with scaffold. After denotes retentate retrieved after shaking overnight. A-E denote the different concentrations of enzyme. MBP $KIVD_{LLM4}$ Doc G is 115 kDa, ADH_{29C8} Doc T is 45 kDa, and FDH_{WT} Doc V is 50 kDa. 64

Figure 27: SDS-PAGE gel of short and long linkers for Doc V FDH_{WT}. E: elution and C: buffer exchanged. Expressed band highlighted with red box. Doc V Short FDH_{WT} is 51.6 kDa and Doc V Long FDH_{WT} is 52.8 kDa..... 66

Figure 28: Doc V FDH activity assays. 66

Figure 29: SDS-PAGE gel of Doc V Long FDH_{WT} binding to scaffold. Stock: stock solution of fusion; Pre: enzyme solution before binding; and Post: retentate retrieved post binding. Doc V Long FDH_{WT} is 52.8 kDa. Red square highlights lack of band. 67

Figure 30: SDS-PAGE gel of full enzymatic binding to scaffold. Pre: enzyme solution before binding and Post: retentate retrieved post binding. Red square highlights change in bands specific to fusion enzymes. MBP $KIVD_{LLM4}$ Doc G is 115 kDa, ADH_{29C8} Doc T is 45 kDa, and FDH_{WT} Doc V is 50 kDa. 69

ACKNOWLEDGEMENTS

I'd first like to express my sincere gratitude to my advisors, Professors Georges Belfort and Mattheos Koffas. Being coadvised is usually thought of as a balancing act for the student, but I was truly fortunate to have two advisors that worked so well together on my behalf. Both were a source of inspiration, insight, and invaluable advice. I came to RPI with little confidence in presenting, little experience in research, and no background in biology. Together they instilled in me the tools and wisdom to carry out research, a breadth of knowledge for both chemical and biological engineering, and the confidence and skill to tell others about it. I've been truly blessed to have these two remarkable men mentor me.

Next, I'd like to thank the rest of my committee for all their help: Professors Marlene Belfort, Jonathan Dordick, and Catherine Royer. Many thanks to Professor Marlene Belfort for providing me with her lab's resources and advice and guidance for my project, as well as being a third coadvisor for the NIH training grant. Thank you, Professor Dordick, for providing me a fulfilling assistantship at the Rensselaer COVID Testing Lab, it was a great learning experience and great place to work.

Thank you, Dr. Jian Zha, for mentoring me during my first years in the program. You taught me the ins and outs of genetic manipulation, with great patience as I had never even heard of a plasmid before. Your work with me on the mutagenesis and expression of the enzymes was invaluable and I wouldn't be where I am without you. I'd also like to thank Dr. Mirco Sorci for his years of mentoring me and his friendship. You were great at coming up with experiment ideas and your figure making can't be matched. Your Italian cooking was amazing. I'd also like to thank both Professor Edward Bayer and Dr. Sarah Morais for their help on my project. It was

an exciting time working with you two on the scaffold. Both of you had patience and wisdom to share, knowing exactly how to fix each problem I encountered. It was great getting to converse with you two over email and on video calls.

Thank you, Rensselaer Polytechnic Institute and the Howard P. Isermann Department of Chemical and Biological Engineering for providing an intellectually stimulating environment, great facilitates, and for the occasional free pizza.

Next, I'd like to thank Pranav Ramesh, Jack Keating, Somdatta Bhattacharya, Bhanushee Sharma, Chenyu Guan, Surya Karla, Riddhi Banik, and the rest of the Belfort lab I interacted with both past and present; as well as Abinaya Badri, Alex Perl, Adeola Awofiranye, Alex Connor, Asher Williams, Karolina Kalbarcyzk, and the rest of the Koffas lab I interacted with both past and present. I hope Pranav continues to keep it real. I'd also like to thank Chris Gasparis, who worked under me as an undergrad. You had a great head on your shoulders and a wonderful work ethic. I'd also like to thank Tanner Fink, for helping make a TA job fun.

Finally, I'd like to thank my old friends and my family for your support during this process. Buddy, Jake, and Anthony thanks for keeping me grounded through video games. Yeming, thanks your friendship and for keeping an eye on me from up there. I'd like to thank my uncle, Dr. William Monaco, and my aunt, Victoria Monaco, for helping me in both my application to graduate school and providing constant advice and a unique perspective, as well as help during trying times. Lastly, I'd like to thank my father, Dr. Edison Wong; mother, Pam Salimeno; and grandfather, Dr. Thomas Salimeno, for their endless support and deep love, for visiting me, keeping the light on for me, always being available at any hour, and as well as the occasional editing of papers. It helps to have a father who's a published doctor and a mother who worked in publishing and a family who could not love you more.

ABSTRACT

With a need for greener fuels, research into production of biofuels is essential. Isobutanol out preforms ethanol in key metrics such as engine compatibility, energy density, and gasoline blending. Current biofuel strategies of fermentation are constrained by the inherent toxicity of alcohol on microbial cells. While work has been performed on engineering these strains for higher tolerance, cell-free production with enzymes offers a novel approach to bypass the toxicity limitations altogether. These enzymes can also be immobilized to retain enzyme activity and facilitate separations. Based on previous work in the Belfort laboratory, the ketoisovaleric acid pathway was chosen for production of the biofuel, isobutanol. High preforming and stable enzymes were selected from the literature, cloned, expressed, and purified and tested for activity, kinetics, and stability. They were utilized in a novel *in vivo* to *in vitro* system, resulting isobutanol titer of 1.78 g/L and yield of 93%. An epoxy immobilized reaction scheme resulted in a titer of 2 g/L and 43% yield. The pathway enzymes were then fused to dockerins, which bound to a cohesin scaffold on cellulose. The reaction utilizing this immobilization scheme resulted in a titer of 5.92 g/L and 78.4% yield. Further work can be done to optimize this reaction, as well as to expand the pathway or scaffold, and incorporate separation of the isobutanol for eventual scaleup.

CHAPTER 1

BACKGROUND

1.1 Biofuel Production

The quest for renewable resources that can address issues of sustainability and climate change has resulted in a global push for "greener" fuels. The first generation of biofuel production using *in vivo* methods, such as corn ethanol [1-2] and vegetable oil derived biodiesel[3], utilized food feedstock. The second generation utilized sustainable, nonfood stock. The fuels produced included lignocellulosic ethanol [1-2], mixed alcohol [4], waste oil derived biodiesel[3, 5], and butanol[4]. Butanol is of particular interest for use with current engines as it is less corrosive, has a higher energy density than ethanol, can blend with gasoline more easily, and can be used with jet planes and large trucks[6]. Of the many isomers of butanol, isobutanol is currently considered attractive due to its branched structure, which provides enhanced fuel properties, such as a higher octane number[7-9].

Historically, biobutanol has been produced via acetone-butanol fermentation using *Clostridium strains* in a large number of plants built following World War I, with one constructed in South Africa operating until 1982[10]. Ultimately, these fermentation strains were not well understood genetically, lacked proper tools to engineer metabolism, and had a lower threshold for butanol toxicity[11]. In the intervening years, research has gradually moved toward more suitable strains, focusing on recombinant DNA technology and metabolic engineering of cells to both overproduce bio-butanol and increase cellular resistance to its toxic effects through years of experience with the prior fermentation strains[11-13].

Portions of this chapter previously appeared as: Wong, M.; Zha, J.; Sorci, M.; Gasparis, C.; Belfort, G.; Koffas, M., Cell-Free Production of Isobutanol: A Completely Immobilized System. *Bioresour Technol* **2019**, *294*, 122104. DOI: 10.1016/j.biortech.2019.122104

1.2 Metabolic Engineering for Butanol Production

Research in metabolic engineering focuses on engineering pathways in a cell to enhance or create production of biofuels, biopharmaceuticals, biochemicals, etc[11]. One method modularly optimizes a chemical pathway by editing the intracellular machinery to alter the expression of enzymes and metabolites in order to maximize production[12]. Another approach focuses on the enzymes themselves, where protein engineering methods are applied in order to increase the activity of the proteins[14]. *Clostridium* historically was used for producing butanol from cellulosic feedstock, but is not an ideal strain for production as mentioned above, so work has been done to engineer pathways in other microbes such as *E. coli* and yeast[11]. Engineered *E. coli*, with extremely well defined genetics, have produced up to 15 g/L of butanol, while more viable strains, such as *Saccharomyces cerevisiae*, have had titers of less than 1 g/L[13, 15]. Current *in vivo* production of bio-butanol is hampered by a combination of product inhibition and cellular toxicity. Cells such as *Ralstonia eutropha*, *S. cerevisiae*, and *E. coli*, encounter growth inhibition with isobutanol concentrations as low as 4 g/L[13, 16]. Production of butanol in a cell-free bioreactor bypasses this cellular limitation.

1.3 In Vitro vs In Vivo

As discussed above, it is important to understand the advantages and disadvantages of utilizing an *in vitro* system over an *in vivo* system for production of biofuels. Currently the main advantage a cellular process has over a cell-free one is that the cellular machinery is produced for "free"[17]. *In vitro* production of chemicals requires purified enzymes and additional cofactors, which raises costs. There are solutions to this issue as the cost of enzyme production has been lowering[17]; cell-free protein synthesis offers an *in vitro* method of constructing this machinery[18]; immobilization can prolong enzyme lifetime[19]; cofactor recycling has become part of cell-free

systems; and cheaper cofactor analogs are being developed[20]. Another advantage associated with *in vivo* production is the cell's natural capacity to control its internal environment, such as pH and metabolite balance. This is not an insurmountable challenge for *in vitro* production, as control schemes for the physiochemical environment of the cell-free solutions have been developed[21-23]. Other advantages include natural cellular compartmentalization and the ability to feed a metabolically engineered pathway's products into cellular growth, yielding a synergistic effect on chemical production[17].

There are also disadvantages to *in vivo* production that can be answered by *in vitro* methods. Cells are naturally driven to sustain and survive, which can conflict with chemical production schemes unable to synergize with those systems. This can result in lower growth of the cells or the engineered pathway being sidelined, especially during production as plasmids can be shed and mutations occur to enhance survivability[24-25]. A cell-free system does not have biological limitations, and so focus solely on production of whatever chemical, protein, or metabolite is being generated is possible. Cell-free production also avoids toxicity issues that plague *in vivo* production of valuable chemicals that can kill the cells that are engineered to produce them[26]. Despite lacking the innate control mechanisms found in a cell, there is potential for even more precise control of reactions due to this very lack of barriers associated with cells, both chemical and physical (cell wall)[24]. Engineering cells for specialized production is also time consuming, with days or weeks needed to properly introduce new pathways in plasmids or mutate and test genes. Cell-free synthesis can reduce these timelines from days to hours[27-28].

Other general advantages to *in vitro* systems include absence of contamination of one's final product by cells or unwanted byproducts, which can be a health and safety issue[29]. These cell-free reactions are also scalable from the laboratory to an industrial reactor[24-25]. Cell-free

production can also incorporate unnatural amino acids in proteins, beyond those found in bacterial factories like *E. coli.* These can impart both new biological function in proteins and physiochemical properties allowing for example click chemistry[30]. Purification of products is easier with *in* vitro production because all the components are well defined and known, and the desirable products are available in solution. The primary issues facing cell-free engineering are standardization and production cost[25]. As mentioned previously, costs of enzymes and cofactors remain a challenge but even these issues pale in comparison with the inherent head start *in vivo* methods of production have in the industry, having been built upon for well over a century. To penetrate the industry, cell-free needs to either have a large advantage in cost for current production of chemicals, proteins, and pharmaceuticals, or provide novel forms of the aforementioned products that are not or cannot be currently developed using a cellular system. This work focuses on a novel biofuel currently lacking production due to cellular toxicity[31].

1.4 Cell-free Butanol Production

Cell-free production offers a novel approach to producing high value chemicals. It is already being applied in industry, with companies such as Sutro Biopharma (San Francisco, CA) utilizing a proprietary technology XpressCF^{TM} to engineer and optimize a variety of protein therapeutics with methods such as unnatural amino acids[27]. *In vitro* production has been demonstrated before by Krutsakorn et al. constructing a 16 enzyme cascade to produce n-butanol[32]; Guterl *et* al. designed an artificial glycolytic reaction cascade for production of isobutanol from glucose. They obtained a molar yield of 53% and a titer of 0.76 g/L[33]. While it would be possible to metabolically engineer a single cell to construct these pathways, it would be more efficient to recombinantly producing the enzymes using different batches of *E. coli*. These methods come with their own challenges such as enzyme stability, diffusion limitations, scale-

up, cofactor costs, and product purification[24, 34-35]. One way to tackle these challenges uses enzyme immobilization to enhance their stability[36-38], enabling industrial scale-up and facilitating purification[36-37].

The Belfort group has previously studied enzyme stability in cavities[39-40], entrapped[41-43], and immobilized enzyme reactions[9, 44]. Grimaldi *et* al.[9, 44] utilized epoxy methacrylate resin, suggested by DuPont, to immobilize enzymes in the ketoisovaleric acid pathway for isobutanol production. The pathway, shown in **Fig. 1**, was chosen due to its wide research focus, particularly a focus on enzyme mutagenesis and gene expression[9]. Keto-acid decarboxylase (KIVD) converts ketoisovaleric acid to isobutyraldehyde which is then converted by alcohol dehydrogenase (ADH) to isobutanol. The cofactor NADH is converted to NAD by ADH and recycled by the enzyme formate dehydrogenase (FDH) utilizing formate.

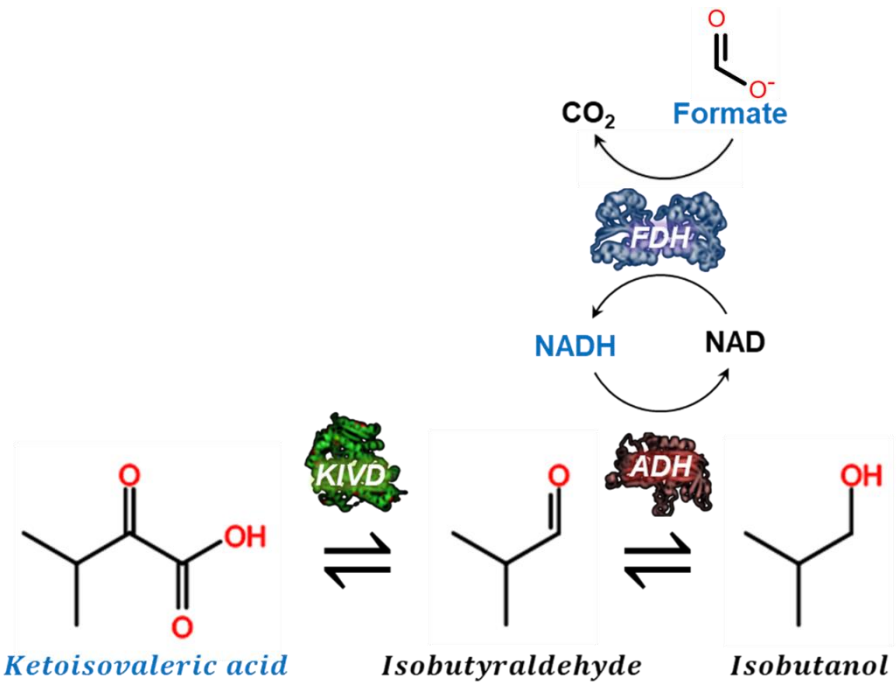

Figure 1: Two step enzymatic production of isobutanol with cofactor recycling using Keto-acid decarboxylase (KIVD), alcohol dehydrogenase (ADH), and formate dehydrogenase (FDH).

Due to stability issues, KIVD was expressed as a fusion with maltose binding protein chosen as the optimal tag for immobilization. The constructed pathway, with FDH free in solution for cofactor recycling, was reacted for 24 hours and had an isobutanol molar yield of 54% and a titer of 2.59 g/L, which correlates to a production rate of 0.11 g/(L·h)[44]. Immobilization adds another layer of modulation to reaction engineering, allowing for easy addition and removal of enzymes. The resins themselves are modular, with multiple varieties available for quick testing and application[9].

1.4.1 Ketoisovalerate Decarboxylase

Ketoisovalerate Decarboxylase (KIVD) is a thiamine dependent keto acid decarboxylase, a group of enzymes that convert keto acid to aldehyde [45-46]. The pathway setup previously in the Belfort lab utilized a recombinant KIVD, but with poor activity[44]. To improve on the performance of the previous enzymes, a literature search was performed to find variants of the pathway enzymes that were more active and had higher stability. A KIVD was found by the Liao lab[45] from *L. lactis* that reportedly had higher activity than that previously reported by our laboratory. Of interest were the mutant enzymes, $KIVD_{LLM3}$ and $KIVD_{LLM4}$, which were reported to have both higher activity (more than double the catalytic efficiency) and higher heat stability than the wild type[45]. To design an industrial friendly reaction scheme, stability of the enzymes is crucial and so mutants with higher stability is essential.

KIVD from *L. lactis* presents as a homodimer. The subunit of the homodimer is seen in **Fig. 2**. It is important to note that lysine, which is a target for epoxy binding, is found throughout the enzyme, possibly presenting a challenge for activity retention.

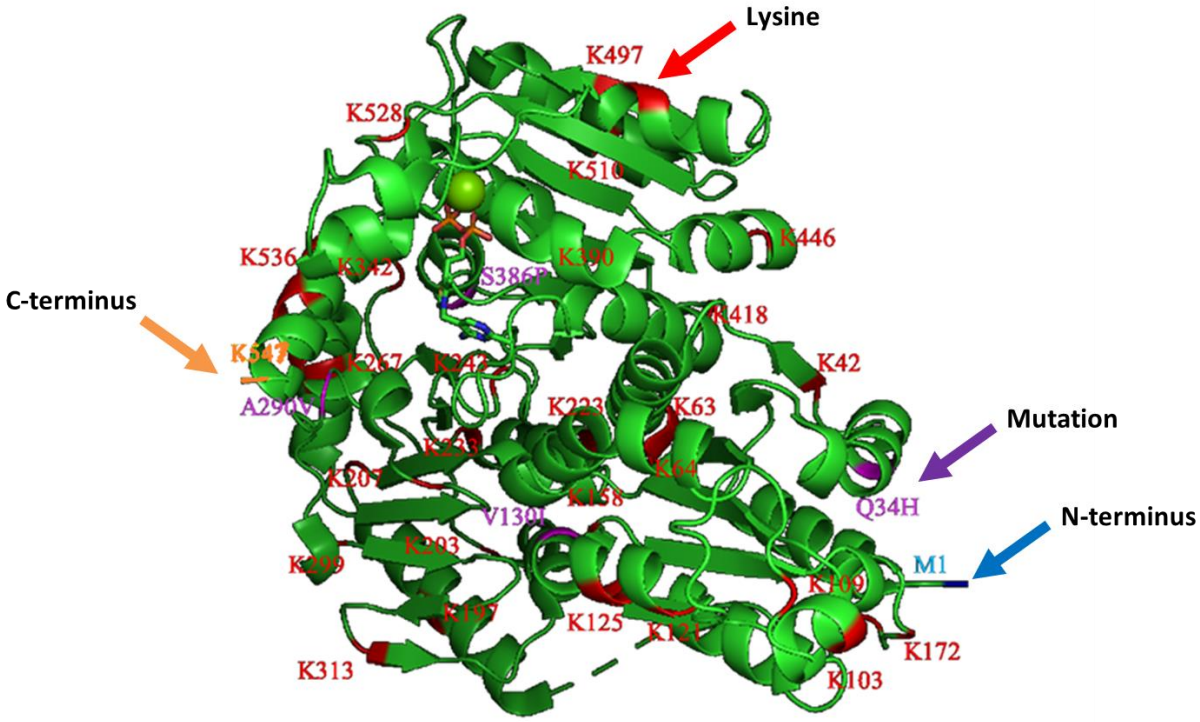

Figure 2: Structure of KIVD (PDB ID: 2VBF) from L. lactis. C-terminus highlighted in orange, N-terminus highlighted in blue, lysines highlighted in red, and mutations of $KIVD_{LLM4}$ highlighted in purple. Figure adapted from [45].

1.4.2 Alcohol Dehydrogenase

Alcohol dehydrogenase is an oxidoreductase known for the essential process of interconverting alcohols, aldehydes, and ketones in living organisms. Often organisms will contain multiple ADHs for these different roles, such as fermentation of alcohol to regenerate NAD or the oxidation of alcohols as a carbon source[47]. For this work, we needed an ADH that could convert isobutyraldehyde to isobutanol with high activity as the reaction is known to be reversible[48]. The ADH used in this work was found again in *L. lactis*, LlAdhA, engineered by the Arnold laboratory at Caltech[49]. This particular ADH belongs to the medium-chain, NAD dependent family of reductases and is also zinc dependent[49]. The mutant 29C8 was of particular

interest and had an almost 200x increase in catalytic efficiency with an increase in kcat and decrease in Km compared with the wild type.

ADH presents as a homodimer[49] which is uncommon since bacterial ADH is usually tetrameric while dimeric ADH is usually found in eukayrotes[50]. As mentioned previously, lysine can serve as a binding site for epoxy groups due to the amine groups. This amino acid is also present over the entire structure of the enzyme, as seen in **Fig.3**, which could affect activity.

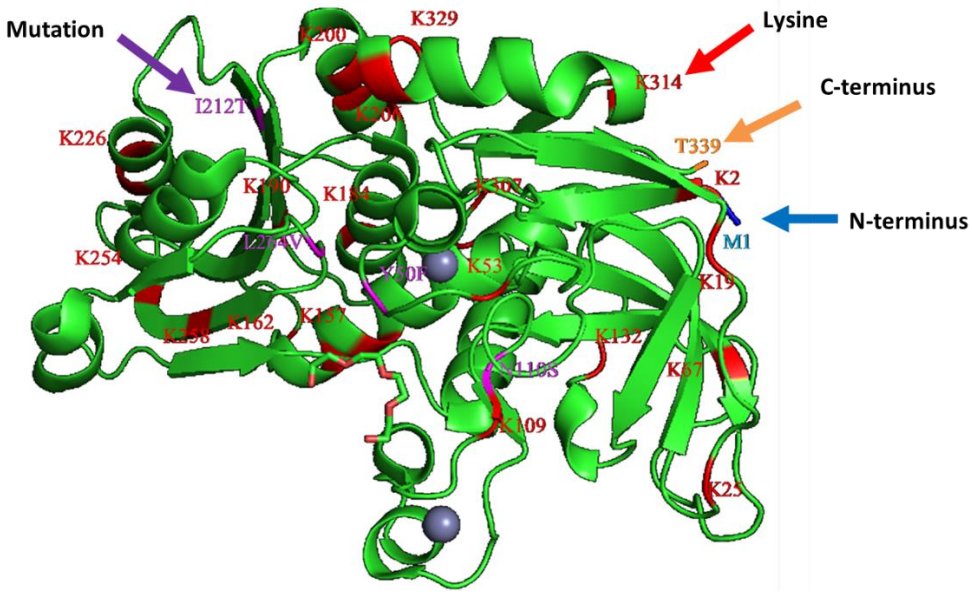

Figure 3: Structure of ADH (PDB ID: 4EEZ) from L. lactis. C-terminus highlighted in orange, N-terminus highlighted in blue, lysines highlighted in red, and mutations of ADH$_{29C8}$ highlighted in purple. Figure adapted from [49].

1.4.3 Formate Dehydrogenase

Formate Dehydrogenase is an oxidoreductase that catabolizes formate *in vivo*, converting it to carbon dioxide. Both aerobes and anaerobes utilize this enzyme and the reaction is reversible[51]. Previously attempts in our laboratory by Grimaldi to immobilize FDH on epoxy resin failed to retain activity, so stability of the enzyme was integral[52]. An NAD dependent FDH was identified from the Lamzin laboratory at the European Molecular Biology Laboratory that is

derived from *Candida boidinii*[53]. Specifically, a mutant was reported to have lower Km (20 vs 5 mM) and higher thermal stability than the wild type[53]. Again, it would be beneficial to the development of this system to have higher activity and stability.

The FDH utilized in this work presents as a homodimer and is divided into two domains: an NAD binding domain and a catalytic domain[53]. The termini of the enzyme are located in the catalytic domain and once again lysine is present through the enzyme as seen in **Fig. 4**. This highlights a challenge of the immobilization strategy.

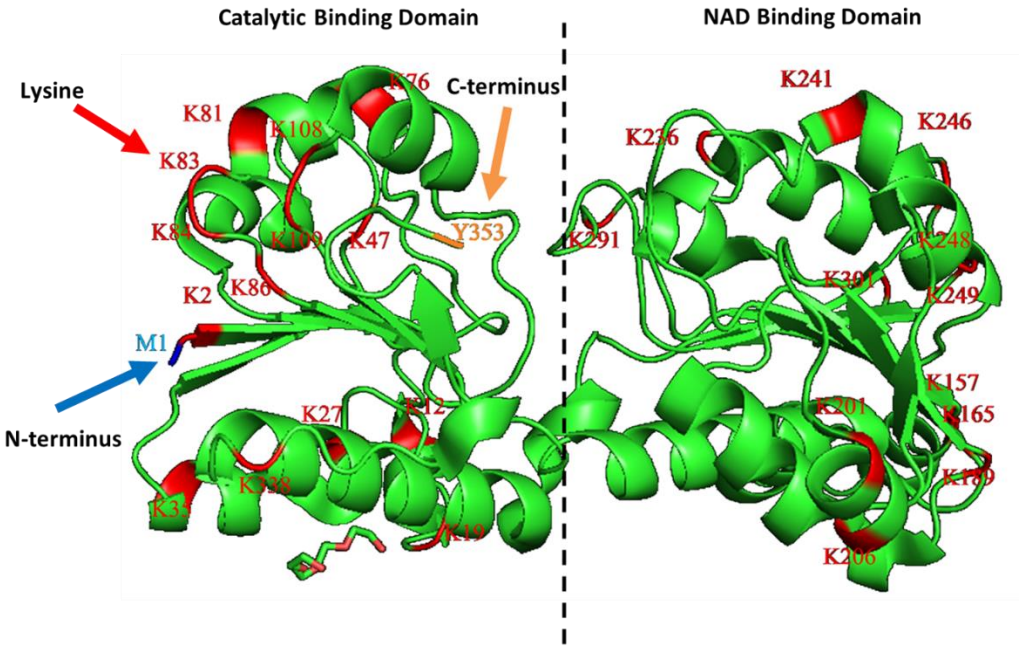

Figure 4: Structure of FDH (PDB ID: 2J6I) from C. boidinii. C-terminus highlighted in orange, N-terminus highlighted in blue, lysines highlighted in red, and mutations of FDH$_{WT}$ highlighted in purple. Figure adapted from [53].

1.5 Objectives and Goals

The objective of this research is to build on the previous results of the Georges Belfort laboratory in collaboration with the Mattheos Koffas laboratory at RPI to engineer an immobilized *in vitro* system to produce isobutanol. As previously mentioned, protein

engineering and metabolic pathway refactoring and balancing are a focus in metabolically engineering these biofuel systems. The previous reaction scheme was also not fully immobilized and can also be modulated for more optimum conditions. This research will examine all of these principles as follows:

1. DNA based cloning procedures were utilized to obtain plasmids with genes for each enzyme and their optimized mutant variants, KIVD from the Liao laboratory[45], ADH from the Arnold laboratory[49], and FDH from the Lamzin laboratory[53], which were transformed into *E. coli* strains suitable for expression of the proteins.
2. Enzymes were tested for activity, kinetics, stability, and immobilization performance with a microplate reader (Biotek Powerwave XS, Winooski, VT).
3. An *E. coli* producing strain of KIV was constructed, providing reagent for a novel *in vivo* to *in vitro* reaction scheme utilizing the pathway enzymes.
4. The reactions were run using the best performing enzymes and ideal reaction conditions while immobilized. The solution was analyzed using both mass spectrometry and gas chromatography.
5. A scaffold system was developed utilizing the pathway enzymes to create a novel, targeted immobilization scheme to produce isobutanol utilizing substrate channeling.

CHAPTER 2

CLONING AND MUTAGENESIS OF ENZYMES

2.1 Introduction

2.1.1 Mutagenesis of Enzymes

Enzymes have been used throughout human history to produce commodities such as bread, beer, and treated leather. Of course at the time humans did not know they were specifically using microbially expressed proteins to catalyze critical reactions[54]. Specified and purposeful use of enzymes in industrial applications came about in the past century with the discovery of recombinant DNA technology, and the development of fermentation processes and enzyme purification[54]. Enzymes derived from natural sources, such as microbes, can perform selective chemical reactions and often work under mild conditions. Though enzymes have the power to accelerate reaction rates, they face issues in industrial applications such as: low environmental and temporal stability, the need for specific conditions and cofactors to function, and the limited capability for unnatural products[55] from highly selective enzymes. Scientists have sought ways to engineer the wild type enzymes to address these issues, utilizing mutagenesis to change the amino acid composition of proteins, and their activity and physicochemical properties.

Enzymes are known to evolve over time through mutation of their DNA blueprint. These mutations can have various affects on the enzyme's properties, potentially changing activity, thermostability, pH stability, or substrate specificity[56]. These natural mutations occur at slow rate, for instance with *E. Coli* the mutation rate was 1.1 per genome per year[57]. The standard or

Portions of this chapter previously appeared as: Wong, M.; Zha, J.; Sorci, M.; Gasparis, C.; Belfort, G.; Koffas, M., Cell-Free Production of Isobutanol: A Completely Immobilized System. *Bioresour Technol* **2019**, *294*, 122104. DOI: 10.1016/j.biortech.2019.122104

usual method to obtain mutated enzymes requires random mutations or the addition of mutagenic agents[58]. Still used to great success with the right strategies, this method enables quick generation of highly active enzymes or ones with production of novel chemicals[14, 59]. In part, proteins are still a relative blackbox when it comes to understanding how specific amino acids will affect performance and structure until observed through tests. But once these mutations are discovered, random mutagenesis will not serve well to obtain these specific mutations on an enzyme. Site directed mutagenesis enables precise and controlled mutation of DNA, allowing for specific mutations. Most commonly, a PCR method utilizes a short oligonucleotide that complements the DNA of the protein of interest, but has a mismatch such as an insertion, a deletion, or a substitution, that will be carried over into subsequent generations of genetic material utilizing a polymerase[60-61]. This work utilizes site directed mutagenesis to replicate mutants generated from other laboratories that were originally generated by site-directed or random mutagenesis.

2.1.2 Fusion Proteins

In some cases, desired function might require a fusion protein. Engineered fusion proteins often take inspiration from naturally occurring ones. These natural fusions enable complex reactions to occur efficiently[62]. Engineered fusion proteins offer benefits such as increased activity, more efficient reactions, enhanced stability and solubility, and reduced toxicity[63]. Fusions can also be used as purification tags, with common ones being maltose binding protein (MBP) and histidine (HIS) tags[64]. In this work, MBP was utilized for its stability and solubility enhancement while HIS was used for purification of the enzymes.

2.1.2.1 Maltose Bind Protein

Maltose binding protein is sourced from *E. coli* and is often used as a fusion candidate due to its ability to bind to amylose columns for purification purposes, but it also has stabilizing and solubilizing effects on proteins[65]. In fact, MBP can be so effective that it has been shown to aid in folding of the partner protein, acting as a chaperone[66]. A protein that is known to aggregate, such as keto-acid decarboxylase (KIVD), could benefit from these properties[44].

2.1.2.2 HIS Tag

The polyhistidine affinity tag is the most widely used tag in recombinant proteins, with 60% of proteins produced for structural studies having one[67]. The imidazole group on the histidine binds to a chelating metal and is unbound with an elution buffer containing imidazole. While HIS tags can be removed to avoid unneeded effects on activity, in this work the HIS tags were left on the proteins of interest following purification.

2.2 Materials and Methods

2.2.1 Materials

Plasmids with the genes for KIVD and mutants were provided by the Liao laboratory[45]. The genes encoding alcohol dehydrogenase (ADH) and formate dehydrogenase (FDH) were synthesized using gene fragments (gBlock, Integrated DNA Technologies, Coralville, Iowa). Plasmid pGS-21a was used as IPTG inducible expression vector (GenScript Co.) *E. coli* DH5α was used as host for cloning and *E. coli* BL21 Star (DE3) as host for plasmid expression.

2.2.2 Plasmid Construction

For converting KIV to isobutanol, the plasmids were constructed for *in vitro* enzyme production. The gene sequences for ADH from *Lactococcus lactis* and FDH from *Candida*

boidinii were cloned into plasmid pGS21a by Nde I and Xho I digestions. The correct plasmids were then confirmed by sequencing (Genewiz, South Plainfield, NJ). The confirmed KIVD and ADH plasmids were then transformed into BL21 star (DE3) cells and FDH plasmid was transformed into Rosetta (DE3) cells.

The mutations of ADH and FDH were obtained from previously described reports by the Arnold and Lamzin groups[53]. Site directed mutagenesis was performed through PCR amplification, followed by Dpn I digestion, transformation into DH5-α for miniprep, and then confirmation of the correct mutation through sequencing (Genewiz, NJ). The fusion of MBP and KIVD was carried out using the Gibson Assembly Ultra Kit purchased from SGI-DNA (La Jolla, CA). Correctly sequenced mutant/fusion protein plasmids were transformed into the expression strains described above. The primers used for PCR and their corresponding mutants are listed in **Table 1**.

Table 1: Primers for mutagenesis. All primers purchased from Integrated DNA Technologies (Coralville, Iowa). 29C8 mutation is in addition to RE1 mutations.

Enzyme	Mutation	Primer	Sequence	Melting Temp °C	GC%
FDH	K47E	K47E-F	CCACGTCTGATGAAGAAGGCGGAAAC	67	54
		K47E-R	GTTTCCGCCTTCTTCATCAGACGTGG	67	54
	K328V	K328V-F	GCTCAAGGTACTGTTAATATCTTGG	63	40
		K328V-R	CCAAGATATTAACAGTACCTTGAGC	63	40
ADH	RE1	Y50F-F	CAGCAGGTGATTTTGGCAACAAAGC	68	48
		Y50F-R	GCTTTGTTGCCAAAATCACCTGCTG	68	48
		I212T-F	GAGCTGATGTGACCATCAATTCTGG	65	48
		I212T-R	CCAGAATTGATGGTCACATCAGCTC	65	48
		L264V-F	GTTGCTGTGGCAGTTCCCAATACTGAG	67	52
		L264V-R	CTCAGTATTGGGAACTGCCACAGCAAC	67	52
	29C8[b]	N110S-F	GAGAAGTTAAAAGCGCAGGATATTC	59	40
		N110S-R	GAATATCCTGCGCTTTTAACTTCTC	59	40

2.2.3 Expression and Purification

Cell lines were cultured overnight in 3 mL of lysogeny broth (LB), shaking at 37°C and 200 rpm. Overnight cultures were mixed with 150 mL of fresh LB and left shaking at 37°C, until OD was between 0.6-0.8. Amp (80 mg/mL), kan (50 mg/mL), strep (100 mg/mL)and Cm

(50 mg/mL) were added when necessary. Protein expression was induced by addition of IPTG at a final concentration of 0.5 mM for ADH and 1 mM for FDH and KIVD[45]. The incubation continued for 14 h at 30°C. Cells were pelleted by centrifugation for 20 minutes at 4°C and 4000 rpm. The supernatant was removed, and the pellet was stored at -80°C. Cells were lysed in an ice bath via sonication for 6 mins, at 70% amplitude with 10 sec on and 5 sec off 10 on, 5 off, and 70% amp. The lysed cells were then centrifuged for one hour at 10,000 g and 4°C. Enzymes were purified using nickel columns and an imidazole gradient. The purification buffer consisted of 20 mM Tris HCl, 10 mM MgCl2, 100 mM NaCl, and varying concentrations of imidazole at pH of 7.4. The lysed extract was left shaking with nickel resin for 3 hours at 4°C. 20 mM imidazole buffer was added to reduce nonspecific binding. The resin settled by gravity and the remaining extract was removed. The resin was then washed with 20 mM imidazole buffer to remove nonspecific proteins. Elution was done with 200 mM imidazole buffer. The enzymes were then buffer exchanged to concentrate the enzyme and remove imidazole. ADH and FDH were stored in 50 mM of Tris HCl and 50% glycerol, at a pH of 7.4. KIVD was stored in 50 mM sodium phosphate, 5 mM MgCl2, 1.5 mM TPP, and 50% glycerol at a pH of 6.5.

2.2.4 Activity Assays

Activity assays were conducted in 96-well plates utilizing the microplate reader (Biotek Powerwave XS, Winooski, VT). Both ketoisovaleric acid and NADH have peak absorbances at 340 nm. Activity was monitored through change in the absorbance at 340 nm over time. The final enzyme concentrations for each well were as follows: 0.125 mg/mL KIVD, 0.001 mg/mL ADH, and 0.25 mg/mL FDH. Each enzyme was mixed with storage buffer to obtain a 150 μL volume. For ADH and FDH, a substrate was also included in excess: isobutyraldehyde and formate respectively. The assay was initiated with the addition of 50 μL of reagent to each well

for an initial concentration of 4 mg/mL ketoisovaleric acid for KIVD, 0.15 mg/mL NADH for ADH, and 1.07 mg/mL NAD for FDH. For KIVD, the temperature was set to 50ºC[45], while for ADH and FDH, the temperature was kept at 24ºC [49, 53].

2.2.5 Kinetic Assays

The kinetic assays for examining the activity of the enzymes were carried out as follows. Enzyme concentration was measured using Bradford assay and then added to storage buffer. 200 µL of the enzyme mix was added to each well. For KIVD, ADH, and FDH, a concentration gradient of the reagents KIV, NADH, and NAD were used respectively. KIV and NADH have an absorbance peak at 340 nm, while NAD does not. Thus, a decrease of absorbance at 340 nm over time was measured for KIVD and ADH as reagent was consumed, while an increase in absorbance at 340 nm was measured for FDH as NADH was produced. ADH and FDH kinetic assays were conducted at room temperature, while the KIVD kinetic assay was conducted at 50°C, while shaking, to facilitate a proper comparison with previously obtained results[45]. Using the initial rate of reaction for each concentration step, the kinetic parameters k_{cat} and K_m were calculated using the Michaelis-Menten equation.

2.2.6 Fusion Protein Development

The fusion of MBP and KIVD was carried out using the Gibson Assembly Ultra Kit (SGI-DNA, La Jolla, CA). Correctly sequenced mutant/fusion protein plasmids were transformed into the expression strains described in Chapter 2. The primers used for fusion protein development are listed in **Table 2**

2.2.7 Heat Stability Screening Conditions

Enzymes were mixed with storage buffer in a 10 mL tube to obtain 800 µL solutions with the same concentrations as used in the activity assay. The solutions were heated in an incubator

for 1 h at the following temperatures: ambient, 35ºC, 45ºC, 50ºC, 55ºC, 60ºC, 65ºC, and 70ºC. The solutions were cooled to room temperature and then assayed for activity as previously described in section 2.2.4. While this won't give the stability while operating at each temperature, it will allow us to ascertain long term stability of the enzymes.

Table 2: Primers for Gibson Assembly. All primers purchased from Integrated DNA Technologies (Coralville, Iowa). Melting temperature calculated using overlap sequence inside brackets.

	Primer	Sequence	Melting Temp °C	GC %
MBP	Forward	[GCATCACCATCACCATCACGGATC]CAGCAGCGGCCTGGTGCC	65	64
KIVD	Reverse	[CCTGAAAATACAGGTTTTCGGATCC]CCTTCCCTCGATCCCGAGG	60	55

2.2.8 pH Stability Screening Conditions

Screening of pH stability was conducted using the activity assay conditions previously described in section 2.2.4 with the pH of the storage buffer used to generate enzyme, reagent, and buffer solutions set to the following pHs: 5.0, 5.5, 6, 6.5, 7, 7.4, 8, 8.5, 9.0. pI values for KIVD and ADH were calculated using the isoelectric point calculator by Kozlowski and are 5.3 and 5.2, respectively[68]. FDH pI value is 5.4[69].

2.2.9 Isobutanol Stability Screening Conditions

Screening of stability to isobutanol was conducted using the activity assay conditions previously described in section 2.2.4 with the storage buffer added to bring the final well volume to 200 µL being replaced with isobutanol to obtain final volume concentrations of: 0%, 0.25%, 0.5%, 1%, 5%, 10%, and 20%. The assay was continuously shaken to keep isobutanol well mixed.

2.3 Results and Discussion

2.3.1 Purification

A uniform purification method was used to purify the three pathway enzymes utilizing nickel columns and genetically attached HIS tags to each enzyme. The efficacy of this purification of the wild type enzymes was confirmed using SDS-PAGE as seen in **Fig. 5**. The molecular weight of KIVD, ADH, and FDH should be ~63, 37, and 41 kDa respectively. The purified elution bands highlighted by the red boxes matches these weights. These bands are in the first elution and so both confirm the uniform purification process used. FDH seemed to overload the well, based on the high concentration obtained.

The mutant variants for each enzyme were then purified and assessed using SDS-PAGE as seen in **Fig. 6**. Despite the enzymes being largely the same between mutant variants, the small mutations could possibly affect binding to the resin, as well as enzyme production, and so checking with a gel was critical. The variants all showed bands corresponding to their correct molecular weights in the elution. KIVD and FDH maintained similar concentrations of proteins, but ADH showed decreasing concentrations with mutant 29C8 having only a faint band when compared to the wild type. Examination of the activity of the wild types and mutants would show if this low concentration would be a problem for what should be the best performing mutant.

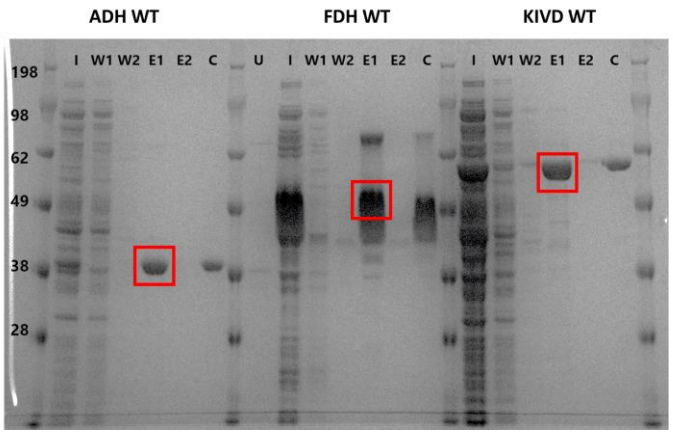

Figure 5: SDS-PAGE gel of wild type enzymes. I: induced, W#: wash number, E#: elution number, and C: buffer exchanged. Purified bands highlighted with red box. KIVD is 63 kDa, ADH is 37 kDa, and FDH is 41 kDa.

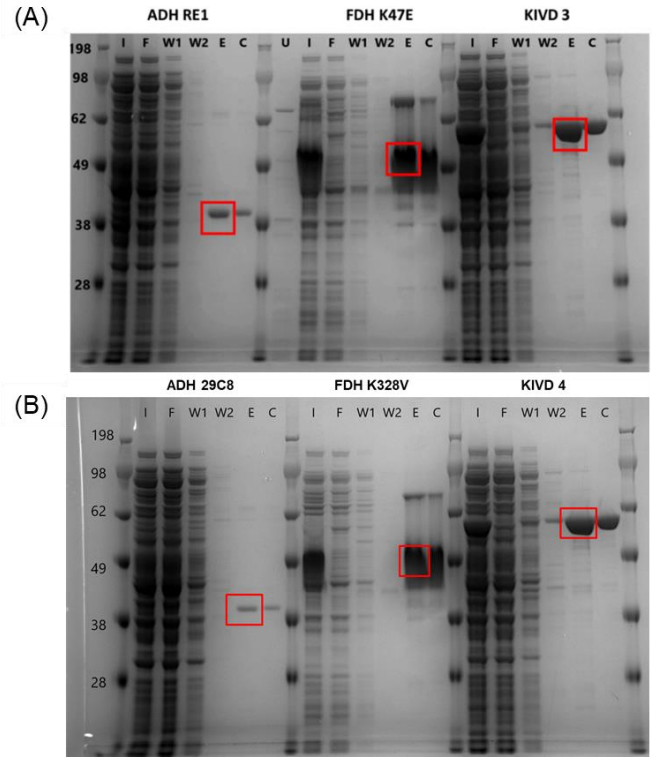

Figure 6: SDS-PAGE gel of mutant enzymes. (A) is the first set of mutants; (B) is the second set of mutants. I: induced, W#: wash number, E: elution, and C: buffer exchanged. Purified bands highlighted with red box. KIVD is 63 kDa, ADH is 37 kDa, and FDH is 41 kDa.

2.3.2 Kinetic Assays of Wild Types

To compare the activities of the enzymes to those found in the literature, kinetic assays of the wild type enzymes were conducted, and the results are shown in **Table 3**. KIVD had a higher Km (9.9 mM) and kcat (500 s^{-1}) than previously reported by Soh, (1.6 mM and 17 s^{-1}, respectively), meaning the binding affinity of KIVD for KIV was lower but the rate at which the substrate is converted was much higher, leading to a larger catalytic efficiency (50 $mM^{-1}s^{-1}$ vs 11 $mM^{-1}s^{-1}$)[45]. It is also worth examining the previous kinetic result for a different strain of KIVD obtained in the Belfort lab, which had a much larger Km (22 mM) and a smaller kcat (0.00058 s^{-1})[44]. Based on these results, it can be concluded that KIVD is quite effective at converting KIV to aldehyde and better than previously reported.

Next, ADH was examined. The enzyme used in this study had both a Km (30 mM) and a kcat (90 s^{-1}) higher than previously reported by Liu (12 mM and 30 s^{-1}, respectively), and a higher catalytic efficiency (3 $mM^{-1}s^{-1}$ versus 2.8 $mM^{-1}s^{-1}$)[49]. NADH is an expensive substrate so a higher catalytic efficiency is useful since the concentration of NADH will be lower than Km. Once again, an enzyme was identified that is more effective at converting its substrate than previously reported. Unlike KIVD and ADH, FDH had a lower kcat (1.2 s^{-1}), Km (0.34 mM^{-1}), and catalytic efficiency (3.5 $mM^{-1}s^{-1}$) compared to what was previously reported (20 s^{-1}, 4.9 mM^{-1}, and 4.1 $mM^{-1}s^{-1}$, respectively)[53]. This underperformance could present a problem; despite it not being part of the main reaction of converting KIV to isobutanol, it is still necessary for recycling NAD back to NADH. To reduce this potential liability for isobutanol production, an excess of formate was utilized, which allowed for high conversion of NAD back to NADH. So, while both KIVD and ADH will have lower reaction rates as their reagents begin to be consumed, NADH recycling will be maintained at a consistent rate.

Table 3: Michaelis-Menten kinetic parameters. Calculated at 25 °C.

Enzyme	K_M (mM)	k_{cat} (s^{-1})	k_{cat}/K_M (mM^{-1} s^{-1})
$KIVD_{WT}$	9.9 ± 0.4	500 ± 15	50 ± 2
ADH_{WT}	30 ± 13	90 ± 40	3 ± 1.8
FDH_{WT}	0.34 ± 0.03	1.2 ± 0.1	3.5 ± 0.4

2.3.3 Activity Assays

The activity in solution at 25ºC of each purified enzyme is shown in **Fig. 7**. In **Fig. 7A**, ketoisovaleric acid uptake is plotted as a measure of KIVD activity. $KIVD_{WT}$ and its variants exhibited expected behavior, namely $KIVD_{LLM4}$ and $KIVD_{LLM3}$ were more active than $KIVD_{WT}$, as seen with the larger decrease in ketoisovaleric acid concentration after 5 minutes. As these results were in line with expectations, LLM4 was selected for further evaluation of stability. ADH_{29C8} showed a large increase in activity compared with the wild type, with the concentration of NADH several times lower after 5 min (**Fig. 7B**). Surprisingly, ADH_{RE1} variant showed a decrease in activity compared with wild type which was inconsistent with the expected activity that was previously reported to be between the wild type and the ADH_{29C8}[49]. Despite having a lower concentration, ADH_{29C8} still showed very high activity with only 1 ug/mL, meaning lower concentrations would not be an issue. ADH_{29C8} was thus selected for further stability testing. In **Fig. 7C**, normalized NADH uptake is plotted as a measure of FDH activity, normalized by the final NADH concentration. FDH_{WT} showed the highest activity compared to the variants. This is not an unexpected result as the selected mutant variants of FDH were largely stability related, so any benefits of mutation would become apparent in stability testing[53]. The variant FDH_{K328V} showed the highest activity of the two variants and was selected for further testing.

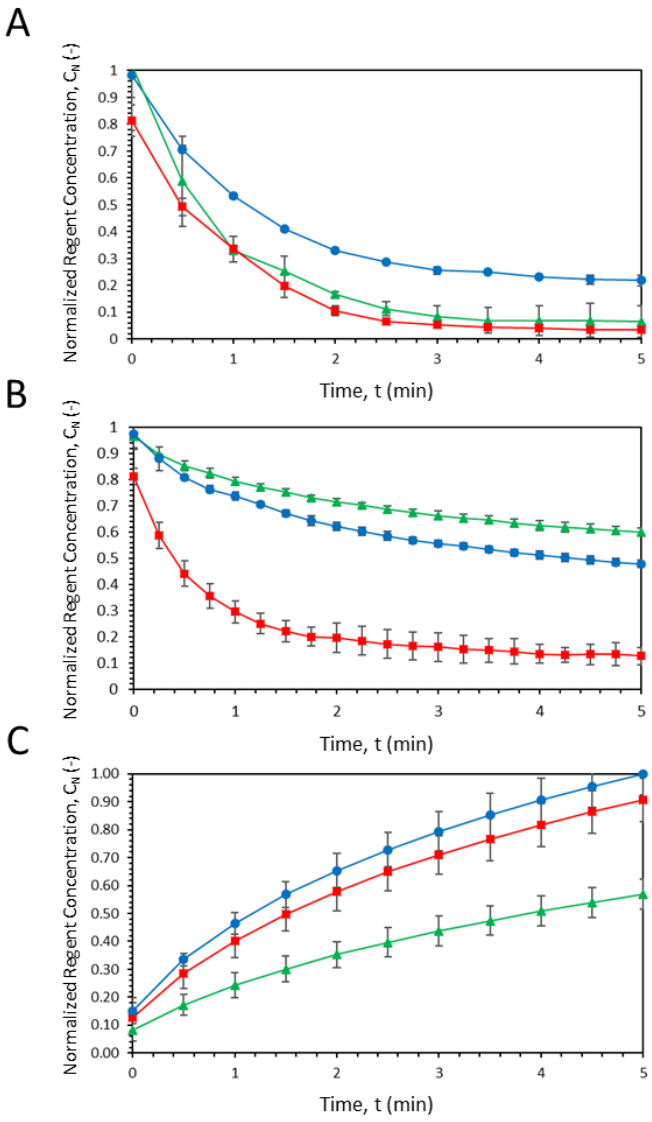

Figure 7: Enzyme activity assays. (A) $KIVD_{WT}$ (●), $KIVD_{LLM3}$ (▲), and $KIVD_{LLM4}$ (■), normalized by initial ketoisovaleric acid concentration (4.4 mg/mL); (B) ADH_{WT} (●), ADH_{RE1} (▲), and ADH_{29C8} (■), normalized by initial NADH concentration (0.034 mg/mL); and (C) FDH_{WT} (●), FDH_{K47E} (▲), and FDH_{K328V} (■), normalized by final wild type NADH concentration (0.13 mg/mL).

Because the KIVD was subject to the previously mentioned, expected aggregation, KIVD was thus fused to the MBP utilizing Gibson assembly to insert the gene for MBP at the N-terminus of the KIVD genes for WT and LLM4. As seen in **Fig. 8**, MBP KIVD WT performs comparably to KIVD WT. There appears to be a bit higher activity that could be a result of the

enhanced solubility for the enzyme. In fact, compared to KIVD WT, which aggregated at -20°C in 50% glycerol after as little a day, MBP KIVD WT never showed any signs of aggregation despite storage for months at the same condition.

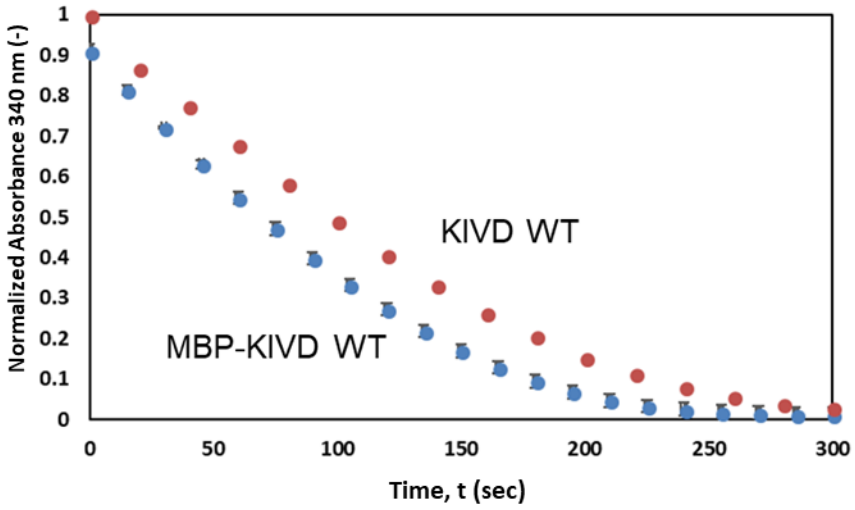

Figure 8: MBP KIVD activity assay. KIVD WT (red) and MBP-KIVD WT (blue) activity assay, normalized by initial ketoisovaleric acid concentration (4.4 mg/mL).

2.3.4 Isobutanol Stability Enzyme Screening

Enzymes were screened for stability in isobutanol at 25°C and the results are shown in **Fig. 9**. The purposes of this testing were to select the best performing variant of each enzyme in the pathway, examining activity rate and identifying which enzyme is the most active in the presence of the product/denaturant, isobutanol. While pH and temperature also affect variant performance, **Figs. 10** and **11** show little difference in activity retention between usable variants. Isobutanol-water mixtures undergo phase separation at concentrations greater than 10% (v/v), so the final measurement in **Fig. 9** includes a sample with two phases, one 10% and the other 87% isobutanol, with the total isobutanol concentration being 20%[70]. $KIVD_{LLM4}$ variant and its fusion variant, MBP-$KIVD_{LLM4}$, show strong stability in isobutanol, remaining active even during the phase separation, while wild type and its fusion variant show weak isobutanol stability,

decreasing steadily over the range tested. For the KIVD fusion proteins, there is crossover in activity between 5 and 10% isobutanol, with the mutant MBP-$KIVD_{LLM4}$ overtaking MBP-$KIVD_{WT}$. As this process is focused on the production of isobutanol, utilizing an enzyme that is stable in isobutanol is essential. Despite being 50% less active than the wild type variant at 0% isobutanol concentration, the MBP fusion variant of $KIVD_{LLM4}$ was chosen for the final reaction due to its stability to isobutanol.

ADH was more straightforward for analysis. ADH_{29C8} was several times more active than the wild type across the isobutanol concertation range and was the clear choice for the final reaction. FDH_{WT} was also straightforward for analysis. Both variants were stable across the isobutanol range. Even during the phase separation, the wild type retained about 100% of its activity, while the FDH_{K328V} variant retained about 70% activity. Given the trend of better performance at higher isobutanol concentrations, FDH_{WT} was chosen for the final reaction. ADH_{29C8} retained less activity compared to $KIVD_{LLM4}$ and FDH_{WT}, but this can also be attributed to isobutanol having dual effects on activity, denaturing and causing product inhibition, as higher concentrations of isobutanol will inhibit further production. Despite these issues ADH_{29C8} was still quite active at moderately high isobutanol concentrations (> 1%), and along with MBP-$KIVD_{LLM4}$ and FDH_{K328V}, was used for the immobilized reaction scheme. The next stability screening carried out was temperature stability.

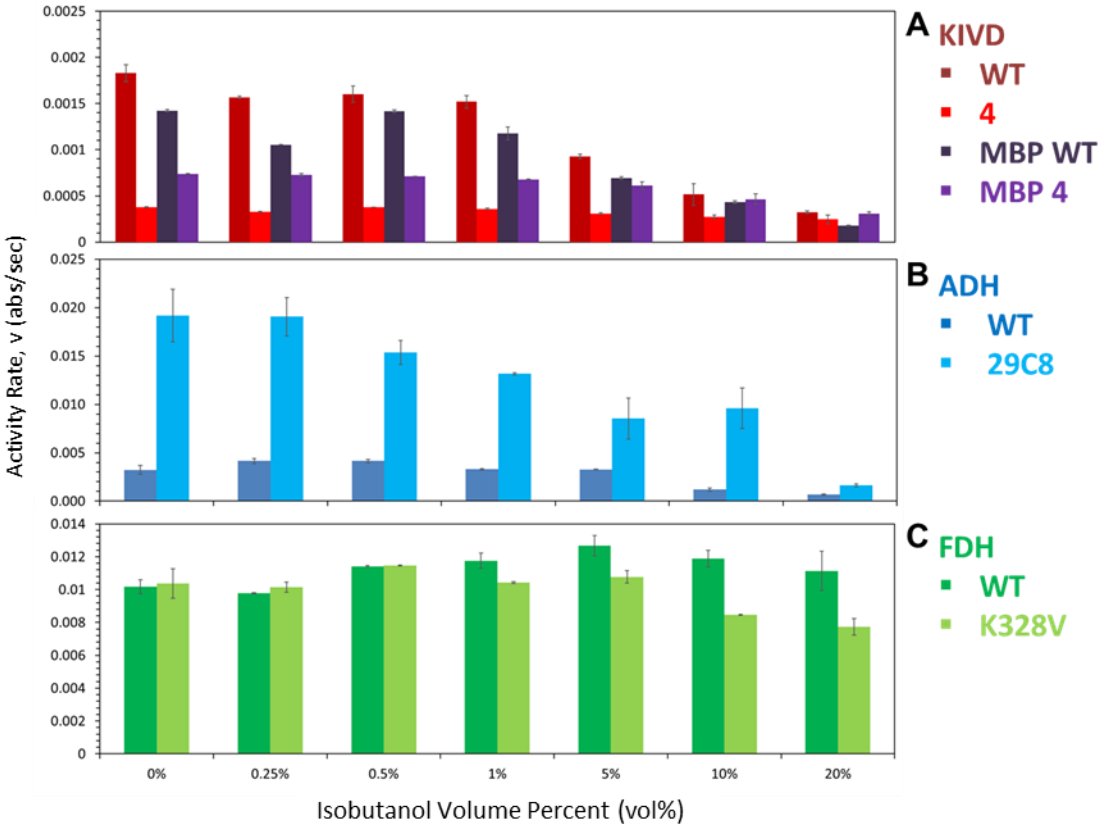

Figure 9: Enzyme isobutanol stability. (A) $KIVD_{WT}$, $KIVD_{LLM4}$, MBP-$KIVD_{WT}$, and MBP-$KIVD_{LLM4}$. (B) ADH_{WT} and ADH_{29C8} (empty). (C) FDH_{WT} and FDH_{K328V}. The 20% concentration is phase separated into two phases with isobutanol concentrations of 10% and 87% (v/v).

2.3.5 Temperature Stability Enzyme Screening

The temperature stability of the enzymes is shown in **Fig. 10**. $KIVD_{WT}$ was remarkably heat stable, with $KIVD_{LLM4}$ variants remaining active after one hour of incubation up to 65°C. The wild type had a more rapid decline in activity compared with $KIVD_{LLM4}$ which was expected based on previous reports[45]. There was a noticeable difference between $KIVD_{LLM4}$ and its MBP fusion variant, but this could be attributed to MBP's own heat stability which has a melting temperature between 60-65°C[71-72]. The two variants of $KIVD_{WT}$ and $KIVD_{LLM4}$ were largely in line with their fusion counterparts up to 60-65°C, after which a sharp decrease for the fusions

was observed. Given this result, a maximum operating temperature of 60°C is recommended for $KIVD_{WT}$.

ADH was noticeably less heat stable than KIVD, with the enzyme retaining activity only up to 35°C and the variant ADH_{29C8} retaining most of its activity compared with the wild type losing greater than 50%. This activity seems quite low; however, *L. lactis* has been shown to have optimum growth between 30-35°C[73-74] which would explain the rapid loss of activity at higher temperatures. FDH_{WT} was remarkably heat stable, like KIVD. Both the wild type and the FDH_{K328V} retained most of their activity after one hour until 60°C. This is slightly better than expected given that the thermal inactivation temperature for both was previously described as being around 55°C[53]. With these results, 60°C would be the recommended operating temperature for FDH_{WT}.

With $KIVD_{WT}$ and FDH_{WT} in agreement with regards to temperature, ADH_{WT} became the limiting enzyme. A temperature of 35°C was chosen, pushing ADH to the limit of its thermal stability, while both FDH and KIVD were comfortably stable. The next condition that was screened was pH.

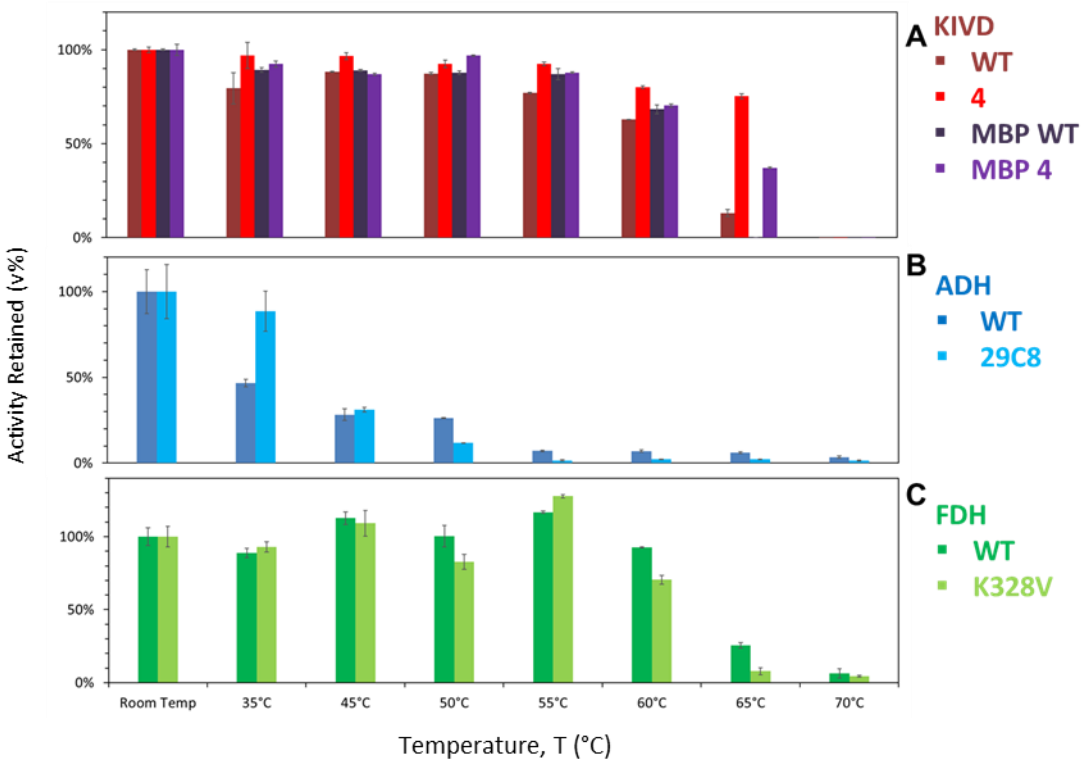

Figure 10: Enzyme temperature stability. The resulting activity was normalized by the room temperature result. (A) KIVD$_{WT}$, KIVD$_{LLM4}$, MBP-KIVD$_{WT}$, and MBP-KIVD$_{LLM4}$. (B) ADH$_{WT}$ and ADH$_{29C8}$. (C) FDH$_{WT}$ and FDH$_{K328V}$.

2.3.6 pH Stability Enzyme Screening

Using the methods described above, enzymes were screened for pH stability as seen in **Fig. 11**. Although 35°C was found to be an optimum operating temperature, for consistency with the isobutanol stability, pH screening was conducted at 25°C. All variants of KIVD, pI 5.3[68], favored acidic conditions, and were stable between pH 5-7.4, with the optimum pH being between 5.5 and 6. At more basic conditions, from pH 8 upwards, KIVD$_{WT}$ and its variant, MBP-KIVD$_{LLM4}$, exhibited rapid decrease in activity. FDH$_{WT}$, pI 5.4, was incredibly pH stable, retaining activity across the entire pH range except the most basic condition, at pH 9. ADH, pI 5.2[68], showed the most divergence between wild type and variant. The wild type was stable between pH 5-7.4, with the apparent optimum being at pH 6. ADH$_{29C8}$ was most stable between

pH 6-8, with the apparent optimum being pH 7.4. FDH_{WT} and FDH_{K328V} were stable across the range, so the optimum pH for the combined reaction was between that optimum value for KIVD and ADH wild type and variants. The ADH_{29C8} variant was selected above as the immobilization variant so the focus was narrowed between the pHs of 6 and 7.4. As **Figs. 9-11** show, ADH_{29C8} was less stable than the MBP fusion variant of $KIVD_{LLM4}$, with reference to the 3 screening variables: it was less heat stable, less isobutanol stable, and the drop of activity from the optimum pH was much larger. Considering these factors, the physiological pH of 7.4, the optimum for ADH_{29C8}, was chosen in an attempt to retain it in more optimal conditions. With all screening of the enzymes completed, the final immobilization reaction was conducted.

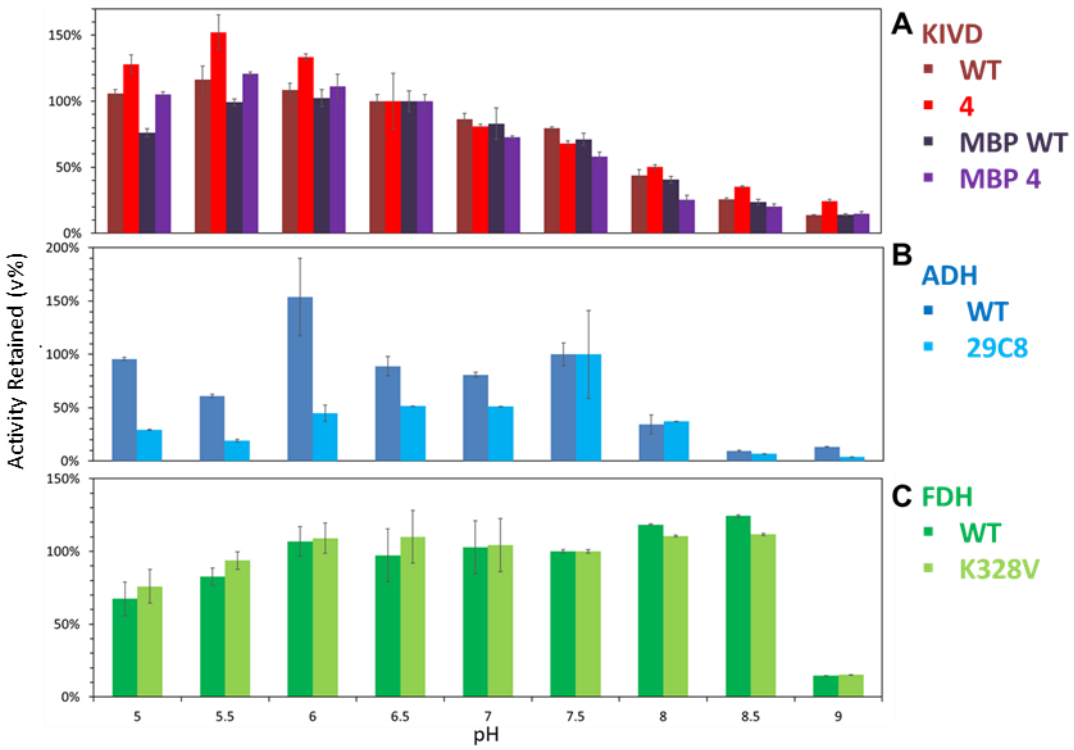

Figure 11: Enzyme pH stability. (A) $KIVD_{WT}$, $KIVD_{LLM4}$, MBP-$KIVD_{WT}$, and MBP-$KIVD_{LLM4}$. Normalized by pH 6.5. (B) ADH_{WT} and ADH_{29C8}. Normalized by pH 7.4. (C) FDH_{WT} and FDH_{K328V}. Normalized by pH 7.4.

2.4 Conclusions

Pathway enzymes and their highly active and/or stable variants were cloned into expression strains of *E. coli* and successfully expressed and purified utilizing a uniform method. The isolated enzymes were tested for activity and the wild types assayed for kinetics to compare to prior literature. The enzymes performed as expected, except for FDH which had the wild type show slightly more activity than the mutants. The fusion of MBP to KIVD both retained activity and completely avoided issues associated with self-aggregation of the enzyme. The enzymes were then tested for stability in three key parameters: isobutanol, temperature, and pH. Based on the isobutanol testing, MBP-$KIVD_{LLM4}$ was chosen as despite not being the most active, it had the strongest stability to isobutanol. ADH_{29C8} had consistently stronger activity and stability in isobutanol compared to the wild type, while FDH_{WT} surprisingly ran counter to prior literature and was both more active and stable than its mutant. KIVD and FDH were relatively stable up to higher temperatures while ADH showed considerable drop off, so a temperature of 35C was chosen to maintain key ADH activity. KIVD and FDH also showed strong stability in a pH range of 4-9, while ADH_{29C8} showed a tighter window of activity for pH, resulting in a pH of 7.4 being chosen to support the key ADH activity.

CHAPTER 3

IN VIVO TO *IN VITRO* PRODUCTION OF ISOBUTANOL

3.1 Introduction

3.1.1 Keto Acid Production

The production of the biofuel, isobutanol, is defined as starting from ketoisovalerate (KIV), an intermediate in the formation of the essential amino acid, valine. In organisms, KIV is produced from glucose[75]. A cell-free system, utilizing the entire pathway, from glucose conversion to isobutanol production, has been achieved[33], but such systems have issues. Expression and purification of each enzyme will compound the labor required[29]. Control of multiple enzymes systems is still a bottleneck, as well as optimization of these systems[76]. Each enzyme will have its own ideal operation temperature and pH, as shown previously in Chapter 2, so the larger the number of enzymes the more difficult optimization becomes. KIV is an expensive chemical, so the ability to start at glucose would be ideal. We propose to link together *in vivo* production of KIV and *in vitro* production of isobutanol, described previously in Chapter 2. This strategy reflects a pseudo co-culture method, allowing for greater flexibility in optimization and splitting the burden between the two systems[77]. Like a co-culture system it would also be modular in nature, which is a benefit since KIV has other uses, such as in therapy for kidney disaese[78]. Work on the *in vivo* system was conducted by Dr. Mamta Gupta, a visiting scholar in the Koffas laboratory. Work for final production of KIV and on the *in vitro* system will be described in this chapter.

3.1.2 CRISPR

Gupta's work for the *in vivo* aspect of this system was to utilize CRISPR-Cas9 to integrate the KIV pathway into *E. coli*. Integration of a pathway into the genome of a cell is a form of modulation that can avoid metabolic burden of plasmids and promote cell growth[79]. Unlike plasmids, a side effect of this approach is that the copy number for the genes is one; however, this has been shown to sometimes be beneficial due to the stress expressing multiple copies of a gene can have on a cell[80]. CRISPRi was used to repress the expression of the ILVE gene responsible for conversion for KIV into valine in *E. coli.* Repression utilizing CRISPR is both fast and affective, while at the same time maintaining the gene, which is essential to the metabolism of the cell[81].

3.2 Materials and Methods

3.2.1 Culture Conditions

Overnight cultures were grown in 5 ml LB Broth containing appropriate antibiotics. Antibiotic concentrations were as follows: ampicillin (Amp 100μg mL-1) and tetracycline (Tet 15μg mL-1) from Fisher BioReagents, chloramphenicol (Cm 25μg mL-1) and kanamycin (Kan 50μg mL-1) from Sigma Aldrich. 1% of the overnight culture was inoculated into 10 mL of the above modified M9 medium (6 g Na2HPO4, 3 g KH2PO4, 1 g NH4Cl, 0.5 g NaCl, 1 mM MgSO4, 1 mM CaCl2, 10 mg L-1 vitamin B1 of solution) with 20 g L-1 glucose, 5 g L-1 yeast extract and 1,000th dilution of Trace Metal Mix A5 (2.86 g H3BO3, 1.81 g MnCl2·4H2O, 0.222 g ZnSO4·7H2O, 0.39 g Na2MoO4·2H2O, 0.079 g CuSO4·5H2O, 49.4 mg Co (NO3)2·6H2O per liter solution).

3.2.2 Fed-batch Conditions

Fed-batch fermentation was performed in a 1 L stirred bioreactor (Applikon). Cells from the glycerol stock were streaked on LB plate containing chloramphenicol and tetracycline. Single colony from the fresh plate was grown overnight in 5 mL LB medium containing respective antibiotics at 37ºC and 180 rpm. Secondary culture was prepared by inoculating 1% of primary culture to 300 mL of M9 medium with 5 g L-1 yeast extract supplemented with 2% glucose and grown at 37ºC until OD600 reached to 3.0. The grown secondary culture was used as seed culture to inoculate in a bioreactor with working volume of 3L having M9 medium along with 5 g L-1 yeast extract and 2% glucose. Dissolved oxygen (DO) was maintained at 20% saturation and pH was maintained at 6.8 via the addition of 10% (v/v) NH4OH base using a PID (proportional, integral, and differential) controller. After 6 h, intermittent linear feeding of glucose solution (500 g L-1) was initiated to maintain a glucose concentration between 20 and 10 g L-1. Samples were collected at different time intervals for measuring cell density and metabolite concentration.

3.2.3 KIV Minimum Inhibitory Concentration

The minimum inhibitory concentration of *E. Coli* was measured utilizing a concentration assay where the change in OD600 was measured at set KIV concentrations after a set time. The concentration for zero change in OD600 was extrapolated from the data.

3.2.4 In Vivo to In Vitro Reaction

The reaction for the conversion of KIV to isobutanol was prepared as follows. Fermentation broth was centrifuged at 14,000 rpm at 25°C for 10 min. Supernatant was set to a pH of 7.4 by addition of NaOH. The reaction volume was 1 mL. 800 μL of supernatant was added to a 200 μL mixture of enzyme together with 1 μmol of NADH and excess formate. The reaction tube was

left shaking in an end-over-end mixer for 24 hours at 35 °C. The tube was then frozen at -20 °C until analysis.

3.2.5 Overexpression of the KIV Pathway

IPTG inducible plasmid pSA69 was a gift from Professor James Liao. The plasmid was transformed into chemically competent MG03. This newly derived strain was compared to the base strain by utilizing the prior culture conditions in 3.2.1.

3.2.6 Analytical Methods

Glucose, acetic acid, KIV, and isobutanol were detected using HPLC Agilent 1,200 series instrument (Agilent) with a refractive index detector. Analytes were separated using the Aminex HPX-87H anion exchange column (Bio-Rad Laboratories) with a 5 mM sulfuric acid mobile phase at 40°C and a flow rate of 0.5 ml min-1. Commercially purchased versions of the reagents were used for quantification of experimental samples by linear interpolation of external standard curves.

3.3 Results

3.3.1 Minimum Inhibitory Concentration

To ascertain the value in producing KIV *in vivo* as opposed to isobutanol, the minimum inhibitory concentration (MIC), or the concentration at which the cellular growth rate is equal to the death rate, for *E. coli* was calculated and compared to isobutanol. Concentrations as low as 8 g/L (1% v/v) have been observed as completely inhibiting growth of cells[82]. The calculated MIC for KIV was found to be 14.7 g/L, based on the linear interpolation found in **Fig. 12**. With KIV having a higher MIC and isobutanol being a known bactericidal agent, it would be advisable to produce KIV in *E. coli*.

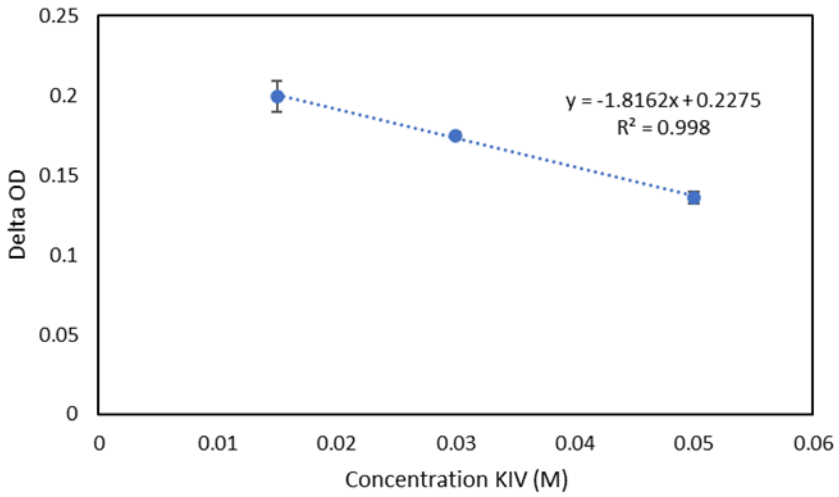

Figure 12: Delta OD600 vs concentration of KIV. Each concentration was done in triplicate. A linear interpolation based on the data is found in the graph.

3.3.2 Bioreactor Run

In a 1 L fed-batch reactor, *E. coli* cells grew for 9 h to an OD600 of 10, beyond which the culture entered stationary phase (**Fig. 13**). Most of the KIV was produced in the first 6 h with KIV yield close to the theoretical maximum. Maximum titer of KIV recorded was 5.6 g/L after 9 h of cultivation at 0.36 g/g glucose, which was 56% of maximum theoretical yield. Following hour 9, the system entered stationary phase and KIV concentration decreased. This would seem to be a result of the repression of the *ilvE* gene. As valine is an essential amino acid, the gene was not silenced, so eventually consumption of the KIV would take place. When the cells enter the death phase, valine production will lessen and so KIV begins to accumulate once more.

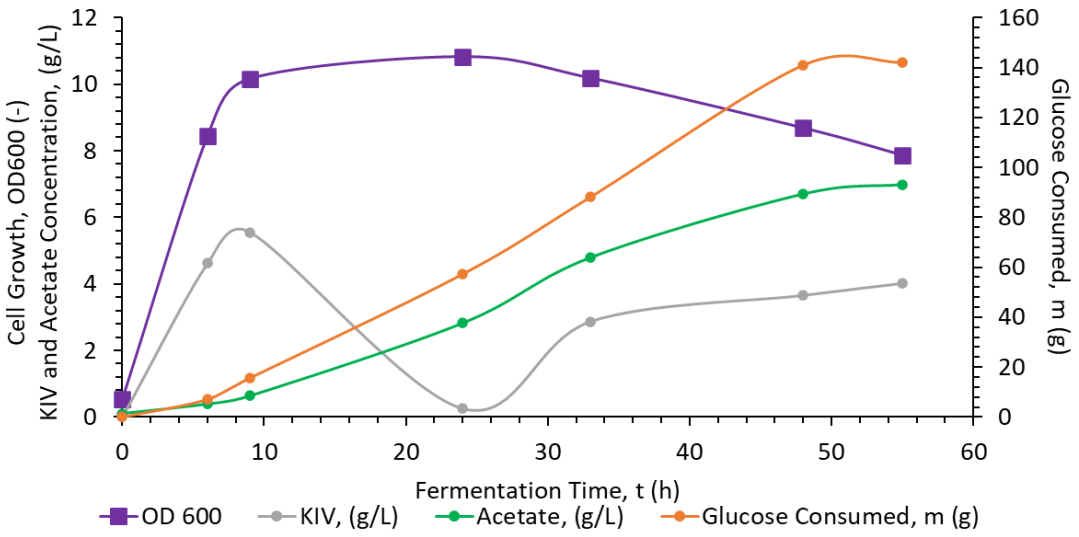

Figure 13: KIV and acetate production pattern in glucose fed batch reactor at different growth stages of MG03. OD600 (-), KIV (g/L) , and Acetate (g/L) share the left axis, while Glucose Consumed (g) utilizes the right axis.

Acetic acid production was restricted in the beginning of the reactor run due to the repression of valine synthesis. That repression slowed the growth rate of the cells, leading to less overflow metabolism and thus less acetic acid secretion[83]. Once the stationary phase was entered and nutrients became scarce, the cells switched to acetic acid production to maintain energy production. Glucose consumption held steady throughout the fermentation, but due to the fluctuating KIV concentration, conversion yield was highest in the initial production phase of KIV. Future optimization around this time point should lead to yields close to the theoretical maximum while increasing KIV titer.

3.3.3 In Vivo to In Vitro Reaction

A cell-free reaction utilizing the previously chosen pathway enzymes and operating conditions was conducted utilizing the reaction broth buffered to pH 7.4. The reaction produced an isobutanol titer of 1.78 g/L, which was a yield of 93% from the starting KIV in the reaction. This result was comparable to plasmid based *in vivo* production[13]. This result shows the viability

of this two-pronged approach as the system was easy to prepare and only required centrifugation and basic buffering of the reaction broth.

3.3.4 Copy Number

To ascertain the effect of copy number on the production of KIV, as seen in **Fig. 14**, the OD600 and concentration of KIV was tracked over a period of 10 hours for two cultures containing MG03 and the same strain with an inducible plasmid containing the KIV pathway. After 10 hours the OD600 was 0.92 ± 0.04 and 0.89 ± 0.02 respectively; KIV concentration was 2.2 ± 0.3 and 2.0 ± 0.3 g L^{-1} respectively (Fig. 6). All values were within error of each other, and further measurements at 24 hours mark showed no difference accounting for error.

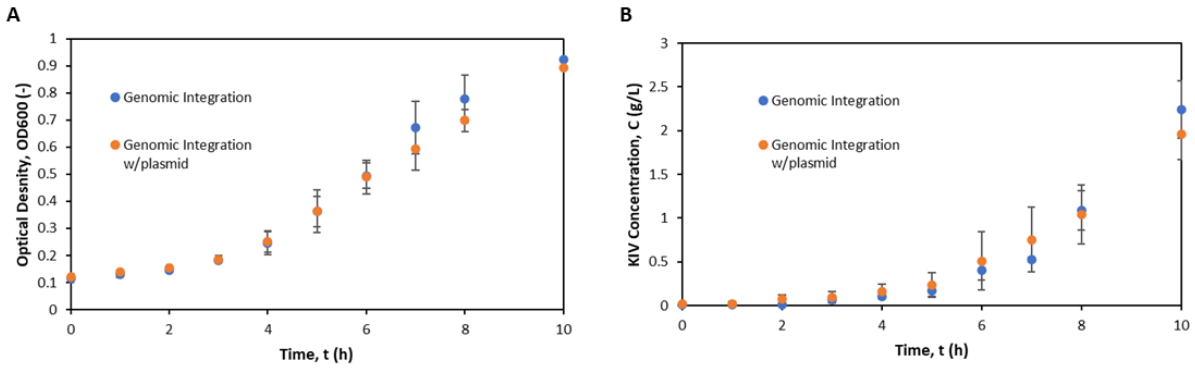

Figure 14: Copy number effect on KIV production. (A) OD of cultures grown at 37oC with and without the inducible KIV pathway plasmid. (B) KIV concentration for cultures grown at 37ºC with and without the inducible KIV pathway plasmid.

Integration of a genetic pathway has often been used to avoid the issues of natural plasmid loss during fermentation as well as high metabolic burden that can occur due to the number of copies of plasmid produced in a cell[80]. In this case a comparison between the integrated pathway strain and the same strain transformed with a low copy number plasmid containing the pathway showed no discernible difference in either growth or production. It has been shown before that a copy number as low as 1 can be the ideal for production of metabolites

in *E. Coli* so it is not surprising that the integrated strain did not need a higher copy number to improve performance[80]. Further experiments could explore plasmid with other copy numbers and further define the system in relation to copy number.

3.4 Conclusions

A novel *in vivo* to *in vitro* system was developed to produce KIV *in vivo* and then convert it to isobutanol *in vitro*, bypassing the innate toxicity of alcohol on the cells. The production of KIV utilized CRISPR-CAS9 to integrate the pathway into the *E. coli* genome, which can both avoid metabolic burden of plasmids and avoid plasmid loss overtime. Ultimately the inserting a plasmid with the pathway into this integrated strain showed no increase in production of cellular growth. KIV was produced at a titer of 5.6 g/L and a yield of 53%, while isobutanol was produced at a titer of 1.78 g/L and yield of 93%. This modular system has room for optimizations of reactor conditions, growth timing, and tuning of the cell-free aspect. The following chapters focus on one optimization, immobilization of the pathway enzymes.

CHAPTER 4

IRREVERSIBLE IMMOBILIZATION

4.1 Introduction

The study of enzyme immobilization has been around for at least a century, with early studies in the first decades of the 1900s focusing on the adsorption and activity of enzymes by charcoal[84-85]. During the 50s and 60s the current field of enzyme immobilization was established, focusing on enzyme adsorption on inorganic materials and covalent binding to organic materials, pioneered by scientists such as the forth president of Israel, Ephraim Katzir[86]. Following that time period the first case of industrially immobilized enzymes was at the Tanake Seiyaku Company, Japan, utilizing immobilized aminoacylase to obtain L enantiomer of amino acids[36]. Since then, immobilized enzymes have been adopted and widely used in industry, with for example six hundred thousand tons of high fructose corn syrup being produced in 1992 utilizing immobilized glucose isomerase[36]. For industry, immobilization of enzymes provides ease of handling, physical separation from the product to avoid contamination, reuse of enzymes, enhanced stability which reduces both time and cost, and finally capability of use in non-aqueous solutions[87]. Thus, the study of an immobilized pathway would be of great interest for industrial production of novel products.

Immobilization of enzymes consists of both irreversible and reversible techniques. The two primary irreversible techniques are covalent binding of the enzyme to a support and entrapment of the enzyme[88]. Covalent binding involves the use of functional groups on a matrix that react with, for example, amino acid residues on the enzyme of choice. Due to this binding,

Portions of this chapter previously appeared as: Wong, M.; Zha, J.; Sorci, M.; Gasparis, C.; Belfort, G.; Koffas, M., Cell-Free Production of Isobutanol: A Completely Immobilized System. *Bioresour Technol* **2019**, *294*, 122104. DOI: 10.1016/j.biortech.2019.122104

consideration of where the amino acids are on the protein, aka proximity to the active site, is essential as the enhanced stability needs to be balanced with the potential loss of activity[88]. The matrix can either be functionalized by the user or purchase prepared functionalized groups. Entrapment avoids the loss of activity associated with covalent binding by instead trapping the enzyme in a matrix, without binding. It is a fast and cheap process and can protect the enzymes from external forces but can have drawbacks with mass transfer of the reactant and product is greatly reduced. There is also encapsulation, where instead of a matrix, the enzyme is entrapped in a semipermeable membrane, which has increased surface area but the encapsulation results in enzyme inactivation[89]. This chapter will be examining the use of epoxy methacrylate resin and N-Hydroxysuccinimide (NHS) ester functionalized agarose beads, both of which were used prior in the Belfort group[44, 90].

4.1.1 NHS Ester

NHS esters are used to covalently bind proteins utilizing amine groups. The reaction is a generally a one-step aminolysis that is performed at physiological pH, with the ester either binding to nucleophilic amines or undergoing hydrolysis. This immobilization technique is commonly used for binding of antibodies[91]. A two-step version involves the use of sulfo-NHS. The resin had carboxylic groups to react with a 1-ethyl-3-(3-dimethylaminopropyl) carbodiimide (EDC) crosslinker and the water soluble sulfo-NHS to create a semi stable NHS ester that in turn could react with the enzymes[92]. Another method is to bind the EDC and sulfo-NHS to the enzyme of choice, creating a modified enzyme that can bind to an amine functionalized surface[93]. This in theory would help avoid the instability associated with the NHS, allowing for complete reaction, as well as being modular for different resins. The downside is that instead of

modifying a surface, the enzyme itself would be exposed to these linkers. This method is shown in **Fig. 15.**

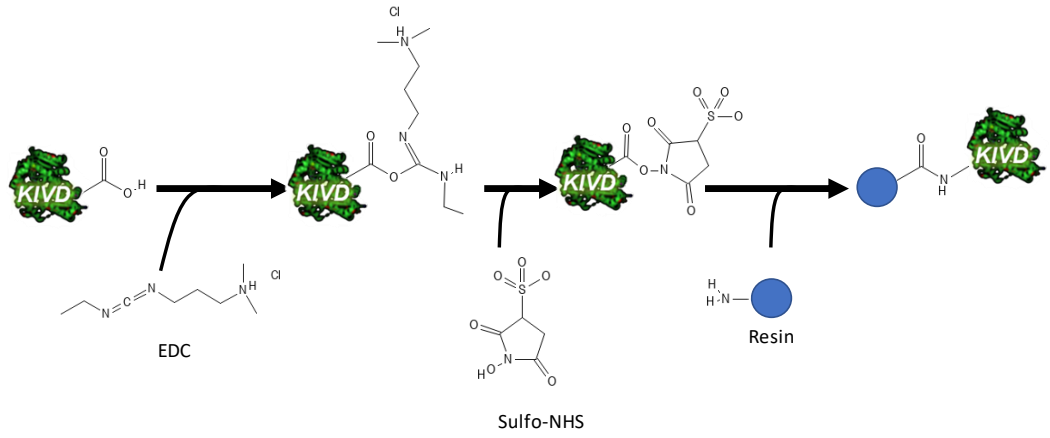

Figure 15: EDC-NHS enzyme immobilization.

4.1.2 Epoxy Resin

Epoxy resin has a similar mode of immobilization compared to NHS ester, nucleophilic attack by amine groups. The immobilization scheme utilizing epoxy resin is seen in **Fig. 16**. The difference is that while not as active, it is far more stable than NHS, stable while stored both dry and in aqueous solution[94]. Prior testing in the Belfort laboratory found that ADH immobilized well to epoxy resin, while FDH and KIVD did not. In order to immobilize the primary pathway, it was decided to genetically fuse maltose binding protein (MBP) to KIVD[44]. MBP served to both increase the stability and solubility of the KIVD[44]. The KIVD used in this study, while different from what was used previously in the Belfort laboratory, could also suffer from immobilization issues that would need to be studied before further testing as immobilization would require adsorption of the enzyme onto the resin, which would be difficult if it aggregates.

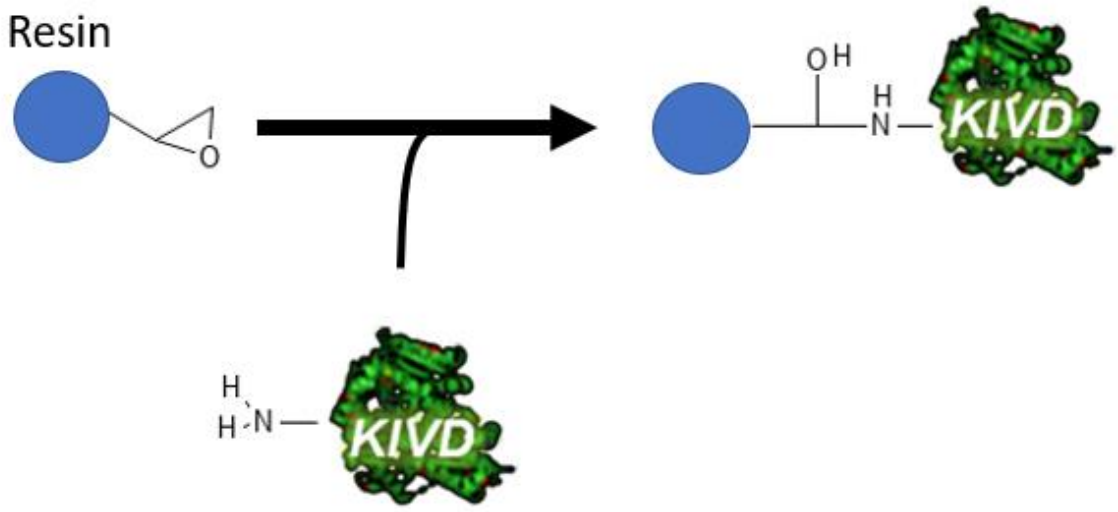

Figure 16: Epoxy enzyme immobilization.

4.1.3 Immobilized Reaction

To further expand on the system developed previously in this lab, it was decided to run a fully immobilized reaction scheme, utilizing the optimized reaction conditions and enzymes[44]. This would allow for further study of the system and for bottlenecks in the reaction to be discovered. While the enzymes can be individually assayed, the full scope of their interactions with all reagents and with each other cannot be explored until the full reaction is run. This also complicates the analysis as the primary reagents examined with a plate reader share a 340 nm peak. As such, mass spectrometry (MS) and gas chromatography (GC) would be needed to ascertain the concentration of KIV and the final product isobutanol.

4.2 Materials and Methods

4.2.1 Materials

Epoxy methacrylate resin was obtained commercially (Resindion, Rome, Italy). EDC and sulfo NHS were purchased from Thermo Fisher.

4.2.2 Enzyme Immobilization- EDC NHS

The following method was adapted from the Thermo Fisher protocol for EDC and Sulfo-NHS[93]. Phosphate buffer (PB) was prepared at pH 6 to avoid side reactions. Phosphate saline buffer (PBS) was prepared at pH 7.4. To start, 0.4 mg of EDC and 0.6 mg of Sulfo-NHS were added to 1 mL of enzyme solution that was buffer exchanged with PB buffer. This was mixed and left at room temperature for 15 mins, then buffer exchanged again, this time with PBS, to remove unreacted chemicals. The modified enzyme solution was then introduced to carboxylate functionalized resin and mixed for two hours. Following that, the resin was washed with PBS to remove unreacted enzyme and stored in PBS until further use.

4.2.3 Enzyme Immobilization- Epoxy Methacrylate

Epoxy methacrylate resin (2 mg) was hydrated with DI water in a 2 mL tube. The resin was allowed to settle, the water was removed, and 1 mL of enzyme solution was added to each tube. The resin-enzyme suspension was shaken at 4°C overnight. Following this, the resin was allowed to settle, and the supernatant removed and assayed using the Bradford assay to check concentration. The resin was then washed with DI water to remove unbound enzyme from the resin. The resin was stored in 400 μL of storage buffer.

4.2.4 Enzyme Activity Assay

Assays were conducted as described previously in Section 2.2.4, but instead of adding enzyme solution to the well, the resin enzyme solutions were resuspended and then pipetted into the well.

4.2.5 Immobilized Reaction Conditions

Immobilized enzyme resin (1 mg) for each enzyme was added to a 2 mL tube. Reagent, cofactor, and KIVD storage buffer were added to the tube to bring the total reactor volume to 1 mL (final concentration: 2 or 64 mM ketoisovaleric acid, 1 mM NADH, and 10x molar excess of formate). The reaction tube was shaken in an incubator for 24 h. Following the specified reaction time, the tubes were frozen to prevent evaporation and to stop the reaction. Ketoisovaleric acid and isobutanol quantification were conducted by MS and GC, respectively.

4.3 Results and Discussion

4.3.1 EDC-NHS vs Epoxy

To decide on which immobilization regime would be used for the final reaction, EDC-NHS and epoxy resins were compared, using ADH activity. **Fig. 17** shows the results of the immobilized activity assays.

The epoxy bound ADH showed higher activity than that of the EDC-NHS bound ADH. Given the nature of the EDC immobilization, modifying the enzyme instead of just binding it to a surface first, this isn't a completely unexpected result. The immobilization itself is also much simpler, being a one-step binding vs a two-step one that requires buffer exchange and supplemental reactants. With this in mind, epoxy was chosen as our immobilization resin of choice for the following reactions.

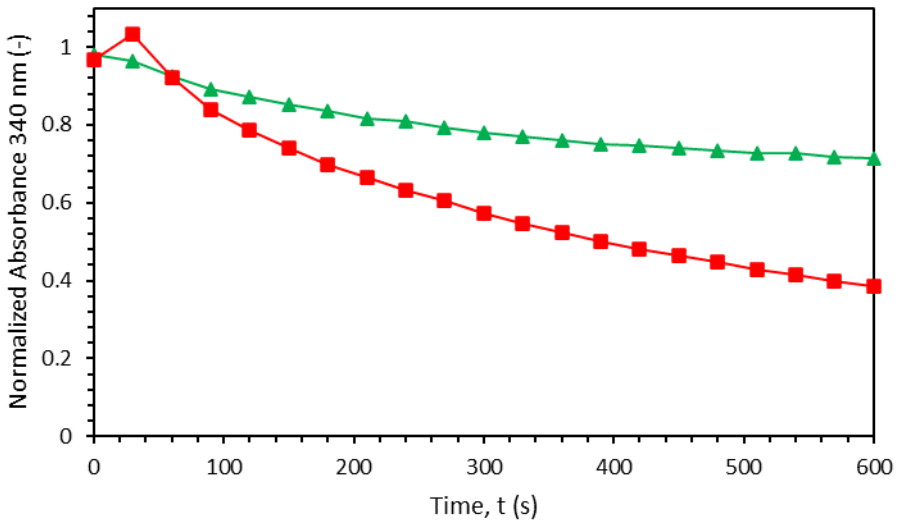

Figure 17: Wild type enzyme epoxy immobilized activity (■) vs EDC-NHS immobilized activity (▲). Absorbance over time was normalized by initial absorbance (1.82).

4.3.2 Immobilized Enzyme Activity

As $KIVD_{WT}$ was inactive when immobilized on epoxy methacrylate resin, as seen in **Fig. 18**, MBP was genetically bound to the N-terminus of the enzyme to impart greater stability and solubility, as seen previously in Chapter 2. The wild type versions of the three enzymes were immobilized onto the resin and their activity was assayed as shown in **Fig. 19**. All enzymes were successfully immobilized. Immobilized ADH_{WT} showed slightly lower activity with time of reaction in comparison with the free enzyme in solution (**Fig. 19B**). A similar trend for the concentration of NADH (i.e. absorbance) is observed. Both MBP-KIVD (**Fig. 19A**) and FDH (**Fig. 19C**) exhibited a decrease in activity when immobilized. The free solution FDH_{WT} showed a sharp increase in the absorbance corresponding to an increase in NADH, while the immobilized enzyme had a shallower slope for its concentration increase. Free MBP-$KIVD_{WT}$ showed a sharp decrease in absorbance corresponding to a decrease in concentration of ketoisovaleric acid, while the immobilized enzyme exhibited a much slower decrease in regent concentration.

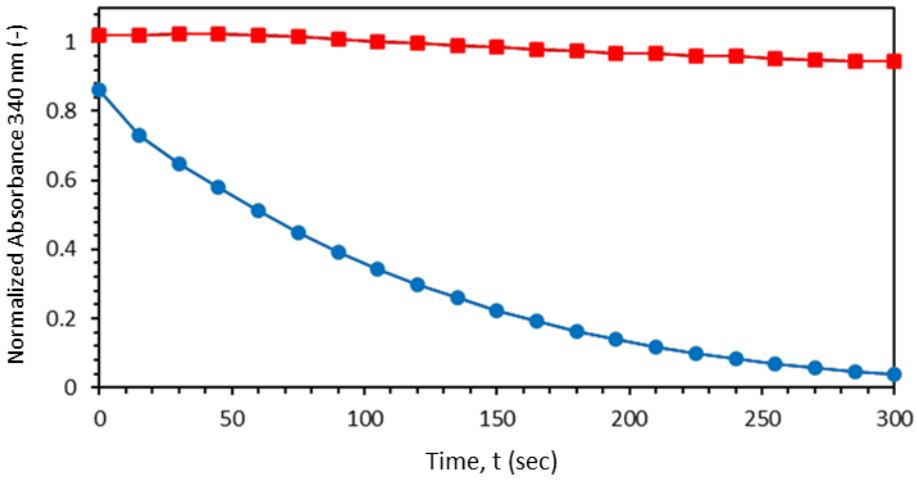

Figure 18: Wild type KIVD immobilized activity (■) vs free in solution (●). Normalized by initial absorbance (0.312).

Decreases in the activity of the immobilized enzymes can be explained primarily by the formation of the covalent bonds between the enzymes and the immobilization supports. The epoxy resin targets amine groups on the enzyme, ideally from the N-terminus, but any amino acid group with an amine group can be a target, namely lysine. All three enzymes have lysine residues in their structures, some of which are close to the active sites. If these lysine groups bind to the epoxy resin, the enzyme could be rendered inactive due to interference with the active site. This could also explain the benefit of the MBP fusion tag for $KIVD_{WT}$, as it contains lysine and can also bind to the resin, anchoring $KIVD_{WT}$ without blocking the $KIVD_{WT}$ active site. **Fig. 19** utilizes normalized absorbances, so removal of a possible resin absorbance artifact would cause a depression of the immobilized assay on all graphs, resulting in ADH_{WT} and MBP-$KIVD_{WT}$ having better activity than shown, while FDH would have lower activity. Either way, all enzymes were immobilized with activity. Prior to implementing the immobilized enzyme pathway, further testing was needed to (i) ascertain acceptable conditions for the reaction, and (ii) select the most active and stable mutant variant or wild type enzyme, which was presented in

Chapter 2. With confirmation that the enzymes could be actively immobilized and knowing that enzymes are often stabilized when immobilized[36-37], it was decided to conduct the fully immobilized reaction.

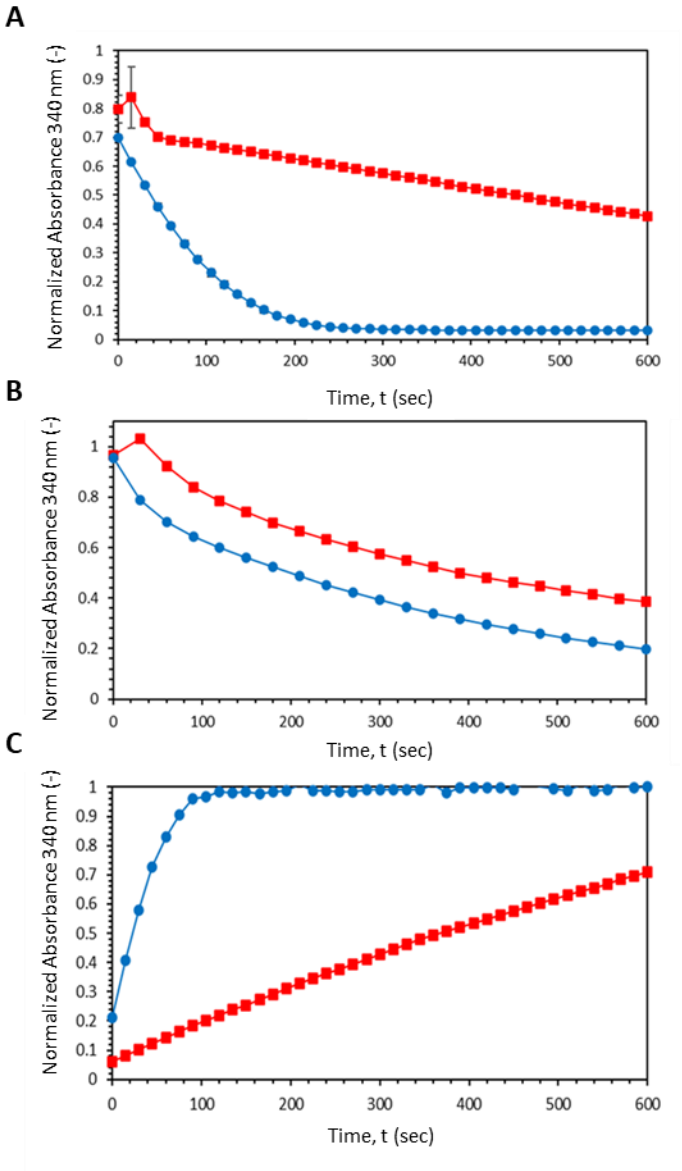

Figure 19: Wild type enzyme immobilized activity (■) vs free in solution (●). (A) MBP-KIVD normalized by initial absorbance (0.742), (B) ADH normalized by initial absorbance (1.82), and (C) FDH normalized by final free in solution absorbance (3.43).

4.3.3 Immobilized In Vitro Reaction

Table 4: Immobilized enzyme reaction scheme. The three enzymes used here were MBP-KIVD$_{LLM4}$, FDH$_{WT}$ and ADH$_{29C8}$: Reaction conditions 24 h, shaking, 35ºC, pH 7.4, 1 mL total volume, 1 µmol of NADH, excess formate.

Scale (mM)	Starting ketoisovaleric acid (mM)	Final ketoisovaleric acid (mM)	Isobutanol (mM)
2	2	Negligible	1.9±0.4
64	64	0.95	27.6±1.7

With the variants of each pathway enzyme chosen, i.e. MBP-KIVD$_{LLM4}$, FDH$_{WT}$ and ADH$_{29C8}$, two reactions were conducted to test the efficacy of the combined immobilized system seen in **Table 4**. Two initial concentrations for ketoisovaleric acid were chosen: 2 mM and 64 mM. The latter was chosen to offer a comparison to previous work from this lab that obtained an isobutanol yield of 55%[44]. The 2 and 64 mM reactions resulted in an approximately 95% and 43% yield of isobutanol from the starting reagent, respectively. The large decrease in yield with the increase in starting reagent could be the result of product inhibition on ADH. This hypothesis is supported by the fact that ketoisovaleric acid conversion to isobutyraldehyde is greater than 98% for the 64 mM reaction. To reduce product inhibition, a membrane separation unit is necessary in order to recover isobutanol from the reactor solution and push the reaction forward as was previously done[95].

The 64 mM reaction exhibited high titer (2 g/L) and yield (43%), larger than what has been reported for *in vivo* systems such as *Ralstonia eutropha*, 0.2 g/L and 5%[96], and *S. cerevisiae*, 0.635 g/L and 2%, as detailed in **Table 5**. This is promising in terms of having both (i) a large titer, comparable with the high performing in vivo systems reported, i.e. *Clostridium*

thermocellum and *Geobacillus thermoglucosidqsius* with titers of 5.4 and 3.3 g/L, respectively, and (ii) a high yield, comparable with other in vitro schemes[33, 44]. This also confirms the system's capability for isobutanol production comparable with in vivo systems without the concerns for cellular growth and maintenance.

One issue that arises from the comparisons is that the yield and titer are less than those this group has previously reported for the same system with incomplete immobilization[44]. The key difference is that in the previous work FDH was not immobilized and kept free in solution. Thus, the enzyme would not be constrained to the resin and would be well mixed in the reactor. Immobilization is key to the scheme as this would facilitate efficient subsequent purification using membrane separation of the reaction broth. Having an enzyme in the solution would result in protein fouling of the membrane, reducing efficiency of the separation and the capability for production of isobutanol. With the immobilized system, one could either genetically fuse the enzymes or bind the enzymes on the same scaffold, reducing diffusional limitations and increasing the local intermediate concentration[97-99]. There is also the consideration of the amount of resin used. 100 mg of resin for KIVD and ADH were used in an earlier study[44], while this current reaction used only 1 mg of resin for each enzyme, resulting in a more efficient production of isobutanol. This was due to selecting greater active mutant enzymes that enhanced the activity of the pathway reactions.

Table 5: Isobutanol production *in vivo* and *in vitro.* (*) Reaction was partially immobilized: ADH_{WT} and MBP-$KIVD_{WT}$ immobilized, FDH_{WT} free in solution

Host Cell	Substrate	Titer (g/L)	Yield (%)	Reference
In vivo				
C. thermocellum	Cellulose	5.4	41	([100])
G. thermoglucosidqsius	Glucose	3.3	22	([101])
	Cellobiose	0.6	8	
R. eutropha	Fructose	0.2	5	([96])
S. cerevisiae	Glucose	0.635	2	([102])
In vitro				
Free in solution	Glucose	0.76	53	([33])
Immobilized*	Keto acid	2.59	54	([44])
Immobilized	Keto acid	2	43	(This work)

4.4 Conclusions

Successful immobilization of each pathway enzyme was carried out, with minimal loss of activity for the primary pathway enzymes MBP KIVD and ADH, and substantial loss for the recycling enzyme FDH. A complete immobilized reaction was conducted under optimized conditions and with the best performing enzymes. The immobilized reaction produced a yield of 43% and a titer of 2 g/L. This result was comparable to prior results both *in vivo* and *in vitro*. There are possible methods to improve this titer and yield further, which will be discussed in the next section, including use of an improved immobilization regime.

CHAPTER 5

COHESIN AND DOCKERIN SCAFFOLD

5.1 Introduction

With a titer of 2 g/L and 43% yield, the complete immobilized cell-free system has proven to be an effective producer of isobutanol, but yield can be improved. ADH, and not FDH, is the limiting enzyme in this process despite having lower kinetics, for two reasons: the cofactor formate is provided in excess for FDH driving the reaction forward, hence FDH is not limiting, and ADH loses activity with increasing isobutanol and temperature compared with FDH, which remains stable. One solution would be substrate channeling, where instead of having the aldehyde in equilibrium with the bulk solution, its concentration could be raised in the presence of ADH, driving the conversion to isobutanol forward, while also lowering the diffusion length for the intermediate, to reduce the Damköhler number and thus diffusion limitations[103]. Channeling thru utilization of a scaffold instead of epoxy resin, results in a more specific immobilization with the enzymes ordered for optimized reactions[104-105]. The type of scaffold binding examined in this chapter was a dockerin-cohesin affinity pair.

5.1.1 Affinity Binding

Affinity binding is an example of reversible immobilization[88]. Unlike an irreversible immobilization like covalent binding to epoxy, affinity interactions are reversible. Despite enhanced enzymatic stability in irreversible immobilization, over time enzyme activity will decrease as the enzyme denatures. By allowing for detachment, fresh enzyme can be substituted in without need to dispose of the prior resin or binding surface, allowing for use of more expensive supports[88]. A previous example of this was seen in Chapter 2 with the HIS affinity tag

purification. Another advantage is by targeting one specific point on the enzyme, one can avoid immobilization binding that interferes with the enzyme's folding or binding pocket[106-107]. The major disadvantage of affinity is the usual high cost of ligand, such as in antibody binding[108].

5.1.2 Cohesin and Dockerin

The specific affinity binding examined for immobilization of the isobutanol producing pathway was a combination of three dockerin-cohesin pairs. This affinity pairing is utilized by cellulolytic bacteria for the solubilization of cellulosic substrates. Scaffoldins are composed of cohesion domains and a separate subunit that binds to cellulose, a cellulose-binding-domain (CBD). Enzymes bind to the scaffoldin cohesin utilizing a docking domain, known as a dockerin[109]. In general affinity pairing, while specific binding of the enzyme at the affinity tag would be expected, ordering multiple different enzymes would be difficult on the same surface. For example, a HIS tag system would have no way to properly channel the substrate as each enzyme would bind randomly to the resin, with the possibility of crowding and interactions favoring one tagged enzyme over another. The cohesin and dockerin pairing has a solution to this, where cohesin-dockerin pairs have specificity, with dockerin binding to the specific cohesin of their own bacterial species and generally ignoring those from another species[110]. The interaction is known to have very high affinity, with dissociation constant (Kd) values between 10^{-8} to 10^{-11} M[111], which is comparable to antibodies[112]. Use of dockerin-cohesin for substrate channeling is a known quantity[113], with the system having been used for yeast display production of methanol[105] as well as cell-free production of fructose 6-phosphate[114], 1-3-Propanediol[115], and xylonic acid[116]. To our knowledge, this system has not been utilized for cell-free production of isobutanol. The Bayer group at the Weizmann institute has long studied this affinity intereaction[117], and provided their expertise as well as materials for this next step in isobutanol

production. In this case, they provided a thermally stable cohesin scaffold, Scaf GTV, and its corresponding dockerins[118]. The proposed system is shown in **Fig. 20.**

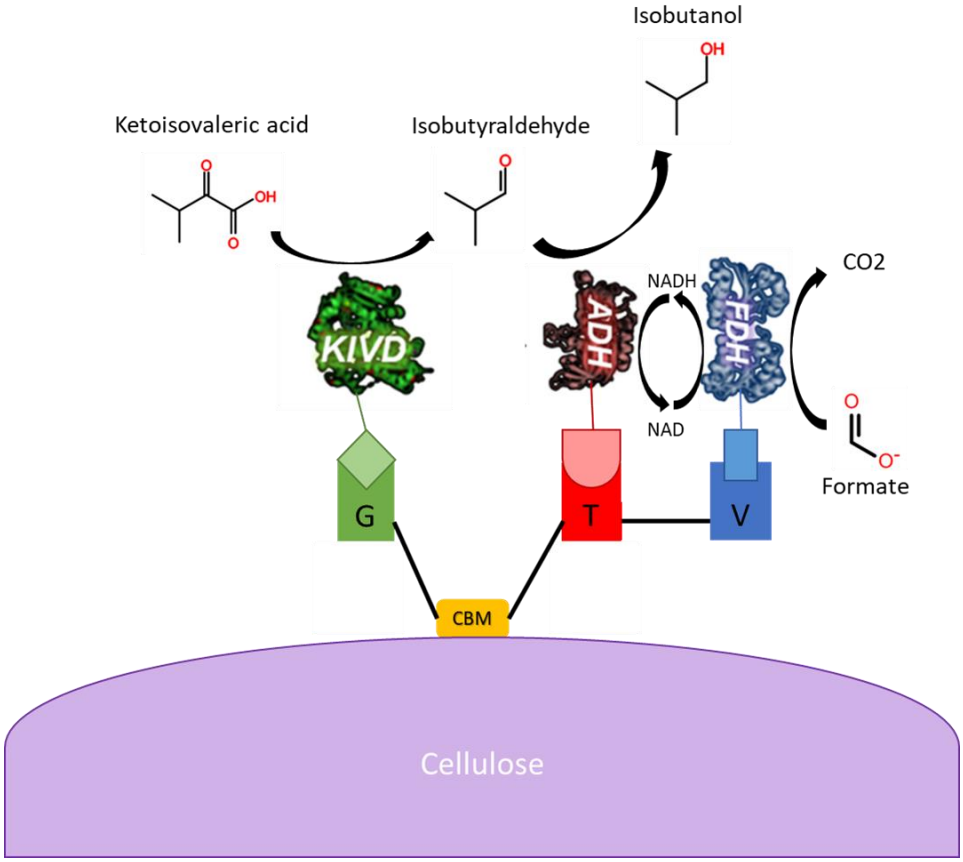

Figure 20: Cell-free production of isobutanol on a scaffold-CBM: cellulose binding module; G, T, V denote cohesin from *A. fulgidus, C. thermocellum,* and *C. clariflavum* respectively; enzymes are shown in monomer form for ease of visualization.

5.2 Materials and Methods

5.2.1 Materials

Cellulose was provided by Asahi Kasei America (New York City, New York). pET9d containing dockerin from *C. thermocellum* (doc T), pET28a containing dockerin from *A. fulgidus* (doc G), pET28a containing dockerin from *C. clariflavum* (doc V), and pET9d containing cohesin scaffold corresponding to the aforementioned dockerin (Scaf GTV) were provided by the

Bayer lab at the Weizmann institute, Rehovot, Israel. Dockerin linker gBlocks were purchased from IDT. NEBuilder was purchased from New England Biolabs.

5.2.2 Fusion Enzyme Assembly

Each pathway enzyme that was chosen for the prior pathway reaction was fused to a dockerin at either the enzyme's N-terminus, utilizing a rigid linker (EAAAK)3, or the C-terminus utilizing the natural linker associated with each dockerin. The primers used for the cloning are listed in the following **Table 6**. The N-terminal fusion of FDH_{WT} was further engineered: adding a stop codon between the enzyme and its stop codon at the C-terminus; adding a HIS tag at the N-terminus of the fusion, and replacing the (EAAAK)3 linker with a short and long linker sourced from the Bayer lab[119]. Primers for this design are listed in **Table 7**. Each plasmid was transformed into BL21(DE3). Plasmids containing ADH and FDH fusion were further transformed into Solu BL21, pGro7, and pLysS to aid in expression.

5.2.3 Expression

Expression was conducted in the same manner as described in Chapter 2 for MBP $KIVD_{LLM4}$ fusions. Fusions of ADH_{29C8} and FDH_{WT}, as well as the scaffold GTV were expressed using an alternative method of shaking at 16°C overnight[118].

Table 6: Primers for assembly of fusions. Primers purchased from Integrated DNA Technologies (Coralville, Iowa).

Protein	Primer	Sequence	Melting Temp °C[a]	GC%
Doc T ADH	Forward	AAGAAGGAGATATACATATGCCAGAAAGCAGCAGC	59	43
	Reverse	ACTACTGCTGCTTTCATATGGGCGCGCCATTTCGC	61	54
ADH Doc T	Forward	TATATACTCGAGCCAGAAAGCAGCAGCG	56	50
	Reverse	CAAATTTCCTGTAGCAGAAAATCCTCTCGAG	56	42
Doc G MBP KIVD	Forward	TGCCGCGCGGCAGCCATATGCCAGAAGAAGC	61	65
	Reverse	CCTTCTTCGATTTTCATATGGATTTTGGCGCGCCATTTCG	60	45
MBP KIVD Doc G	Forward	TTGCTGAACAAAATAAATCACCAGAAGAAGCAAACAAGGGAG	59	38
	Reverse	TATTTGATGCCTCTAGATTACTCGAGCTTACCCAGTAAGCC	59	44
Doc V FDH	Forward	AAGAAGGAGATATACATATGTCTAGAGATCTGCGGTACCGTCTC	50	43
	Reverse	ACTAAAACGATCTTCATATGGGCGCGCCATTTCGC	61	49
FDH Doc V	Forward	AACACGATAAGAAACTCGAGAGATCTGCGGTACCGTCTC	59	49
	Reverse	GTGGTGGTGGTGCTCGAGTTGTTCTTCAACTGGGAATAAGGATATTTTTCC	55	45

Table 7: Primers for Doc V linker FDH design. Primers purchased from Integrated DNA Technologies (Coralville, Iowa).

Purpose	Primer	Sequence	Melting Temp °C[a]	GC%
Stop insertion	Forward	CACGATAAGAAACTCGAGTGACACCACCACC	56	52
	Reverse	GGTGGTGGTGTCACTCGAGTTTCTTATCGTG	56	52
HIS insertion	Forward	CTTTAAGAAGGAGATATACATATGTCTAGACACCAC	59	36
	Reverse	ATAAATTTATGAGACGGTACCGCCAG	59	42
Linker insertion	Forward	GTACTCGGAAAAATATCCTTATTCCCAGTTGAAG	60	38
	Reverse	GCGTGTTTACCAGCATCATATAAGACTAAAACG	61	39

5.2.4 Purification

Purification of HIS tagged fusion enzymes was conducted as described previously in Chapter 2. The scaffold GTV was purified using the following adapted protocol[120]. Tris-buffered saline (TBS) was prepared with the following concentrations: 137 mM NaCl, 2.7 mM KCL, and 25 mM Tris-HCl, at pH 7.4[120]. The cellulose inserted into a gravity column and washed with six column volumes of TBS. The scaffold containing cells were lysed as previously described, with TBS instead of buffer A, and left shaking with the washed cellulose overnight. Afterwards the flowthrough was collected, and the cellulose was washed with six volumes of TBS, followed by six volumes of 1M NaCl TBS, and then finally six volumes of TBS again.

5.2.5 Activity Assays

Activity assays were conducted in ninety-six well plates. 50 µL of KIVD and FDH enzymes or 1 µL of ADH enzyme were added to the well. For KIVD enzymes, 2 mg of KIV was

utilized. For ADH enzymes, 200 µM of NADH was utilized as well as excess isobutanol. For FDH enzymes, 0.25 mg of NAD was utilized as well as excess formate. Total well volume for each assay was 200 µL. The microplate reader was used as described previously.

5.2.6 Binding Experiments

To determine if the fusions would bind to the cohesin scaffold, 400 mg of cellulose with bound Scaf GTV was inserted into a tube and left in contact with 1 mL of a 50% stock enzyme mixture and left over shaking overnight at 4°C. The 50% mixture as well as the post shaking retentate, obtained by centrifuging the tube, was examined using SDS-PAGE to gauge if binding occurred.

5.2.7 Complete Immobilization

A three-enzyme bound scaffold was constructed utilizing the following: 500 mg of cellulose with bound Scaf GTV was deposited into a 5 mL tube. It was then shaken overnight at 4°C with a 4.5 mL mixture of three enzymes, MBP $KIVD_{LLM4}$ Doc G, ADH_{29C8} Doc T, and Doc V Long FDH_{WT}, at equal volumes. The equal volume mixture of enzymes, as well as the post shaking retentate was examined using SDS-PAGE to ascertain if binding occurred.

5.2.8 Immobilized Reaction

Following binding of the enzymes to the scaffold, the cellulose was washed with storage buffer, shaken, centrifuged, and then decanted to remove excess unbound enzyme. A 3 mL mixture containing 102 µmol of KIV, 4 µmol of NADH, and a tenfold excess of formate was pipetted into the 5 mL tube and then left shaking for 24 hours at 37°C. Following that, the tube was centrifuged, and a pipette was used to remove the supernatant which was analyzed using HPLC.

5.3 Results

5.3.1 Expression of Dockerin Fusions

As seen in **Fig. 21**, the initial expression of dockerin fusions was only successful with MBP KIVD Doc G fusions. The cohesin scaffold also binds quite well to the cellulose, with the band disappearing from the lysis and not washing out. FDH and ADH fusions had no noticeable bands that would indicate successful expression. This is not a completely unexpected result when dealing with fusion proteins. Fusion proteins may be toxic to the cell and hinder expression. Fusion proteins may also misfold and aggregate. In fact, that appears to be the issue, as seen in **Fig. 22** with the ADH N-terminal fusion of doc T. The lysed extract does show an expression band corresponding to ADH doc T (52 kDa).

A solution suggested by the Bayer laboratory to this issue of solubility was to run the expression at a lower temeprature[118, 121], slowing expression and avoiding misfolding. Another solution was to utilize cell lines that specialize in expressing troublesome recombinant proteins, which in this work were BL21(DE3) pLysS, BL21(DE3) pGro7, and SoluBl21. pLysS is a plasmid which expresses T7 lysozyme, which is known to inhibit basal expression, enabling better expression of proteins which utilize T7 RNA polymerase[122]. pGro7 is a plasmid that expresses additional chaperones, which aid in folding and can help prevent protein aggregation[123]. Finally, SoluBL21 is an engineered BL21 strain designed for expression of proteins with poor solubilty[124]. Low temperature expression utilizing these cell lines was performed to assess viability of fusions expressed.

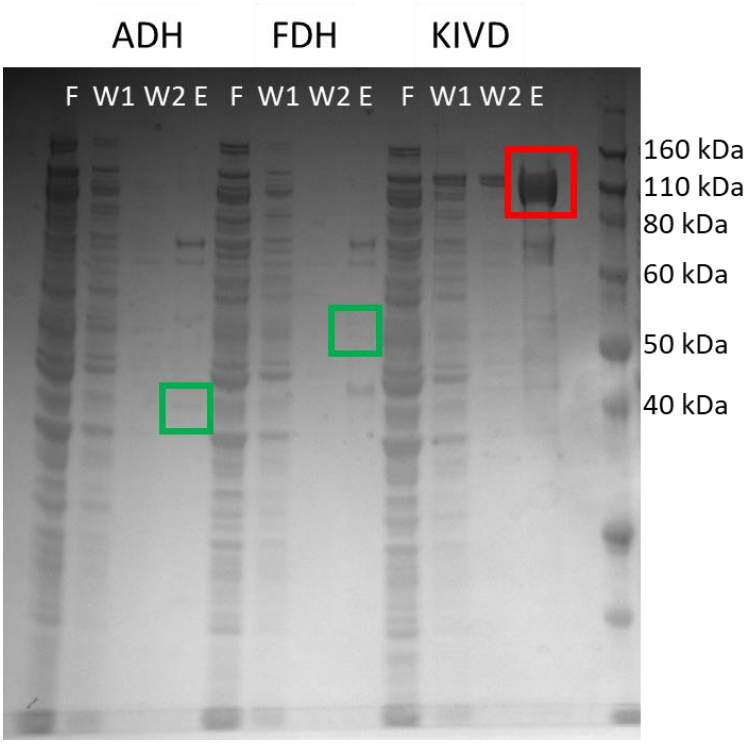

Figure 21: SDS-PAGE gel of N-terminal dockerin fusion enzymes. F: flowthrough, W#: wash number, E: elution. Purified band highlighted with red box. Theoretical location of purified bands highlighted with green box. MBP KIVD$_{LLM4}$ Doc G is 115 kDa, ADH$_{29C8}$ Doc T is 45 kDa, and FDH$_{WT}$ Doc V is 50 kDa.

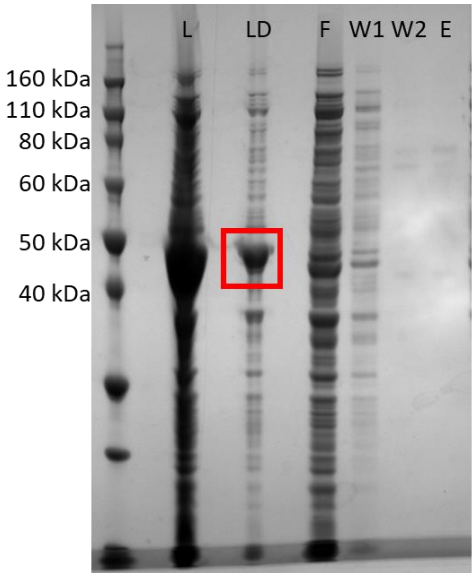

Figure 22: SDS-PAGE gel of dockerin N-terminal ADH Doc T. L: Lysate, LD: diluted lysate, F: flowthrough, W#: wash number, E: elution. Expressed band highlighted with red box. ADH Doc T is 45 kDa.

As seen in **Fig. 23**, all three cell lines were able to express the protein of interest, ADH_{29C8} Doc T. To differentiate the options, an activity assay was conducted in **Fig. 24** to compare their activities. pGro7 showed no activity, while both SoluBL21 and pLysS were active. While SoluBL21 produced more active enzyme per unit, pLysS expressed far more enzyme and thus the potential total activity for each batch was higher. Thus, pLysS was chosen for further low temperature expressions. The other troublesome fusions were examined with pLysS, but only the N-terminal fusion of Doc V FDH_{WT} was viable. With at least one fusion expressing for each pathway enzyme, work could then be pursued to ascertain if the enzymes were active.

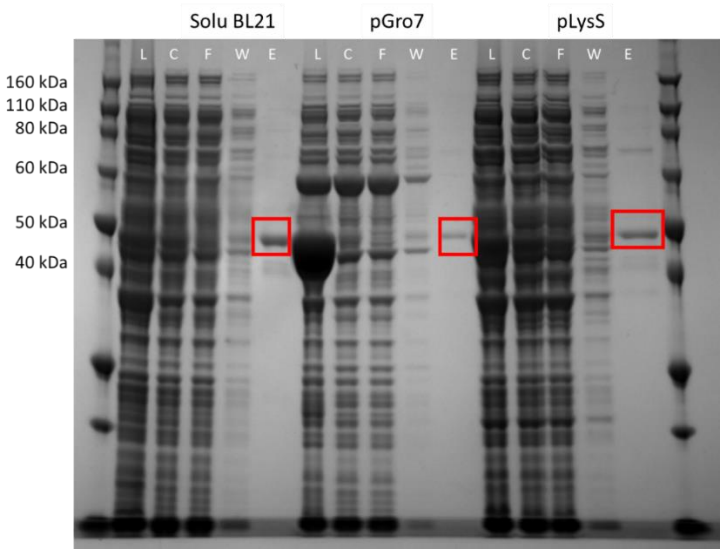

Figure 23: SDS-PAGE gel of dockerin N-terminal ADH Doc T in different cell lines. L: lysate, C: clarified lysate, F: flowthrough, W: wash, E: elution. Expressed band highlighted with red box. ADH Doc T is 45 kDa.

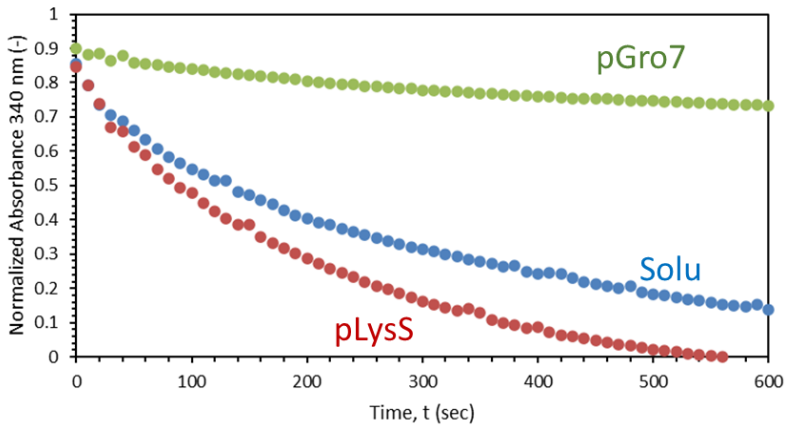

Figure 24: ADH Doc T activity assay. Absorbance normalized by initial NADH absorbance.

5.3.2 Fusion Activity

Fusion activity compared to the free in solution wild type is shown in **Fig. 25**. The N-terminal fusion of Doc G to MBP $KIVD_{LLM4}$ showed little to no activity, which could be related to the weaker expression of the fusion compared to the C-terminal fusion. Both KIVD and ADH C-terminal fusions were as active as their non-fused forms, a good result for future production of isobutanol given these are the primary pathway enzymes. Doc V FDH_{WT} showed activity but was much lower than that of FDH_{WT}. Interestingly despite showing excellent stability in chapter 2, FDH_{WT} struggles with fusion to the dockerin. Since FDH is only the recycling enzyme, it was decided to go forward with the immobilization tests.

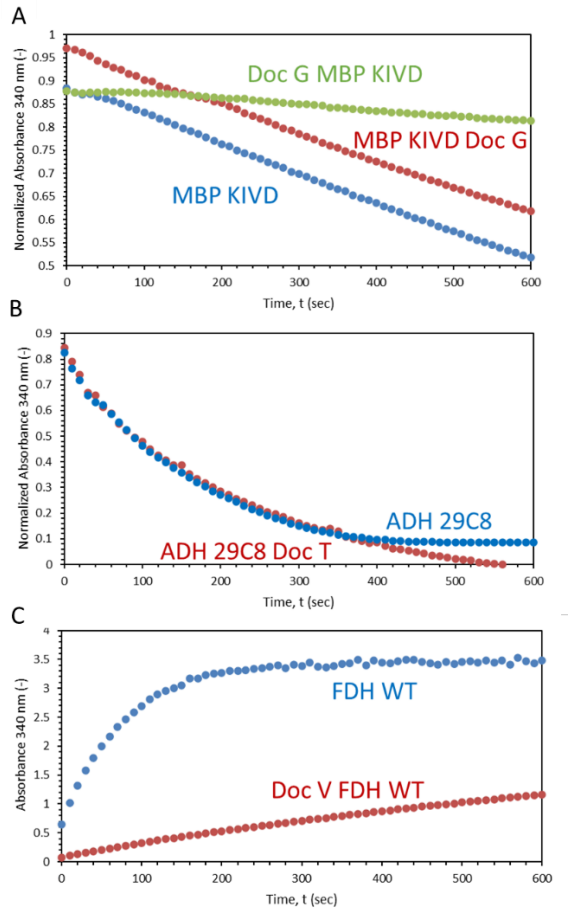

Figure 25: Enzyme activity assays. (A) Comparison of fused and non-fused MBP KIVD$_{LLM4}$ variants. Position of Doc G in label denoted position in fusion. Absorbance normalized by initial ketoisovaleric acid absorbance; (B) comparison of fused and non-fused ADH$_{29C8}$ variants. Absorbance normalized by initial NADH absorbance; and (C) comparison of fused and non-fused FDH$_{WT}$.

5.3.3 Binding to Cohesin Scaffold

Fig. 26 shows the gels for serial dilutions for the initial binding experiments of the dockerin fusions to the cohesin scaffolds. Both KIVD and ADH bound to the cohesin scaffold, as shown by the disappearance of the corresponding band in the retentate. This was a promising result when coupled with the earlier high activity of the fusions, highlighting great potential for the system. Unfortunately, the Doc T FDH$_{WT}$ fusion had issues binding. The clearest band of FDH did not bind to the scaffold; this band was utilized as proof of expression earlier, but this

was a mistake. It was assumed general differences in how proteins will run on the gel explained why the band was slightly below 50 kDa, while Doc T FDH_{WT} should be around 52 kDa. Here in this binding experiment, you can see a faint band in the page gel, just above 50 kDa that vanishes post binding. This points to an issue with the EAAAK linker; a possible cleavage is occurring. Because the wild type enzyme has the HIS tag at the C-terminus, if cleavage occurred, what is essentially FDH_{WT} with a small N-terminal tag would be purified by the nickel resin, resulting in the large bright band below the light fusion band. It was suggested by the Bayer lab to redesign the FDH fusion utilizing a linker known to work with dockerin. These linkers, which didn't improve performance of the enzymes in the prior work, had no negative effects and could be a better choice than the rigid linker chosen[119].

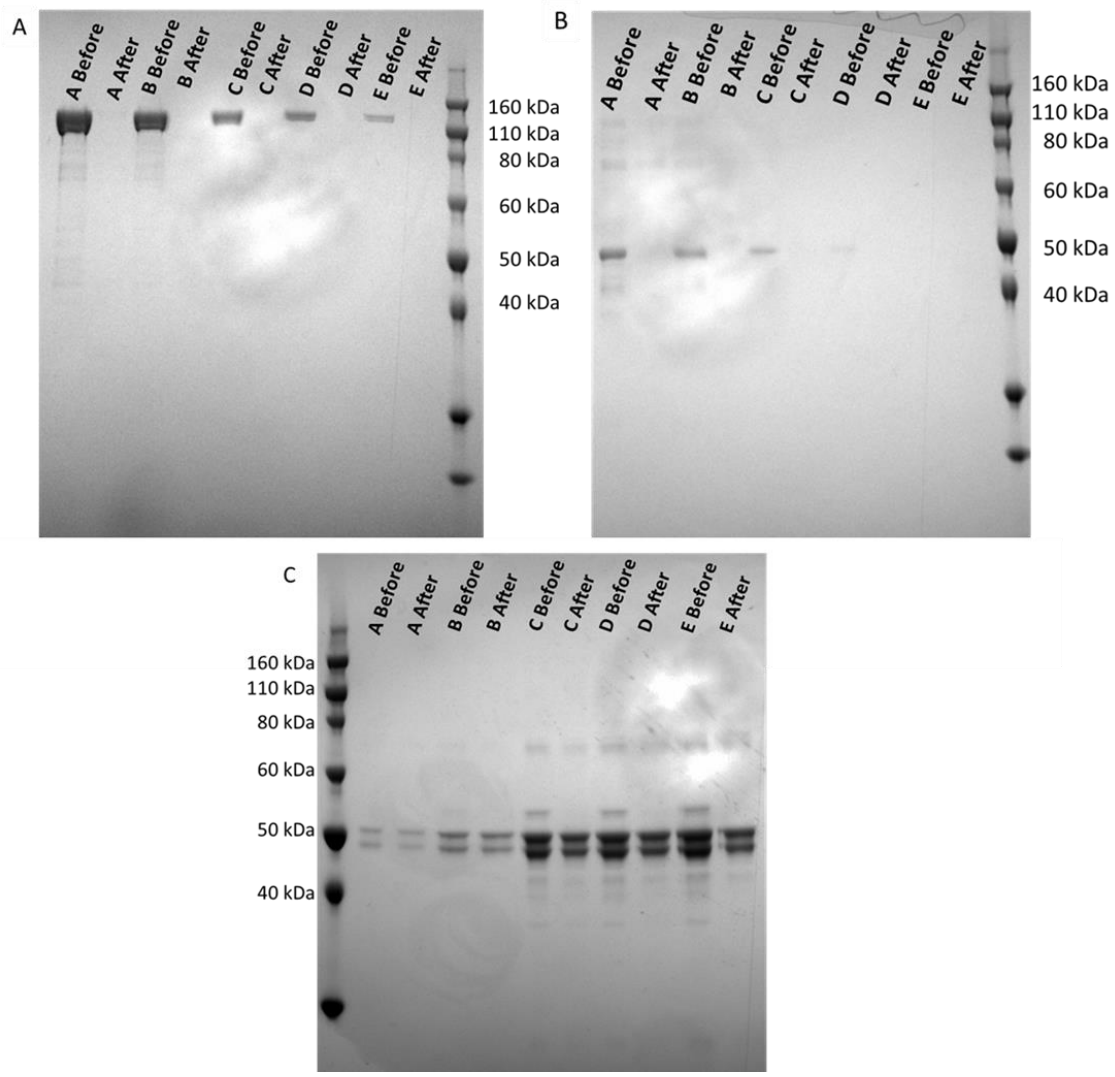

Figure 26: SDS-PAGE gel of enzyme binding. (A) MBP KIVD Doc G serial dilution and binding, A: 0.43 mg/mL, B: 0.25 mg/mL, C: 0.12 mg/mL, D: 0.06 mg/mL, and E: 0.03 mg/mL; (B) ADH_{29C8} Doc T serial dilution and binding, A: 0.18 mg/mL, B: 0.1 mg/mL, C: 0.05 mg/mL, D: 0.03 mg/mL, and E: 0.01 mg/mL; and (C) Doc V FDH_{WT} serial dilution and binding, A: 0.03 mg/mL, B: 0.07 mg/mL, C: 0.1 mg/mL, D: 0.14 mg/mL, and E: 0.17 mg/mL. Before denotes enzyme solution before contact with cellulose bound with scaffold. After denotes retentate retrieved after shaking overnight. A-E denote the different concentrations of enzyme. MBP $KIVD_{LLM4}$ Doc G is 115 kDa, ADH_{29C8} Doc T is 45 kDa, and FDH_{WT} Doc V is 50 kDa.

5.3.4 Doc V FDH_{WT} Redesign

To address the issues with the potential cleavage of the linker, two parts of the fusion were redesigned: the linker was switched out for a long or short one described by the Bayer

labratory[119] and the HIS tag was moved from the C-terminus to the N-terminus. The reasoning behind these design changes was to avoid prior cleavage issues and have only the entire fusion purified by both nickel purification and buffer exchange, which would remove cleaved dockerin with only a HIS tag attached due to the molecular weight being below the cutoff of 30 kDa. **Fig. 27** shows the result of low temperature expression in pLysS for Doc V FDH_{WT} for both long and short linkers. While both appear to have been expressed, the long linker has better expression, with a denser band. Of note is the additional bands present in the SDS-PAGE. This is an effect of the change of nickel resin utilized for purification, resulting in more nonspecific binding. Thus, the binding to the cohesin scaffold has new importance, as it needs to also overcome this purity issue.

The activity of both the short and long linker fusions of Doc V FDH_{WT} is seen in **Fig. 28**. In keeping with the better expression levels, the long linker fusion is also more active than the short linker fusion. Like before, issues with expression, such as aggregation and misfolding would obviously affect activity of the enzyme itself. Neither fusion is as active as the wild type version, which is not particularly surprising given the difficulty FDH has had with fusions, but because FDH is the recycle enzyme and formate is kept at excess due to being inexpensive, this activity disparity can be overcome easily.

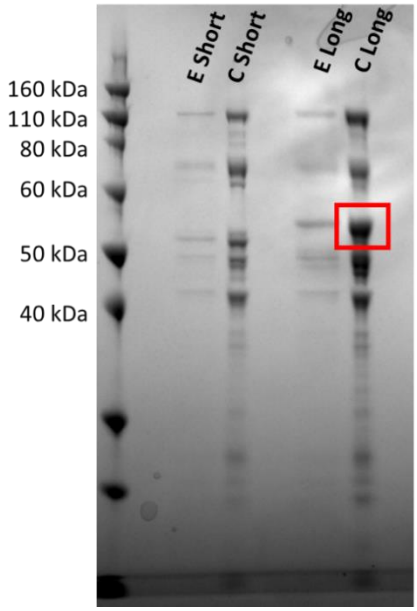

Figure 27: SDS-PAGE gel of short and long linkers for Doc V FDH$_{WT}$. E: elution and C: buffer exchanged. Expressed band highlighted with red box. Doc V Short FDH$_{WT}$ is 51.6 kDa and Doc V Long FDH$_{WT}$ is 52.8 kDa.

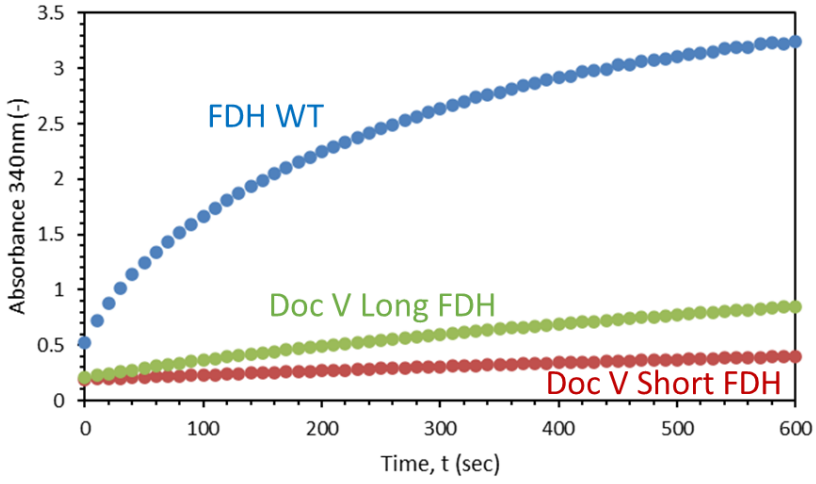

Figure 28: Doc V FDH activity assays.

The final test before an immobilized reaction could be conducted, was to bind the dockerin fusion for FDH to the scaffold. As seen in **Fig. 29**, the band that should correspond to a 50+kDa protein successfully disappears in the retentate. The prior issue with purity is also not an issue as the other bands have remained unbound, accounting for the dilution that would occur

due to the cellulose retaining solution post washes. This is expected as cohesin is known to be selective and cellulose is known to have low nonspecific binding[125]. With this result, all three enzymes now had active dockerin fusions that were successful at binding to the cohesin scaffold.

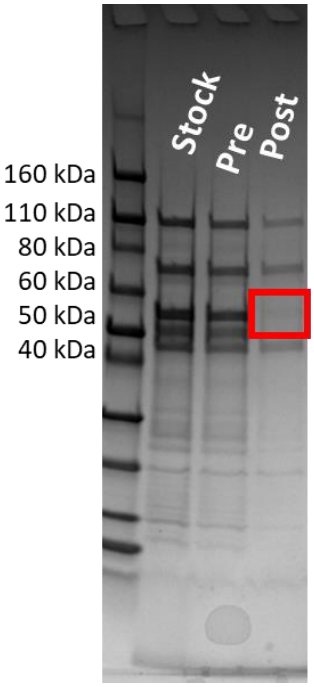

Figure 29: SDS-PAGE gel of Doc V Long FDH$_{WT}$ binding to scaffold. Stock: stock solution of fusion; Pre: enzyme solution before binding; and Post: retentate retrieved post binding. Doc V Long FDH$_{WT}$ is 52.8 kDa. Red square highlights lack of band.

5.3.5 Immobilized Reaction

An advantage of the scaffold system is that all three pathway enzymes with respective dockerin will be localized on the same support once bound to their respective cohesin. The result of this binding is found in **Fig. 30**. The three previously discussed bands are displayed in the initial enzyme mixture and dissipate in the retentate. Unlike before, the bands do not disappear, but still show a significant decrease. The impurities associated with the current nickel purification serves as a guidepost, showing unlike before on the lower scale, dilution is not a present concern comparing the lanes as the impure bands retain strength post shaking. There are

two possible explanations for the enzyme fusion bands not fully binding: the concentration could be too high compared to the scaffold or there could be an issue of crowding the scaffold. The former seems unlikely given the concentration of FDH and ADH fusions was already significantly lower than KIVD, so the unform increase of stock volume used should not be visible in FDH and ADH's bands. The more likely possibility is that due to the scaffold binding randomly to the cellulose, all three enzymes binding in a relatively close space, and all three being dimers, there could be an aspect of crowding where binding is slowed and/or hindered due to enzyme(s) already bound to the scaffold blocking another from reaching its cohesin. It would be possible to forgo the cellulose aspect of the scaffold to try and alleviate crowding, but this would result in another issue, the dimers could cause a crosslinking like effect of linking different cohesin scaffolds together, which could have unforeseen consequences, such as aggregation. Beyond these concerns though, the enzymes were binding to the scaffold and a full reaction run could be evaluated.

Like the immobilized reaction seen previously, a fully immobilized reaction was run with the scaffold. A higher starting concentration of KIV was chosen because utilization of substrate channeling should help alleviate the potential problem a higher concentration of final isobutanol would have on final yield. As stated previously in Chapter 2, ADH is sensitive to isobutanol concentration, so higher starting reagent would naturally increase the final concentration of isobutanol which would have a negative effect on ADH activity, lowering yield. If substrate channeling is realized and the Damköhler number is lowered; however, yield will be increased as the intermediate aldehyde is pushed toward conversion to isobutanol. The final concentration of isobutanol after 24 hours was 80 mM, representing a 78.4% yield. This validates the choice of switching the immobilization strategy for the system: it is simpler than the prior epoxy

immobilization, yields better results, the scaffold theoretically allows for regeneration not possible with the epoxy, and the system itself is also more modular allowing for different pathways if they are fused to a specific dockerin.

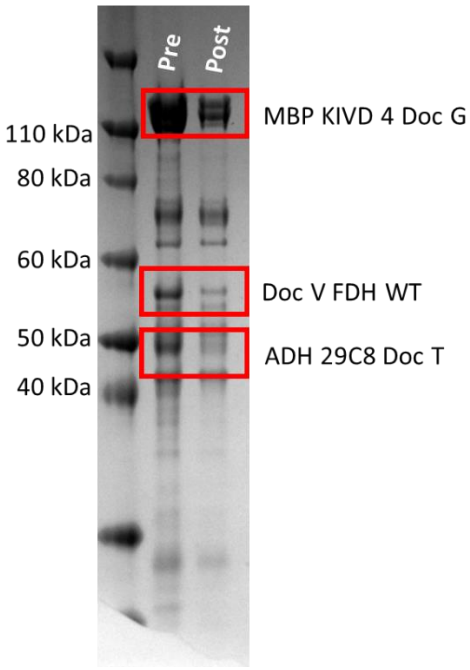

Figure 30: SDS-PAGE gel of full enzymatic binding to scaffold. Pre: enzyme solution before binding and Post: retentate retrieved post binding. Red square highlights change in bands specific to fusion enzymes. MBP KIVD$_{LLM4}$ Doc G is 115 kDa, ADH$_{29C8}$ Doc T is 45 kDa, and FDH$_{WT}$ Doc V is 50 kDa.

Referring to **Table 5** in Chapter 4 for comparison, this system is now quite favorable in both yield and titer. However, new developments in cell-free systems have altered the field radically: a full glucose to isobutanol system was developed, producing an isobutanol titer of 275 g/L, far above even the best *E. coli* production schemes and ethanol fermentation in general[126]. It is important to note that there are limitations to this system. A massive amount of enzyme was needed, with loading of 5 g/L in a system with a 15 mL aqueous phase and 50 mL organic phase, and additional input of enzyme was needed to sustain production. Due to the system having the

enzymes in solution, a liquid-liquid system was developed to extract the isobutanol using a large amount of organic phase which would require thermal separation downstream. Use of an immobilized scaffold scheme would allow for far easier separation of isobutanol from the reaction broth and could address the stability concerns; however obviously the system would need to be developed further given the number of enzymes used in the pathway[126].

This scaffold reaction was proof-of-concept and so has room for improvement. Stability tests should be conducted on the fusion enzymes to ascertain optimal conditions/need for engineering to address issues with isobutanol tolerance. Optimization of binding to the scaffold to better bind the enzymes would be ideal. Given the large volume used compared to the tube size, addressing the amount of CO_2 and possible pH changes is necessary. There are also possible fusion protein developments, such as fusing enzymes together or changing the scaffold, that will be discussed in the next chapter. Overall, system modularity results in a high potential for future applications beyond isobutanol production, as the dockerin can be fused to any enzyme of relevance and with minimal engineering needed to run the system.

5.4 Conclusions

Following the successful immobilization onto epoxy, the KIV pathway was altered to accommodate a cohesin scaffold. Each enzyme was genetically fused to a unique dockerin, which corresponded to a specific cohesin on a scaffold that was bound to cellulose. The activity of each fusion enzyme and binding to the scaffold was confirmed. A fully immobilized reaction produced a titer of 5.92 g/L titer and 78.4% yield. This offers a solid start for the system with potential for further engineering and tuning, especially given no prior case study of the cohesin dockerin system used for cell-free isobutanol production.

CHAPTER 6

SUMMARY AND FUTURE WORK

6.1 Summary

This project was designed to both advance and expand on prior work on a cell-free system developed in the Belfort laboratory. High preforming and stable enzymes were chosen from the literature, cloned, expressed, and purified. The enzymes were tested for activity, kinetics, and stability. With this wide range of information, optimal reaction conditions were chosen using the best enzymes for production of isobutanol. In one case, they were utilized in the creation of a unique, *in vivo* to *in vitro* system. They were also immobilized on epoxy resin, obtaining a titer of 2 g/L and 43% yield. Work was done on this system to push for substrate channeling and lowering the Damköhler number; the enzymes were further engineered, fusing them to dockerin and immobilizing them on a cohesin scaffold, bound to cellulose. This upgraded system provided a 5.9 g/L titer and a yield of 78.4%. The complete immobilized cell-free system has proven to be an effective producer of isobutanol, and its evolution from being covalently bound to a resin to a targeted scaffold bound to cellulose has potential for improvements. Four key future areas of work will be discussed in this chapter with respect to future plans: optimization of the scaffold system, optimization of the *in vivo* to *in vitro* system, engineering of the pathway itself, and product purification.

Portions of this chapter previously appeared as: Wong, M.; Zha, J.; Sorci, M.; Gasparis, C.; Belfort, G.; Koffas, M., Cell-Free Production of Isobutanol: A Completely Immobilized System. *Bioresour Technol* **2019**, *294*, 122104. DOI: 10.1016/j.biortech.2019.122104

6.2 Future Plans

6.2.1 Optimization of In Vivo to In Vitro System

Several optimizations to this unique *in vivo* to *in vitro* system could be implemented to increase the titer. An increase in the production of KIV will increase the titer, but at the potential cost of the high yield. Immobilization of the enzymes is a useful strategy to retain activity as the concentration of biofuel increases [127-128], reduce diffusion limitations, and for purification of isobutanol[95]. These immobilized enzymes have higher thermal and chemical stability and can be separated from the biofuel with ease[37]. By immobilizing enzymes, along with having a higher concentration of starting reagent, a cell-free system can be created that has both the high yield obtained so far as well as higher titer. Because the system is divided into two parts, it is also modular: the cell-free enzymes can be swapped out with other pathways to produce other bioproducts from KIV such as biopharmaceuticals or flavoring compounds[129].

6.2.2 Optimization of the Scaffold System

Despite the excellent results, ways to improve this scaffold system exist from an operational standpoint. New assays should be conducted with the fusions, to examine the effect the dockerins have on the specific pathway enzymes. As was shown in Chapter 2, fusions can have both positive and negative effects on changing activity, stability, solubility, and other functions. These assays could reveal any changes in operating temperature, pH, or even isobutanol stability. Since the reaction was conducted using the prior operating parameters from the epoxy resin reaction in Chapter 4, there could be further fine tuning.

Another consideration is reaction time used. A 24-hour reaction time is a hold-over from previous work by Grimaldi et al[44]. Analysis of the reaction at different time points would allow for a more tuned operation, as well as allow for more production from the enzymes, which decay

in activity with time. Since it is known that the conversion carried out by ADH is reversible, there could be unforeseen affects with the reaction going too long, resulting in lower apparent yield, as well as issues with cofactor stabilty[130-131] as well as enzyme stability. Of note with cofactor stability is that while all buffers are prepared at pH 7.4, the pathway as designed releases CO_2 during conversion. This will lead to carbonic acid formation in the aqueous solution, which could overcome the buffer and lower the pH and affect both enzymes and cofactors[131]. Thus, there should be consideration for capturing CO_2, utilizing either adsorption[132] or perhaps a membrane seperation[133], which will drive the reaction forward as well as tighten the pH control during the reaction. Of course, scale up would be needed, as pH control at a 1-3 mL range seems rather unrealistic.

Given the dockerin-cohesin affinity used for immobilization, another consideration would be to forgo HIS tag purification. This would have the advantages of both quickening time from expression to application, as well as avoiding losses of enzyme mass and activity during nickel purification and buffer exchange. A possible issue could be nonspecific binding, to which cellulose is resistant and cohesin are species selective[110].

Finally, consideration should be given to changing how the reaction occurs. Currently the reaction is run in a batch formation, but a continuous mode, such as a packed column with membrane filtration would be more applicable to an industrial setting for producing purified isobutanol[134]. Of course, examination of reaction time would be key, and a separation method developed to allow for recycle of unreacted solution.

6.2.3 Engineering the Pathway

Chapter 5 focused on the design of a scaffold immobilization scheme to address the bottleneck at the ADH conversion of aldehyde by promoted substrate channeling. Another

solution to explore is fusion of KIVD, ADH, and/or FDH together utilizing linkers which have been shown to accomplish substrate channeling and possibly improving activity and stability[135]. The principle of substrate channeling is to drive the substrate to the enzyme and reduce diffusion length. By fusing KIVD and ADH, the aldehyde would be available quickly for ADH to convert to alcohol. Fusing ADH and FDH would allow for the cofactor NADH to be regenerated in proximity to ADH. Either case would push the reaction forward, which if combined with a quicker reaction and product recovery would help overcome equilibrium. An issue would be that all three are dimers, and so on top of issues of folding while fused, their dimeric interactions could also be affected. Care would need to be taken to keep the two enzymes separate, perhaps with a long linker, so that they can still dimerize properly. Another possibility is to redesign the scaffold. As seen in **Fig. 23**, crowding influenced binding of the fusion proteins to the scaffold. One solution increases the size of linkers between cohesin or the dockerin in the fusions, giving the pathway enzymes more room, while still localizing them. One of the pathway enzymes could also be fused directly to the scaffold, which would both avoid any kind of crowding and simplify the binding needed. Of course, it would also reduce the capacity of regeneration and so would need to be an exceptionally stable enzyme, such as MPB KIVD. There are also ordering considerations, where alternative scaffolds with more cohesin could be used allowing for use of additional versions of pathway enzymes[136]. Surrounding KIVD with ADH could be more beneficial than having ADH in one direction from KIVD, “catching” more aldehyde to convert to alcohol.

The pathway could also be expanded, utilizing different enzymes than the ones in this study. As noted in Chapter 2, ADH has stability issues that could be rectified by utilizing a more stable ADH[126]. Indeed, the study by Sherkhanov et al. provides a glimpse into multiple enzymes

that could be utilized with this scaffold system to improve and expand upon production of isobutanol. The enzymes could be fused to dockerin and bound to a scaffold like in this work, allowing for more environmentally friendly separation methods to be used, rather than the liquid-liquid extraction used.

6.2.4 Separation of Biofuel

Finally, there is a desire to continue the previous work by Grimaldi et al.[95], examining new membrane morphologies for filtration of isobutanol and water. Often alcohol separations are thought of in a distillation context; however, it is energy intensive and not ideal for a green process. The Belfort lab has focused on pervaporation membranes for this separation. That is still a thermal process but has energy savings that give it a large advantage over distillation. While a nanofiltration membrane would be ideal, and there has been work done[137] to facilitate organic solvent nanofiltration with the use of surface modified membranes[138] or membranes assembled with novel mateirals[139], filtration of organic solvents size differentiation is incredibly difficult given the two hydrogen difference between the alcohol and its aldehyde. Of interest are novel material membranes such as zeolite membranes, with their adsorptive properties that have selective flux for isobutanol[140-141]. Other adsorptive materials of interest for isobutanol separations are metal organic frameworks[142] and activated carbon[143]. Separation of isobutanol from the reaction solution would be essential to industrial scaleup, transitioning a batch system to a continuous one.

REFERENCES

1. Baeyens, J.; Kang, Q.; Appels, L.; Dewil, R.; Lv, Y.; Tan, T., Challenges and Opportunities in Improving the Production of Bio-Ethanol. *Prog Energy Combust Sci* **2015,** *47*, 60-88. DOI: 10.1016/j.pecs.2014.10.003
2. Kang, Q.; Van der Bruggen, B.; Dewil, R.; Baeyens, J.; Tan, T., Hybrid Operation of the Bio-Ethanol Fermentation. *Sep Purif Technol* **2015,** *149*, 322-330. DOI: 10.1016/j.seppur.2015.05.007
3. Nie, K.; Xie, F.; Wang, F.; Tan, T., Lipase Catalyzed Methanolysis to Produce Biodiesel: Optimization of the Biodiesel Production. *J Mol Catal B: Enzym* **2006,** *43* (1-4), 142-147. DOI: 10.1016/j.molcatb.2006.07.016
4. Naik, S. N.; Goud, V. V.; Rout, P. K.; Dalai, A. K., Production of First and Second Generation Biofuels: A Comprehensive Review. *Renewable Sustainable Energy Rev* **2010,** *14* (2), 578-597. DOI: 10.1016/j.rser.2009.10.003
5. Wang, M.; Nie, K.; Cao, H.; Deng, L.; Wang, F.; Tan, T., Biodiesel Production by Combined Fatty Acids Separation and Subsequently Enzymatic Esterification to Improve the Low Temperature Properties. *Bioresour Technol* **2014,** *174*, 302-305. DOI: 10.1016/j.biortech.2014.08.011
6. Han, X.; Yang, Z.; Wang, M.; Tjong, J.; Zheng, M., Clean Combustion of N -Butanol as a Next Generation Biofuel for Diesel Engines. *Appl Energy* **2017,** *198*, 347-359. DOI: 10.1016/j.apenergy.2016.12.059
7. Peralta-Yahya, P. P.; Zhang, F.; del Cardayre, S. B.; Keasling, J. D., Microbial Engineering for the Production of Advanced Biofuels. *Nature* **2012,** *488* (7411), 320-328. DOI: 10.1038/nature11478
8. Minty, J. J.; Singer, M. E.; Scholz, S. A.; Bae, C. H.; Ahn, J. H.; Foster, C. E.; Liao, J. C.; Lin, X. N., Design and Characterization of Synthetic Fungal-Bacterial Consortia for Direct Production of Isobutanol from Cellulosic Biomass. *Proc Natl Acad Sci U S A* **2013,** *110* (36), 14592-14597. DOI: 10.1073/pnas.1218447110
9. Grimaldi, J.; Collins, C. H.; Belfort, G., Toward Cell-Free Biofuel Production: Stable Immobilization of Oligomeric Enzymes. *Biotechnol Prog* **2014,** *30* (2), 324-331. DOI: 10.1002/btpr.1876
10. Jones, D. T.; Woods, D. R., Acetone-Butanol Fermentation Revisited. *Microbiol Rev* **1986,** *50* (4), 484-524. DOI: 10.1128/mr.50.4.484-524.1986
11. Xu, P.; Koffas, M. A., Metabolic Engineering of Escherichia Coli for Biofuel Production. *Biofuels* **2010,** *1* (3), 493-504.
12. Jones, J. A.; Toparlak, O. D.; Koffas, M. A., Metabolic Pathway Balancing and Its Role in the Production of Biofuels and Chemicals. *Curr Opin Biotechnol* **2015,** *33*, 52-59. DOI: 10.1016/j.copbio.2014.11.013
13. Chen, C. T.; Liao, J. C., Frontiers in Microbial 1-Butanol and Isobutanol Production. *FEMS Microbiol Lett* **2016,** *363* (5), fnw020. DOI: 10.1093/femsle/fnw020
14. Arnold, F. H.; Volkov, A. A., Directed Evolution of Biocatalysts. *Curr Opin Chem Biol* **1999,** *3* (1), 54-59. DOI: 10.1016/s1367-5931(99)80010-6
15. Shi, S.; Si, T.; Liu, Z.; Zhang, H.; Ang, E. L.; Zhao, H., Metabolic Engineering of a Synergistic Pathway for N-Butanol Production in Saccharomyces Cerevisiae. *Sci Rep* **2016,** *6* (1), 25675. DOI: 10.1038/srep25675

16. Bernardi, A. C.; Gai, C. S.; Lu, J.; Sinskey, A. J.; Brigham, C. J., Experimental Evolution and Gene Knockout Studies Reveal Acra-Mediated Isobutanol Tolerance in Ralstonia Eutropha. *J Biosci Bioeng* **2016,** *122* (1), 64-69. DOI: 10.1016/j.jbiosc.2015.12.015
17. Claassens, N. J.; Burgener, S.; Vogeli, B.; Erb, T. J.; Bar-Even, A., A Critical Comparison of Cellular and Cell-Free Bioproduction Systems. *Curr Opin Biotechnol* **2019,** *60*, 221-229. DOI: 10.1016/j.copbio.2019.05.003
18. Gregorio, N. E.; Levine, M. Z.; Oza, J. P., A User's Guide to Cell-Free Protein Synthesis. *Methods Protoc* **2019,** *2* (1), 24. DOI: 10.3390/mps2010024
19. Beilke, M. C.; Klotzbach, T. L.; Treu, B. L.; Sokic-Lazic, D.; Wildrick, J.; Amend, E. R.; Gebhart, L. M.; Arechederra, R. L.; Germain, M. N.; Moehlenbrock, M. J.; Sudhanshu; Minteer, S. D., Enzymatic Biofuel Cells. In *Micro Fuel Cells*, Zhao, T. S., Ed. Academic Press, 2009; pp 179-241.
20. Knaus, T.; Paul, C. E.; Levy, C. W.; de Vries, S.; Mutti, F. G.; Hollmann, F.; Scrutton, N. S., Better Than Nature: Nicotinamide Biomimetics That Outperform Natural Coenzymes. *J Am Chem Soc* **2016,** *138* (3), 1033-1039. DOI: 10.1021/jacs.5b12252
21. Karim, A. S.; Heggestad, J. T.; Crowe, S. A.; Jewett, M. C., Controlling Cell-Free Metabolism through Physiochemical Perturbations. *Metab Eng* **2018,** *45*, 86-94. DOI: 10.1016/j.ymben.2017.11.005
22. Yamamoto, T.; Fujii, T.; Nojima, T., Pdms-Glass Hybrid Microreactor Array with Embedded Temperature Control Device. Application to Cell-Free Protein Synthesis. *Lab Chip* **2002,** *2* (4), 197-202. DOI: 10.1039/b205010b
23. Opgenorth, P. H.; Korman, T. P.; Bowie, J. U., A Synthetic Biochemistry Molecular Purge Valve Module That Maintains Redox Balance. *Nat Commun* **2014,** *5* (1), 4113. DOI: 10.1038/ncomms5113
24. Swartz, J. R., Transforming Biochemical Engineering with Cell-Free Biology. *AIChE J* **2012,** *58* (1), 5-13. DOI: 10.1002/aic.13701
25. Bundy, B. C.; Hunt, J. P.; Jewett, M. C.; Swartz, J. R.; Wood, D. W.; Frey, D. D.; Rao, G., Cell-Free Biomanufacturing. *Curr Opin Chem Eng* **2018,** *22*, 177-183. DOI: 10.1016/j.coche.2018.10.003
26. Zhang, Y.-H. P.; Myung, S.; You, C.; Zhu, Z.; Rollin, J. A., Toward Low-Cost Biomanufacturing through in Vitro Synthetic Biology: Bottom-up Design. *J Mater Chem* **2011,** *21* (47), 18877-18886.
27. Zawada, J. F.; Yin, G.; Steiner, A. R.; Yang, J.; Naresh, A.; Roy, S. M.; Gold, D. S.; Heinsohn, H. G.; Murray, C. J., Microscale to Manufacturing Scale-up of Cell-Free Cytokine Production--a New Approach for Shortening Protein Production Development Timelines. *Biotechnol Bioeng* **2011,** *108* (7), 1570-1578. DOI: 10.1002/bit.23103
28. Karim, A. S.; Jewett, M. C., A Cell-Free Framework for Rapid Biosynthetic Pathway Prototyping and Enzyme Discovery. *Metab Eng* **2016,** *36*, 116-126. DOI: 10.1016/j.ymben.2016.03.002
29. Tinafar, A.; Jaenes, K.; Pardee, K., Synthetic Biology Goes Cell-Free. *BMC Biol* **2019,** *17* (1), 64. DOI: 10.1186/s12915-019-0685-x
30. Gao, W.; Cho, E.; Liu, Y.; Lu, Y., Advances and Challenges in Cell-Free Incorporation of Unnatural Amino Acids into Proteins. *Front Pharmacol* **2019,** *10*, 611. DOI: 10.3389/fphar.2019.00611
31. Su, Y.; Zhang, W.; Zhang, A.; Shao, W., Biorefinery: The Production of Isobutanol from Biomass Feedstocks. *Appl Sci* **2020,** *10* (22), 8222. DOI: 10.3390/app10228222

32. Krutsakorn, B.; Honda, K.; Ye, X.; Imagawa, T.; Bei, X.; Okano, K.; Ohtake, H., In Vitro Production of N-Butanol from Glucose. *Metab Eng* **2013,** *20*, 84-91. DOI: 10.1016/j.ymben.2013.09.006
33. Guterl, J. K.; Garbe, D.; Carsten, J.; Steffler, F.; Sommer, B.; Reisse, S.; Philipp, A.; Haack, M.; Ruhmann, B.; Koltermann, A.; Kettling, U.; Bruck, T.; Sieber, V., Cell-Free Metabolic Engineering: Production of Chemicals by Minimized Reaction Cascades. *ChemSusChem* **2012,** *5* (11), 2165-2172. DOI: 10.1002/cssc.201200365
34. Wilding, K. M.; Schinn, S. M.; Long, E. A.; Bundy, B. C., The Emerging Impact of Cell-Free Chemical Biosynthesis. *Curr Opin Biotechnol* **2018,** *53*, 115-121. DOI: 10.1016/j.copbio.2017.12.019
35. Zhang, Y. H., Production of Biocommodities and Bioelectricity by Cell-Free Synthetic Enzymatic Pathway Biotransformations: Challenges and Opportunities. *Biotechnol Bioeng* **2010,** *105* (4), 663-677. DOI: 10.1002/bit.22630
36. Katchalski-Katzir, E., Immobilized Enzymes — Learning from Past Successes and Failures. *Trends Biotechnol* **1993,** *11* (11), 471-478. DOI: 10.1016/0167-7799(93)90080-s
37. Sheldon, R. A., Enzyme Immobilization: The Quest for Optimum Performance. *Adv Synth Catal* **2007,** *349* (8-9), 1289-1307. DOI: 10.1002/adsc.200700082
38. Moelans, D.; Cool, P.; Baeyens, J.; Vansant, E. F., Using Mesoporous Silica Materials to Immobilise Biocatalysis-Enzymes. *Catal Commun* **2005,** *6* (4), 307-311. DOI: 10.1016/j.catcom.2005.02.005
39. Radhakrishna, M.; Grimaldi, J.; Belfort, G.; Kumar, S. K., Stability of Proteins inside a Hydrophobic Cavity. *Langmuir* **2013,** *29* (28), 8922-8928. DOI: 10.1021/la4014784
40. Grimaldi, J.; Radhakrishna, M.; Kumar, S. K.; Belfort, G., Stability of Proteins on Hydrophilic Surfaces. *Langmuir* **2015,** *31* (3), 1005-1010. DOI: 10.1021/la503865b
41. Wu, D. R.; Belfort, G.; Cramer, S. M., Enzymic Resolution with a Multiphase Membrane Bioreactor: A Theoretical Analysis. *Ind Eng Chem Res* **1990,** *29* (8), 1612-1621. DOI: 10.1021/ie00104a006
42. Wu, D. R.; Cramer, S. M.; Belfort, G., Kinetic Resolution of Racemic Glycidyl Butyrate Using a Multiphase Membrane Enzyme Reactor: Experiments and Model Verification. *Biotechnol Bioeng* **1993,** *41* (10), 979-990. DOI: 10.1002/bit.260411009
43. Yokoi, H.; Belfort, G., High-Rate Membrane Supported Aqueous-Phase Enzymatic Conversion in Organic Solvent. *Bioseparation* **1994,** *4* (3), 213-220.
44. Grimaldi, J.; Collins, C. H.; Belfort, G., Towards Cell-Free Isobutanol Production: Development of a Novel Immobilized Enzyme System. *Biotechnol Prog* **2016,** *32* (1), 66-73. DOI: 10.1002/btpr.2197
45. Soh, L. M.; Mak, W. S.; Lin, P. P.; Mi, L.; Chen, F. Y.-H.; Damoiseaux, R.; Siegel, J. B.; Liao, J. C., Engineering a Thermostable Keto Acid Decarboxylase Using Directed Evolution and Computationally Directed Protein Design. *ACS Synth Biol* **2017,** *6* (4), 610-618. DOI: 10.1021/acssynbio.6b00240
46. de la Plaza, M.; Fernandez de Palencia, P.; Pelaez, C.; Requena, T., Biochemical and Molecular Characterization of Alpha-Ketoisovalerate Decarboxylase, an Enzyme Involved in the Formation of Aldehydes from Amino Acids by Lactococcus Lactis. *FEMS Microbiol Lett* **2004,** *238* (2), 367-374. DOI: 10.1016/j.femsle.2004.07.057
47. Reid, M. F.; Fewson, C. A., Molecular Characterization of Microbial Alcohol Dehydrogenases. *Crit Rev Microbiol* **1994,** *20* (1), 13-56. DOI: 10.3109/10408419409113545

48. Hayes Jr, J. E.; Velick, S. F., Yeast Alcohol Dehydrogenase: Molecular Weight, Coenzyme Binding, and Reaction Equilibria. *J Biol Chem* **1954,** *207* (1), 225-244. DOI: 10.1016/S0021-9258(18)71263-5
49. Liu, X.; Bastian, S.; Snow, C. D.; Brustad, E. M.; Saleski, T. E.; Xu, J.-H.; Meinhold, P.; Arnold, F. H., Structure-Guided Engineering of Lactococcus Lactis Alcohol Dehydrogenase Lladha for Improved Conversion of Isobutyraldehyde to Isobutanol. *J Biotechnol* **2013,** *164* (2), 188-195. DOI: 10.1016/j.jbiotec.2012.08.008
50. Guy, J. E.; Isupov, M. N.; Littlechild, J. A., The Structure of an Alcohol Dehydrogenase from the Hyperthermophilic Archaeon Aeropyrum Pernix. *J Mol BIol* **2003,** *331* (5), 1041-1051. DOI: 10.1016/s0022-2836(03)00857-x
51. Ferry, J. G., Formate Dehydrogenase. *FEMS Microbiol Rev* **1990,** *7* (3-4), 377-382. DOI: 10.1111/j.1574-6968.1990.tb04940.x
52. Grimaldi, J. Cell Free Production of a Liquid Fuel. PhD Dissertation, Rensselaer Polytechnic Institute, Troy, NY, 2014.
53. Schirwitz, K.; Schmidt, A.; Lamzin, V. S., High-Resolution Structures of Formate Dehydrogenase from Candida Boidinii. *Protein Sci* **2007,** *16* (6), 1146-1156. DOI: 10.1110/ps.062741707
54. Kirk, O.; Borchert, T. V.; Fuglsang, C. C., Industrial Enzyme Applications. *Curr Opin Biotechnol* **2002,** *13* (4), 345-351. DOI: 10.1016/s0958-1669(02)00328-2
55. Farinas, E. T.; Bulter, T.; Arnold, F. H., Directed Enzyme Evolution. *Curr Opin Biotechnol* **2001,** *12* (6), 545-551. DOI: 10.1016/s0958-1669(01)00261-0
56. Nevalainen, H. K. M.; Te'o, V. S. J., Enzyme Production in Industrial Fungi-Molecular Genetic Strategies for Integrated Strain Improvement. In *Fungal Genomics*, Vol. 3, Arora, D. K.; Khachatourians, G. G., Eds. Elsevier, 2003; pp 241-259.
57. Reeves, P. R.; Liu, B.; Zhou, Z.; Li, D.; Guo, D.; Ren, Y.; Clabots, C.; Lan, R.; Johnson, J. R.; Wang, L., Rates of Mutation and Host Transmission for an Escherichia Coli Clone over 3 Years. *PLoS One* **2011,** *6* (10), e26907. DOI: 10.1371/journal.pone.0026907
58. Ling, M. M.; Robinson, B. H., Approaches to DNA Mutagenesis: An Overview. *Anal Biochem* **1997,** *254* (2), 157-178. DOI: 10.1006/abio.1997.2428
59. Arnold, F. H., Directed Evolution: Bringing New Chemistry to Life. *Angew Chem Int Ed Engl* **2018,** *57* (16), 4143-4148. DOI: 10.1002/anie.201708408
60. Carter, P., Site-Directed Mutagenesis. *Biochem J* **1986,** *237* (1), 1-7. DOI: 10.1042/bj2370001
61. Mendel, D.; Cornish, V. W.; Schultz, P. G., Site-Directed Mutagenesis with an Expanded Genetic Code. *Annu Rev Biophys Biomol Struct* **1995,** *24* (1), 435-462. DOI: 10.1146/annurev.bb.24.060195.002251
62. Yu, K.; Liu, C.; Kim, B. G.; Lee, D. Y., Synthetic Fusion Protein Design and Applications. *Biotechnol Adv* **2015,** *33* (1), 155-164. DOI: 10.1016/j.biotechadv.2014.11.005
63. Yang, H.; Liu, L.; Xu, F., The Promises and Challenges of Fusion Constructs in Protein Biochemistry and Enzymology. *Appl Microbiol Biotechnol* **2016,** *100* (19), 8273-8281. DOI: 10.1007/s00253-016-7795-y
64. Terpe, K., Overview of Tag Protein Fusions: From Molecular and Biochemical Fundamentals to Commercial Systems. *Appl Microbiol Biotechnol* **2003,** *60* (5), 523-533. DOI: 10.1007/s00253-002-1158-6

65. Fox, J. D.; Kapust, R. B.; Waugh, D. S., Single Amino Acid Substitutions on the Surface of Escherichia Coli Maltose-Binding Protein Can Have a Profound Impact on the Solubility of Fusion Proteins. *Protein Sci* **2001,** *10* (3), 622-630. DOI: 10.1110/ps.45201
66. Kapust, R. B.; Waugh, D. S., Escherichia Coli Maltose-Binding Protein Is Uncommonly Effective at Promoting the Solubility of Polypeptides to Which It Is Fused. *Protein Sci* **1999,** *8* (8), 1668-1674. DOI: 10.1110/ps.8.8.1668
67. Arnau, J.; Lauritzen, C.; Petersen, G. E.; Pedersen, J., Current Strategies for the Use of Affinity Tags and Tag Removal for the Purification of Recombinant Proteins. *Protein Expr Purif* **2006,** *48* (1), 1-13. DOI: 10.1016/j.pep.2005.12.002
68. Kozlowski, L. P., Ipc–Isoelectric Point Calculator. *Biol Direct* **2016,** *11* (1), 55. DOI: 10.1186/s13062-016-0159-9
69. Yoshimoto, M.; Yamashita, T.; Yamashiro, T., Stability and Reactivity of Liposome-Encapsulated Formate Dehydrogenase and Cofactor System in Carbon Dioxide Gas-Liquid Flow. *Biotechnol Prog* **2010,** *26* (4), 1047-1053. DOI: 10.1002/btpr.409
70. Barton, A. F., *Alcohols with Water: Solubility Data Series*. Elsevier, 2013.
71. Ganesh, C.; Shah, A. N.; Swaminathan, C. P.; Surolia, A.; Varadarajan, R., Thermodynamic Characterization of the Reversible, Two-State Unfolding of Maltose Binding Protein, a Large Two-Domain Protein. *Biochemistry* **1997,** *36* (16), 5020-5028. DOI: 10.1021/bi961967b
72. Novokhatny, V.; Ingham, K., Thermodynamics of Maltose Binding Protein Unfolding. *Protein Sci* **1997,** *6* (1), 141-146. DOI: 10.1002/pro.5560060116
73. Chen, J.; Shen, J.; Solem, C.; Jensen, P. R., Oxidative Stress at High Temperatures in Lactococcus Lactis Due to an Insufficient Supply of Riboflavin. *Appl Environ Microbiol* **2013,** *79* (19), 6140-6147. DOI: 10.1128/AEM.01953-13
74. Lee, D. A.; Collins, E. B., Influences of Temperature on Growth of Streptococcus Cremoris and Streptococcus Lactis. *J Dairy Sci* **1976,** *59* (3), 405-409. DOI: 10.3168/jds.S0022-0302(76)84220-8
75. Leonardi, R.; Jackowski, S., Biosynthesis of Pantothenic Acid and Coenzyme A. *EcoSal Plus* **2007,** *2* (2), 10.1128/ecosalplus.3.6.3.4. DOI: 10.1128/ecosalplus.3.6.3.4
76. Morgado, G.; Gerngross, D.; Roberts, T. M.; Panke, S., Synthetic Biology for Cell-Free Biosynthesis: Fundamentals of Designing Novel in Vitro Multi-Enzyme Reaction Networks. In *Synthetic Biology – Metabolic Engineering*, Zhao, H.; Zeng, A.-P., Eds. Springer International Publishing, 2018; pp 117-146.
77. Wang, R.; Zhao, S.; Wang, Z.; Koffas, M. A., Recent Advances in Modular Co-Culture Engineering for Synthesis of Natural Products. *Curr Opin Biotechnol* **2020,** *62*, 65-71. DOI: 10.1016/j.copbio.2019.09.004
78. Aparicio, M.; Bellizzi, V.; Chauveau, P.; Cupisti, A.; Ecder, T.; Fouque, D.; Garneata, L.; Lin, S.; Mitch, W. E.; Teplan, V.; Zakar, G.; Yu, X., Keto Acid Therapy in Predialysis Chronic Kidney Disease Patients: Final Consensus. *J Ren Nutr* **2012,** *22* (2 Suppl), S22-24. DOI: 10.1053/j.jrn.2011.09.006
79. Wong, M.; Badri, A.; Gasparis, C.; Belfort, G.; Koffas, M., Modular Optimization in Metabolic Engineering. *Crit Rev Biochem Mol Biol* **2021,** *56* (6), 587-602. DOI: 10.1080/10409238.2021.1937928
80. Englaender, J. A.; Jones, J. A.; Cress, B. F.; Kuhlman, T. E.; Linhardt, R. J.; Koffas, M. A. G., Effect of Genomic Integration Location on Heterologous Protein Expression and Metabolic Engineering in E. Coli. *ACS Synth Biol* **2017,** *6* (4), 710-720. DOI: 10.1021/acssynbio.6b00350

81. Cress, B. F.; Leitz, Q. D.; Kim, D. C.; Amore, T. D.; Suzuki, J. Y.; Linhardt, R. J.; Koffas, M. A., Crispri-Mediated Metabolic Engineering of E. Coli for O-Methylated Anthocyanin Production. *Microb Cell Fact* **2017,** *16* (1), 10. DOI: 10.1186/s12934-016-0623-3
82. Atsumi, S.; Wu, T. Y.; Machado, I. M.; Huang, W. C.; Chen, P. Y.; Pellegrini, M.; Liao, J. C., Evolution, Genomic Analysis, and Reconstruction of Isobutanol Tolerance in Escherichia Coli. *Mol Syst Biol* **2010,** *6*, 449. DOI: 10.1038/msb.2010.98
83. Szenk, M.; Dill, K. A.; de Graff, A. M. R., Why Do Fast-Growing Bacteria Enter Overflow Metabolism? Testing the Membrane Real Estate Hypothesis. *Cell Syst* **2017,** *5* (2), 95-104. DOI: 10.1016/j.cels.2017.06.005
84. Nelson, J.; Griffin, E. G., Adsorption of Invertase. *J Am Chem Soc* **1916,** *38* (5), 1109-1115. DOI: 10.1021/ja02262a018
85. Hedin, S. G., A Case of Specific Adsorption of Enzymes. *Biochem J* **1907,** *2* (3), 112-116. DOI: 10.1042/bj0020112
86. Messing, R., *Immobilized Enzymes for Industrial Reactors*. Elsevier, 2012.
87. Riou, C.; Salmon, J. M.; Vallier, M. J.; Gunata, Z.; Barre, P., Purification, Characterization, and Substrate Specificity of a Novel Highly Glucose-Tolerant Beta-Glucosidase from Aspergillus Oryzae. *Appl Environ Microbiol* **1998,** *64* (10), 3607-3614. DOI: 10.1128/AEM.64.10.3607-3614.1998
88. Brena, B. M.; Batista-Viera, F., Immobilization of Enzymes. In *Immobilization of Enzymes and Cells*, Guisan, J. M., Ed. Humana Press, 2006; pp 15-30.
89. Nisha, S.; Karthick, S. A.; Gobi, N., A Review on Methods, Application and Properties of Immobilized Enzyme. *Chem Sci Rev Lett* **2012,** *1* (3), 148-155.
90. Hayama, R.; Sorci, M.; Keating Iv, J. J.; Hecht, L. M.; Plawsky, J. L.; Belfort, G.; Chait, B. T.; Rout, M. P., Interactions of Nuclear Transport Factors and Surface-Conjugated Fg Nucleoporins: Insights and Limitations. *PLoS One* **2019,** *14* (6), e0217897. DOI: 10.1371/journal.pone.0217897
91. Lim, C. Y.; Owens, N. A.; Wampler, R. D.; Ying, Y.; Granger, J. H.; Porter, M. D.; Takahashi, M.; Shimazu, K., Succinimidyl Ester Surface Chemistry: Implications of the Competition between Aminolysis and Hydrolysis on Covalent Protein Immobilization. *Langmuir* **2014,** *30* (43), 12868-12878. DOI: 10.1021/la503439g
92. Thermo Fisher Scientific, *Carbodiimide Crosslinker Chemistry*. 2016. https://www.thermofisher.com/us/en/home/life-science/protein-biology/protein-biology-learning-center/protein-biology-resource-library/pierce-protein-methods/carbodiimide-crosslinker-chemistry.html (accessed 2022-07-20).
93. Thermo Scientific, *Nhs and Sulfo-Nhs*. 2011. https://tools.thermofisher.com/content/sfs/manuals/MAN0011309_NHS_SulfoNHS_UG.pdf (accessed 2022-07-20).
94. Mateo, C.; Abian, O.; Fernández-Lorente, G.; Pedroche, J.; Fernández-Lafuente, R.; Guisan, J. M., Epoxy Sepabeads: A Novel Epoxy Support for Stabilization of Industrial Enzymes Via Very Intense Multipoint Covalent Attachment. *Biotechnol Prog* **2002,** *18* (3), 629-634. DOI: 10.1021/bp010171n
95. Grimaldi, J.; Imbrogno, J.; Kilduff, J.; Belfort, G., New Class of Synthetic Membranes: Organophilic Pervaporation Brushes for Organics Recovery. *Chem Mater* **2015,** *27* (11), 4142-4148. DOI: 10.1021/acs.chemmater.5b01326

96. Black, W. B.; Zhang, L.; Kamoku, C.; Liao, J. C.; Li, H., Rearrangement of Coenzyme a-Acylated Carbon Chain Enables Synthesis of Isobutanol Via a Novel Pathway in Ralstonia Eutropha. *ACS Synth Biol* **2018,** *7* (3), 794-800. DOI: 10.1021/acssynbio.7b00409
97. Dueber, J. E.; Wu, G. C.; Malmirchegini, G. R.; Moon, T. S.; Petzold, C. J.; Ullal, A. V.; Prather, K. L.; Keasling, J. D., Synthetic Protein Scaffolds Provide Modular Control over Metabolic Flux. *Nat Biotechnol* **2009,** *27* (8), 753-759. DOI: 10.1038/nbt.1557
98. Jia, F.; Narasimhan, B.; Mallapragada, S., Materials-Based Strategies for Multi-Enzyme Immobilization and Co-Localization: A Review. *Biotechnol Bioeng* **2014,** *111* (2), 209-222. DOI: 10.1002/bit.25136
99. Zhao, S.; Jones, J. A.; Lachance, D. M.; Bhan, N.; Khalidi, O.; Venkataraman, S.; Wang, Z.; Koffas, M. A. G., Improvement of Catechin Production in Escherichia Coli through Combinatorial Metabolic Engineering. *Metab Eng* **2015,** *28*, 43-53. DOI: 10.1016/j.ymben.2014.12.002
100. Cress, B. F.; Toparlak, O. D.; Guleria, S.; Lebovich, M.; Stieglitz, J. T.; Englaender, J. A.; Jones, J. A.; Linhardt, R. J.; Koffas, M. A., Crispathbrick: Modular Combinatorial Assembly of Type Ii-a Crispr Arrays for Dcas9-Mediated Multiplex Transcriptional Repression in E. Coli. *ACS Synth Biol* **2015,** *4* (9), 987-1000. DOI: 10.1021/acssynbio.5b00012
101. Lin, P. P.; Rabe, K. S.; Takasumi, J. L.; Kadisch, M.; Arnold, F. H.; Liao, J. C., Isobutanol Production at Elevated Temperatures in Thermophilic Geobacillus Thermoglucosidasius. *Metab Eng* **2014,** *24*, 1-8. DOI: 10.1016/j.ymben.2014.03.006
102. Avalos, J. L.; Fink, G. R.; Stephanopoulos, G., Compartmentalization of Metabolic Pathways in Yeast Mitochondria Improves the Production of Branched-Chain Alcohols. *Nat Biotechnol* **2013,** *31* (4), 335-341. DOI: 10.1038/nbt.2509
103. Wheeldon, I.; Minteer, S. D.; Banta, S.; Barton, S. C.; Atanassov, P.; Sigman, M., Substrate Channelling as an Approach to Cascade Reactions. *Nature Chem* **2016,** *8* (4), 299-309. DOI: 10.1038/nchem.2459
104. Lim, S.; Jung, G. A.; Glover, D. J.; Clark, D. S., Enhanced Enzyme Activity through Scaffolding on Customizable Self-Assembling Protein Filaments. *Small* **2019,** *15* (20), e1805558. DOI: 10.1002/smll.201805558
105. Liu, F.; Banta, S.; Chen, W., Functional Assembly of a Multi-Enzyme Methanol Oxidation Cascade on a Surface-Displayed Trifunctional Scaffold for Enhanced Nadh Production. *Chem Commun (Camb)* **2013,** *49* (36), 3766-3768. DOI: 10.1039/c3cc40454d
106. Andreescu, S.; Bucur, B.; Marty, J.-L., Affinity Immobilization of Tagged Enzymes. In *Immobilization of Enzymes and Cells*, Springer, 2006; pp 97-106.
107. Rao, S. V.; Anderson, K. W.; Bachas, L. G., Oriented Immobilization of Proteins. *Microchim Acta* **1998,** *128* (3), 127-143. DOI: 10.1007/BF01243043
108. Brena, B.; González-Pombo, P.; Batista-Viera, F., Immobilization of Enzymes: A Literature Survey. In *Immobilization of Enzymes and Cells*, 3rd ed.; Guisan, J. M., Ed. Humana Press, 2013; pp 15-31.
109. Yaron, S.; Morag, E.; Bayer, E. A.; Lamed, R.; Shoham, Y., Expression, Purification and Subunit-Binding Properties of Cohesins 2 and 3 of the Clostridium Thermocellum Cellulosome. *FEBS Lett* **1995,** *360* (2), 121-124. DOI: 10.1016/0014-5793(95)00074-j
110. Pagès, S.; Bélaïch, A.; Bélaïch, J. P.; Morag, E.; Lamed, R.; Shoham, Y.; Bayer, E. A., Species-Specificity of the Cohesin-Dockerin Interaction between Clostridium Thermocellum and Clostridium Cellulolyticum: Prediction of Specificity Determinants of the Dockerin Domain.

Proteins: Struct, Funct, Bioinf **1997,** *29* (4), 517-527. DOI: 10.1002/(SICI)1097-0134(199712)29:4<517::AID-PROT11>3.0.CO;2-P
111. Slutzki, M.; Barak, Y.; Reshef, D.; Schueler-Furman, O.; Lamed, R.; Bayer, E. A., Indirect Elisa-Based Approach for Comparative Measurement of High-Affinity Cohesin-Dockerin Interactions. *J Mol Recognit* **2012,** *25* (11), 616-622. DOI: 10.1002/jmr.2178
112. Friguet, B.; Chaffotte, A. F.; Djavadi-Ohaniance, L.; Goldberg, M. E., Measurements of the True Affinity Constant in Solution of Antigen-Antibody Complexes by Enzyme-Linked Immunosorbent Assay. *J Immunol Methods* **1985,** *77* (2), 305-319. DOI: 10.1016/0022-1759(85)90044-4
113. Rollin, J. A.; Tam, T. K.; Zhang, Y.-H. P., New Biotechnology Paradigm: Cell-Free Biosystems for Biomanufacturing. *Green Chem* **2013,** *15* (7), 1708-1719. DOI: 10.1039/C3GC40625C
114. You, C.; Zhang, Y. H., Self-Assembly of Synthetic Metabolons through Synthetic Protein Scaffolds: One-Step Purification, Co-Immobilization, and Substrate Channeling. *ACS Synth Biol* **2013,** *2* (2), 102-110. DOI: 10.1021/sb300068g
115. Xu, Q.; Alahuhta, M.; Hewitt, P.; Sarai, N. S.; Wei, H.; Hengge, N. N.; Mittal, A.; Himmel, M. E.; Bomble, Y. J., Self-Assembling Metabolon Enables the Cell Free Conversion of Glycerol to 1, 3-Propanediol. *Front Energy Res* **2021,** *9*. DOI: 10.3389/fenrg.2021.680313
116. Lee, C. C.; Kibblewhite, R. E.; Paavola, C. D.; Orts, W. J.; Wagschal, K., Production of D-Xylonic Acid from Hemicellulose Using Artificial Enzyme Complexes. *J Microbiol Biotechnol* **2017,** *27* (1), 77-83. DOI: 10.4014/jmb.1606.06041
117. Bayer, E. A.; Kenig, R.; Lamed, R., Adherence of Clostridium Thermocellum to Cellulose. *J Bacteriol* **1983,** *156* (2), 818-827. DOI: 10.1128/jb.156.2.818-827.1983
118. Morais, S.; Stern, J.; Kahn, A.; Galanopoulou, A. P.; Yoav, S.; Shamshoum, M.; Smith, M. A.; Hatzinikolaou, D. G.; Arnold, F. H.; Bayer, E. A., Enhancement of Cellulosome-Mediated Deconstruction of Cellulose by Improving Enzyme Thermostability. *Biotechnol Biofuels* **2016,** *9* (1), 164. DOI: 10.1186/s13068-016-0577-z
119. Caspi, J.; Barak, Y.; Haimovitz, R.; Irwin, D.; Lamed, R.; Wilson, D. B.; Bayer, E. A., Effect of Linker Length and Dockerin Position on Conversion of a Thermobifida Fusca Endoglucanase to the Cellulosomal Mode. *Appl Environ Microbiol* **2009,** *75* (23), 7335-7342. DOI: 10.1128/AEM.01241-09
120. Moraïs, S.; David, Y. B.; Bensoussan, L.; Duncan, S. H.; Koropatkin, N. M.; Martens, E. C.; Flint, H. J.; Bayer, E. A., Enzymatic Profiling of Cellulosomal Enzymes from the Human Gut Bacterium, R Uminococcus Champanellensis, Reveals a Fine-Tuned System for Cohesin-Dockerin Recognition. *Enviorn Microbiol* **2016,** *18* (2), 542-556. DOI: 10.1111/1462-2920.13047
121. Clark, E. D., Protein Refolding for Industrial Processes. *Curr Opin Biotechnol* **2001,** *12* (2), 202-207. DOI: 10.1016/s0958-1669(00)00200-7
122. Francis, D. M.; Page, R., Strategies to Optimize Protein Expression in E. Coli. *Curr Protoc Protein Sci* **2010,** *Chapter 5* (1), 1-29. DOI: 10.1002/0471140864.ps0524s61
123. Callejon, S.; Sendra, R.; Ferrer, S.; Pardo, I., Recombinant Laccase from Pediococcus Acidilactici Cect 5930 with Ability to Degrade Tyramine. *PLoS One* **2017,** *12* (10), e0186019. DOI: 10.1371/journal.pone.0186019
124. Weick, E.-M.; Zinder, J. C.; Lima, C. D., Strategies for Generating Rna Exosome Complexes from Recombinant Expression Hosts. In *The Eukaryotic Rna Exosome: Methods and Protocols*, LaCava, J.; Vaňáčová, Š., Eds. Springer, 2020; pp 417-425.

125. Shpigel, E.; Goldlust, A.; Eshel, A.; Ber, I. K.; Efroni, G.; Singer, Y.; Levy, I.; Dekel, M.; Shoseyov, O., Expression, Purification and Applications of Staphylococcal Protein a Fused to Cellulose-Binding Domain. *Biotechnol Appl Biochem* **2000,** *31* (3), 197-203. DOI: 10.1042/ba20000002
126. Sherkhanov, S.; Korman, T. P.; Chan, S.; Faham, S.; Liu, H.; Sawaya, M. R.; Hsu, W.-T.; Vikram, E.; Cheng, T.; Bowie, J. U., Isobutanol Production Freed from Biological Limits Using Synthetic Biochemistry. *Nature Commun* **2020,** *11* (1), 1-10. DOI: 10.1038/s41467-020-18124-1
127. Eiteman, M. A.; Altman, E., Overcoming Acetate in Escherichia Coli Recombinant Protein Fermentations. *Trends Biotechnol* **2006,** *24* (11), 530-536. DOI: 10.1016/j.tibtech.2006.09.001
128. Wong, M.; Zha, J.; Sorci, M.; Gasparis, C.; Belfort, G.; Koffas, M., Cell-Free Production of Isobutanol: A Completely Immobilized System. *Bioresour Technol* **2019,** *294*, 122104. DOI: 10.1016/j.biortech.2019.122104
129. Lu, J.; Brigham, C. J.; Plassmeier, J. K.; Sinskey, A. J., Characterization and Modification of Enzymes in the 2-Ketoisovalerate Biosynthesis Pathway of Ralstonia Eutropha H16. *Appl Microbiol Biotechnol* **2015,** *99* (2), 761-774. DOI: 10.1007/s00253-014-5965-3
130. Morrison, C. S.; Paskaleva, E. E.; Rios, M. A.; Beusse, T. R.; Blair, E. M.; Lin, L. Q.; Hu, J. R.; Gorby, A. H.; Dodds, D. R.; Armiger, W. B.; Dordick, J. S.; Koffas, M. A. G., Improved Soluble Expression and Use of Recombinant Human Renalase. *PLoS One* **2020,** *15* (11), e0242109. DOI: 10.1371/journal.pone.0242109
131. Wu, J. T.; Wu, L. H.; Knight, J. A., Stability of Nadph: Effect of Various Factors on the Kinetics of Degradation. *Clin Chem* **1986,** *32* (2), 314-319. DOI: 10.1093/clinchem/32.2.314
132. Koytsoumpa, E. I.; Bergins, C.; Kakaras, E., The Co2 Economy: Review of Co2 Capture and Reuse Technologies. *J Supercrit Fluids* **2018,** *132*, 3-16. DOI: 10.1016/j.supflu.2017.07.029
133. Yu, J.; Xie, L. H.; Li, J. R.; Ma, Y.; Seminario, J. M.; Balbuena, P. B., Co2 Capture and Separations Using Mofs: Computational and Experimental Studies. *Chem Rev* **2017,** *117* (14), 9674-9754. DOI: 10.1021/acs.chemrev.6b00626
134. Basso, A.; Serban, S., Industrial Applications of Immobilized Enzymes—a Review. *Mol Catal* **2019,** *479*, 110607. DOI: 10.1016/j.mcat.2019.110607
135. Elleuche, S., Bringing Functions Together with Fusion Enzymes—from Nature's Inventions to Biotechnological Applications. *Appl Microbiol* **2015,** *99* (4), 1545-1556. DOI: 10.1007/s00253-014-6315-1
136. Vanderstraeten, J.; Briers, Y., Synthetic Protein Scaffolds for the Colocalisation of Co-Acting Enzymes. *Biotechnol Adv* **2020,** *44*, 107627. DOI: 10.1016/j.biotechadv.2020.107627
137. Marchetti, P.; Jimenez Solomon, M. F.; Szekely, G.; Livingston, A. G., Molecular Separation with Organic Solvent Nanofiltration: A Critical Review. *Chem Rev* **2014,** *114* (21), 10735-10806. DOI: 10.1021/cr500006j
138. Ramesh, P.; Xu, W. L.; Sorci, M.; Trant, C.; Lee, S.; Kilduff, J.; Yu, M.; Belfort, G., Organic Solvent Filtration by Brush Membranes: Permeability, Selectivity and Fouling Correlate with Degree of Set-Lrp Grafting. *J Membr Sci* **2021,** *618*, 118699. DOI: 10.1016/j.memsci.2020.118699
139. Thompson, K. A.; Mathias, R.; Kim, D.; Kim, J.; Rangnekar, N.; Johnson, J. R.; Hoy, S. J.; Bechis, I.; Tarzia, A.; Jelfs, K. E.; McCool, B. A.; Livingston, A. G.; Lively, R. P.; Finn, M. G., N-Aryl-Linked Spirocyclic Polymers for Membrane Separations of Complex Hydrocarbon Mixtures. *Science* **2020,** *369* (6501), 310-315. DOI: 10.1126/science.aba9806

140. Qureshi, N.; Meagher, M. M.; Hutkins, R. W., Recovery of Butanol from Model Solutions and Fermentation Broth Using a Silicalite/Silicone Membrane. *J Membr Sci* **1999,** *158* (1-2), 115-125. DOI: 10.1016/s0376-7388(99)00010-1
141. Bowen, T., Driving Force for Pervaporation through Zeolite Membranes. *J Membr Sci* **2003,** *225* (1-2), 165-176. DOI: 10.1016/j.memsci.2003.07.016
142. Saint Remi, J. C.; Remy, T.; Van Hunskerken, V.; van de Perre, S.; Duerinck, T.; Maes, M.; De Vos, D.; Gobechiya, E.; Kirschhock, C. E.; Baron, G. V.; Denayer, J. F., Biobutanol Separation with the Metal-Organic Framework Zif-8. *ChemSusChem* **2011,** *4* (8), 1074-1077. DOI: 10.1002/cssc.201100261
143. Claessens, B.; De Staercke, M.; Verstraete, E.; Baron, G. V.; Cousin-Saint-Remi, J.; Denayer, J. F. M., Identifying Selective Adsorbents for the Recovery of Renewable Isobutanol. *ACS Sustainable Chem. Eng.* **2020,** *8* (24), 9115-9124. DOI: 10.1021/acssuschemeng.0c02316